原子核のE1,M1励起

A. Tamii

Research Center for Nuclear Physics, Osaka University

勉強会, July 26, 2011

原子核
この多彩で魅力的な世界

量子少数多体系

“形”の始まり

変形、対称性の自発的破れ

“表面”の存在

配位混合・分散

2種の構成子

強・弱・電磁相互作用

集団運動（秩序）

量子カオス

強相関システム

対相関（準粒子）

テンソル相関

クラスタリング

自己束縛系

対象（核構造）とプローブ（核反応）の不可分性

独立粒子描像⇔平均場描像

複雑さの中に普遍的な構造を見つける
＝ 物理

Simple structure in a complex system

Origin of Order

原子核の励起モード

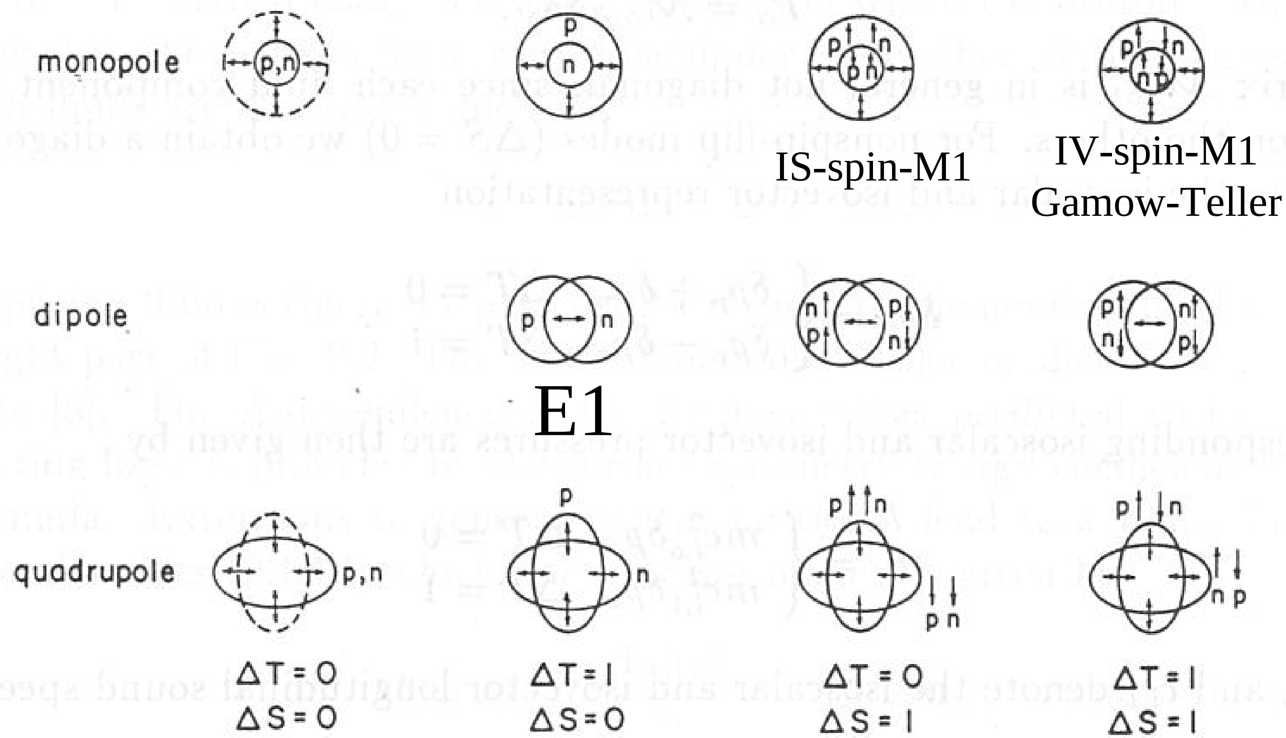

Fig. 2.1. The first three multipoles of oscillations of a four-component nuclear droplet. Isoscalar ($\Delta T = 0$) and isovector ($\Delta T = 1$) as well as nonspin-flip ($\Delta S = 0$) and spin-flip ($\Delta S = 1$) modes are shown separately.

原子核のE1応答

Pygmy (Soft) Dipole Resonance (PDR)

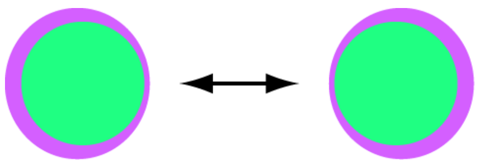

coreとskinの
相対振動？

Giant Dipole Resonance (GDR)

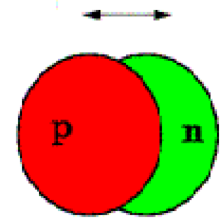

中性子と陽子の
重心の相対振動

Troidal E1 Mode

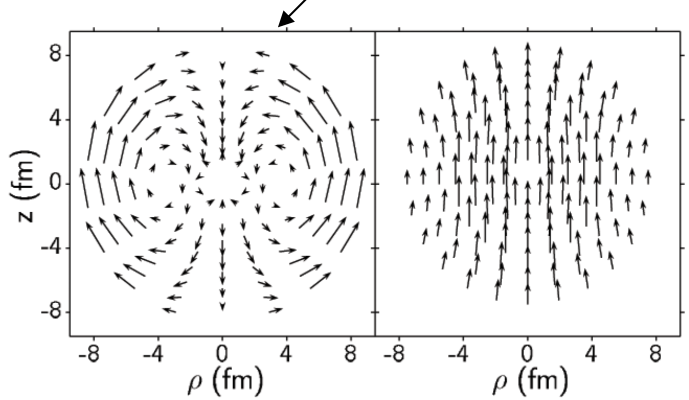

FIG. 4. The QPM prediction for the velocity distributions of $E1$ excitations at $E_x = 6.5$–10.5 MeV (left) and $E_x >$ 10.5 MeV (right) in ^{208}Pb.

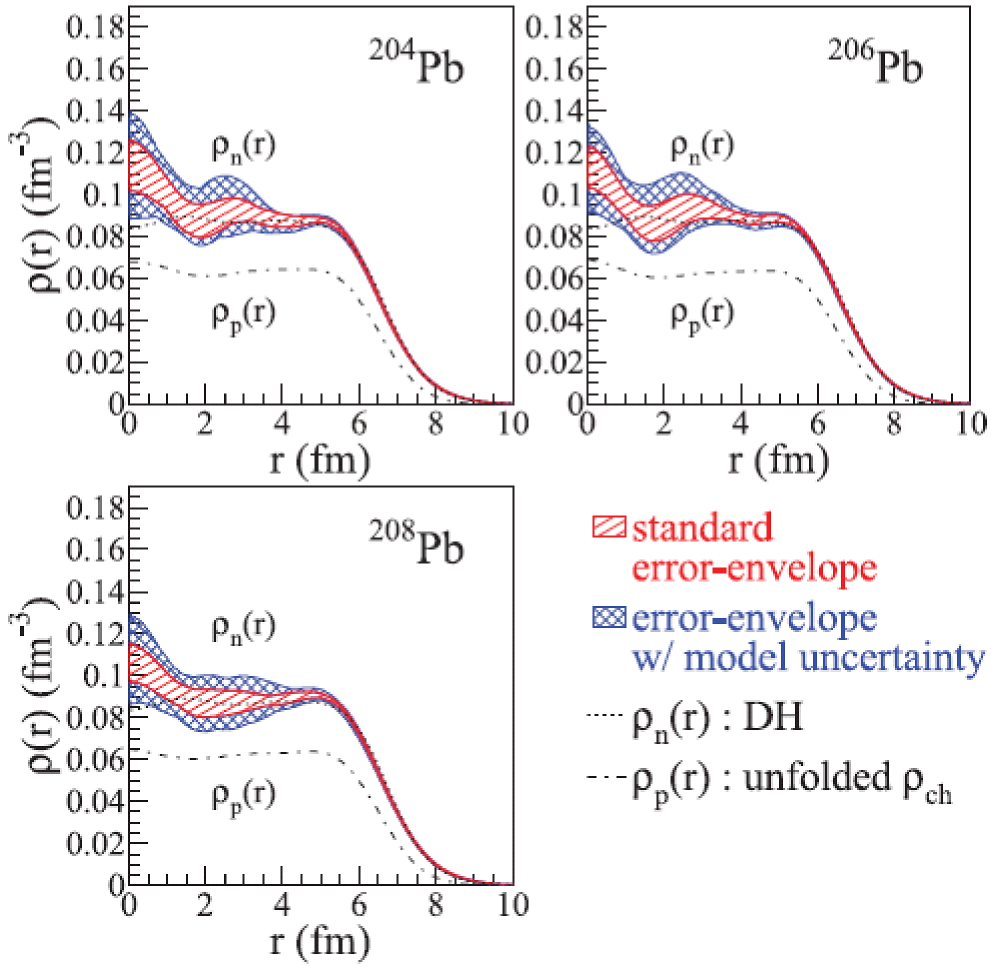

FIG. 7. (Color online) Extracted neutron densities for ^{204,206,208}Pb with two types of error envelopes shown together with DH neutron densities (dotted lines) and point proton densities by unfolding charge densities (dash-dotted lines). The cross-hatched and hatched error envelopes were estimated by Eqs. (8) and (6), respectively.

J. Zenihiro et al., PRC82, 044611 (2010).

E1,M1 励起強度を一網打尽にする！

原子核のE1応答を調べる

↓

原子核を電子レンジに入れて
反応を見る

振動電場
→ E1 Field

E1 Response

E1 Response は、外部振動電場に対する分極の振動に対応する。

E1 Field（振動電場）

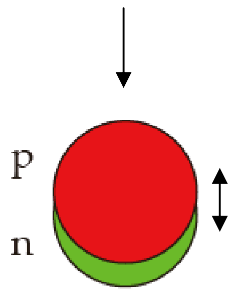

E1 response of a nucleus

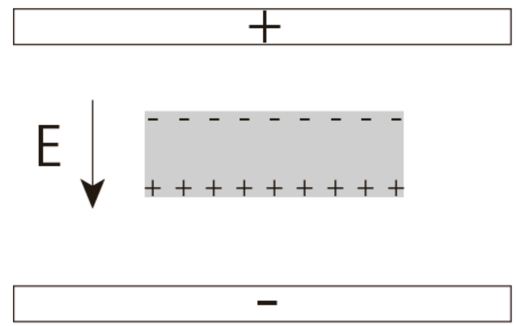

Static

誘電分極

E1-Field を実光子(γ線)で作らず、陽子ビームによる仮想光子(Virtual Photon)を用いて作る。

振動電場

電子レンジ

Probing EM response of the target nucleus

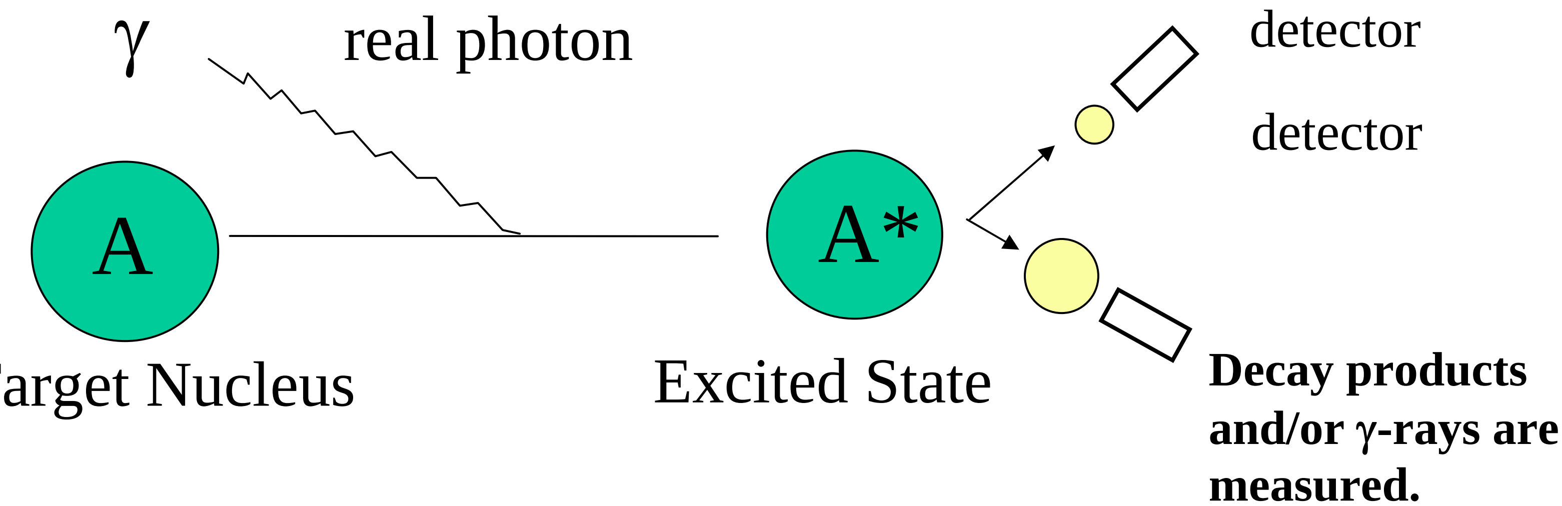

Missing Mass Spectroscopy:

Insensitive to the decay channel.

Total strengths are measured.

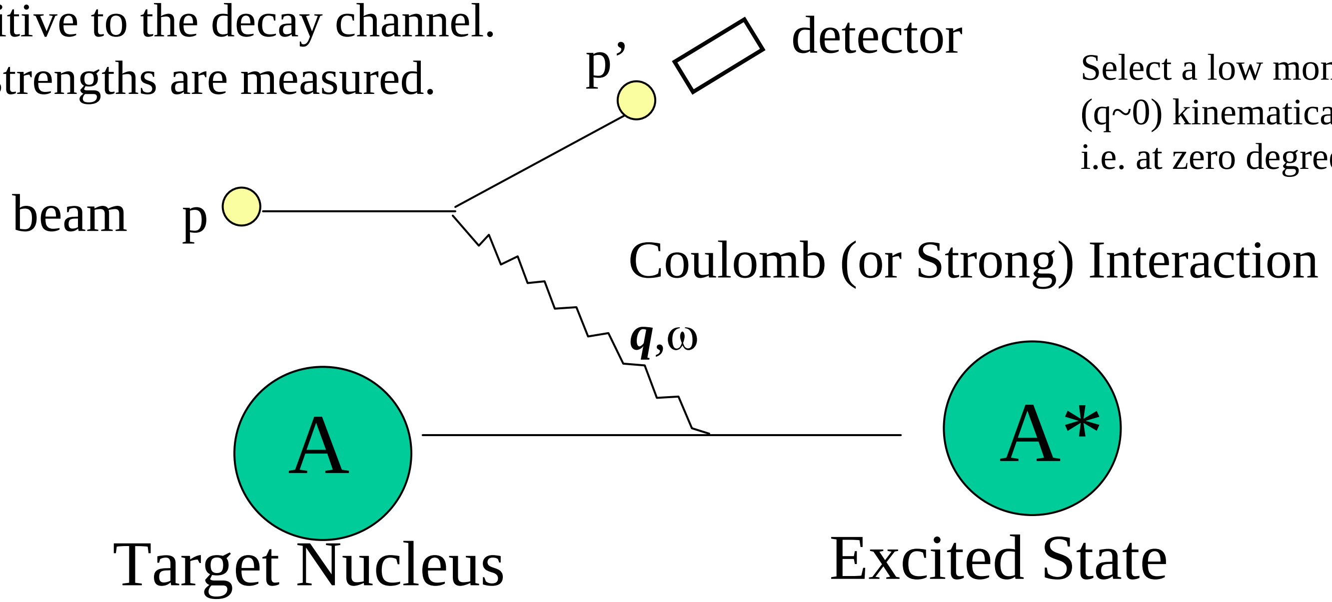

Select a low momentum transfer (q~0) kinematical condition, i.e. at zero degrees

Experimental Method

High-Resolution (*p*,*p*’) measurement at close to zero degrees

AT *et al*., NIM A605, 326 (2009)

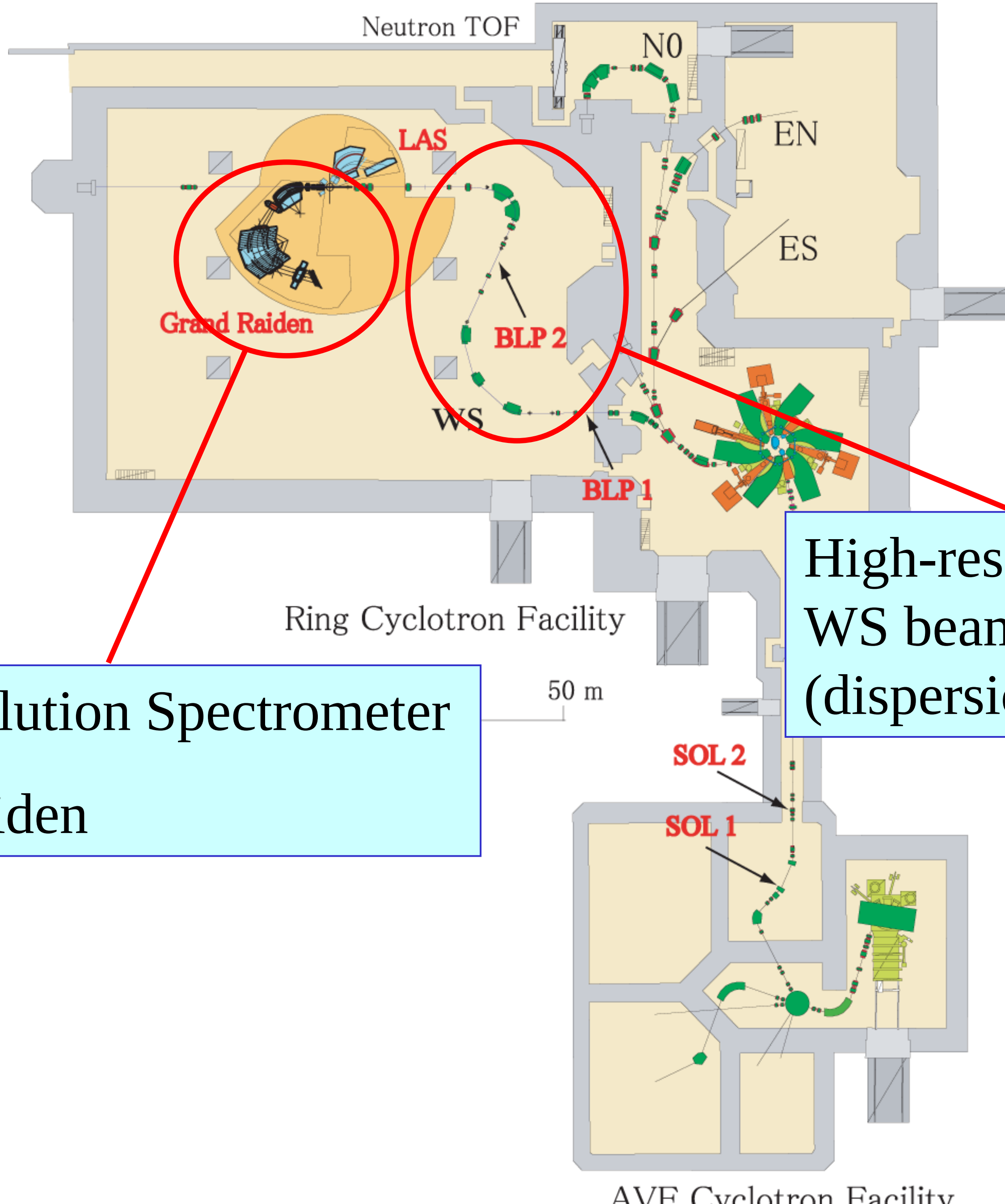

High-resolution Spectrometer

Grand Raiden

High-resolution
WS beam-line
(dispersion matching)

Spectrometers in the 0-deg. experiment setup

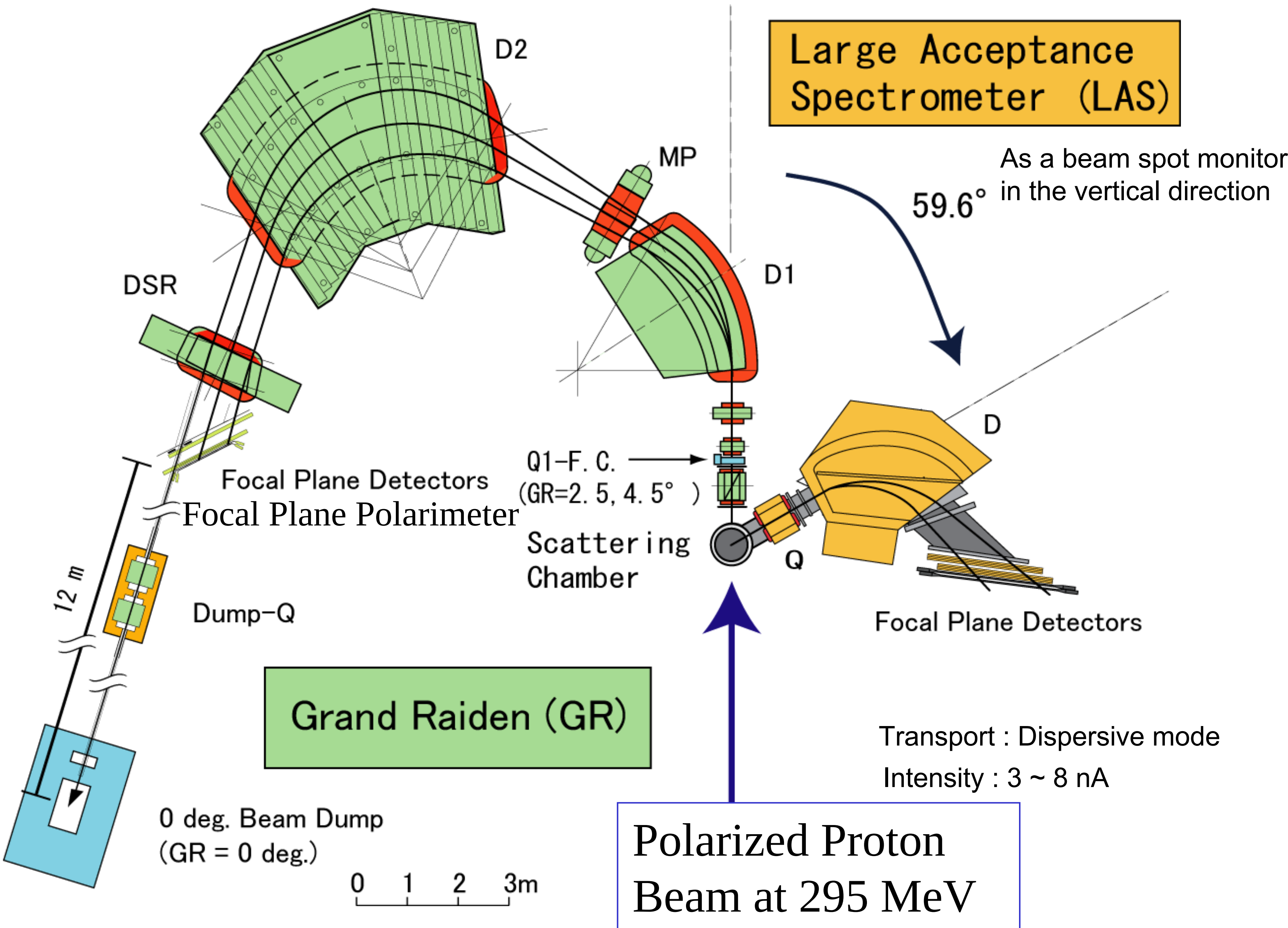

Spin Precession in the Spectrometer

$$\theta_p = \gamma(\frac{g}{2} - 1)\theta_b$$

θ_p: precession angle with respect to the beam direction
θ_b: bending angle of the beam
g: Lande's g-factor
γ: gamma in special relativity

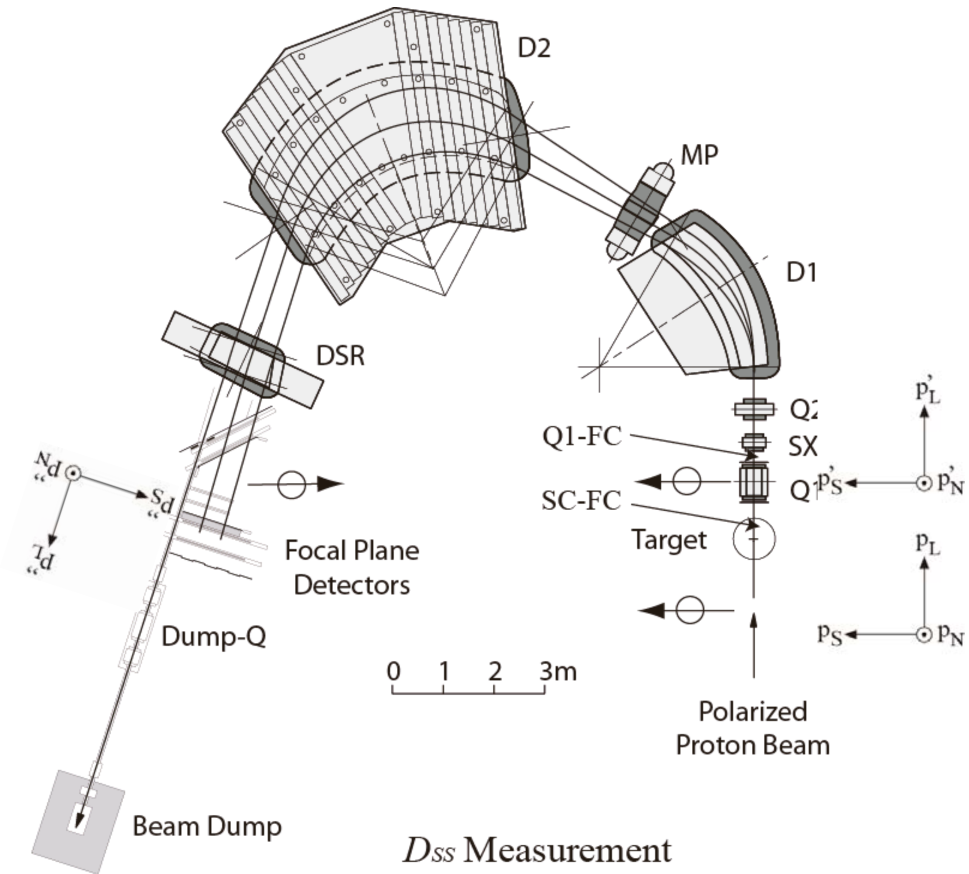

D_{SS} Measurement

$\theta_b \cong 162°$

2006-Oct

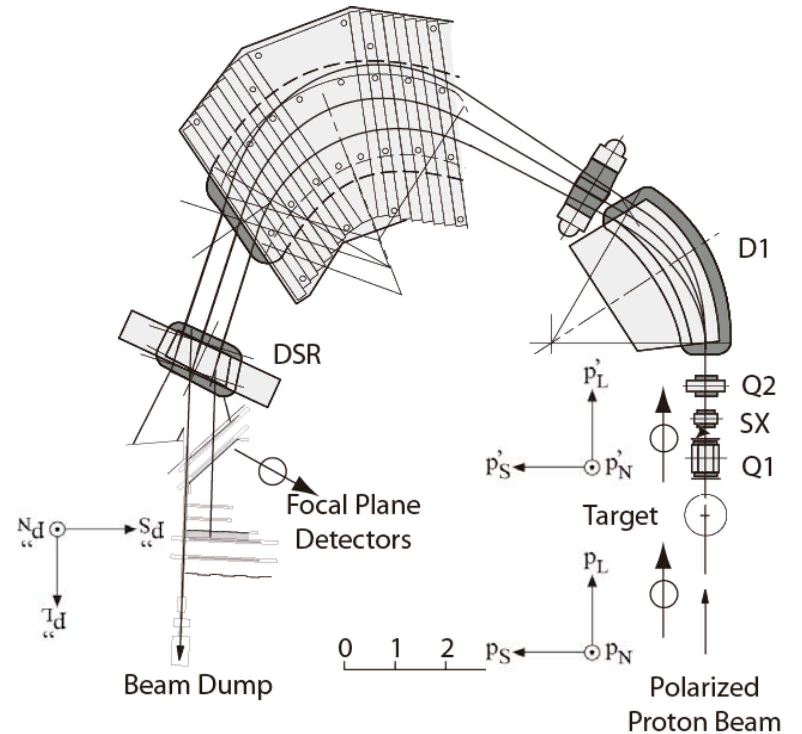

D_{LL} Measurement

$\theta_b \cong 180°$

2008-Nov

E1 Strength Distribution in ^{208}Pb

Illustrative View of E1 Strength Distribution and Measurements

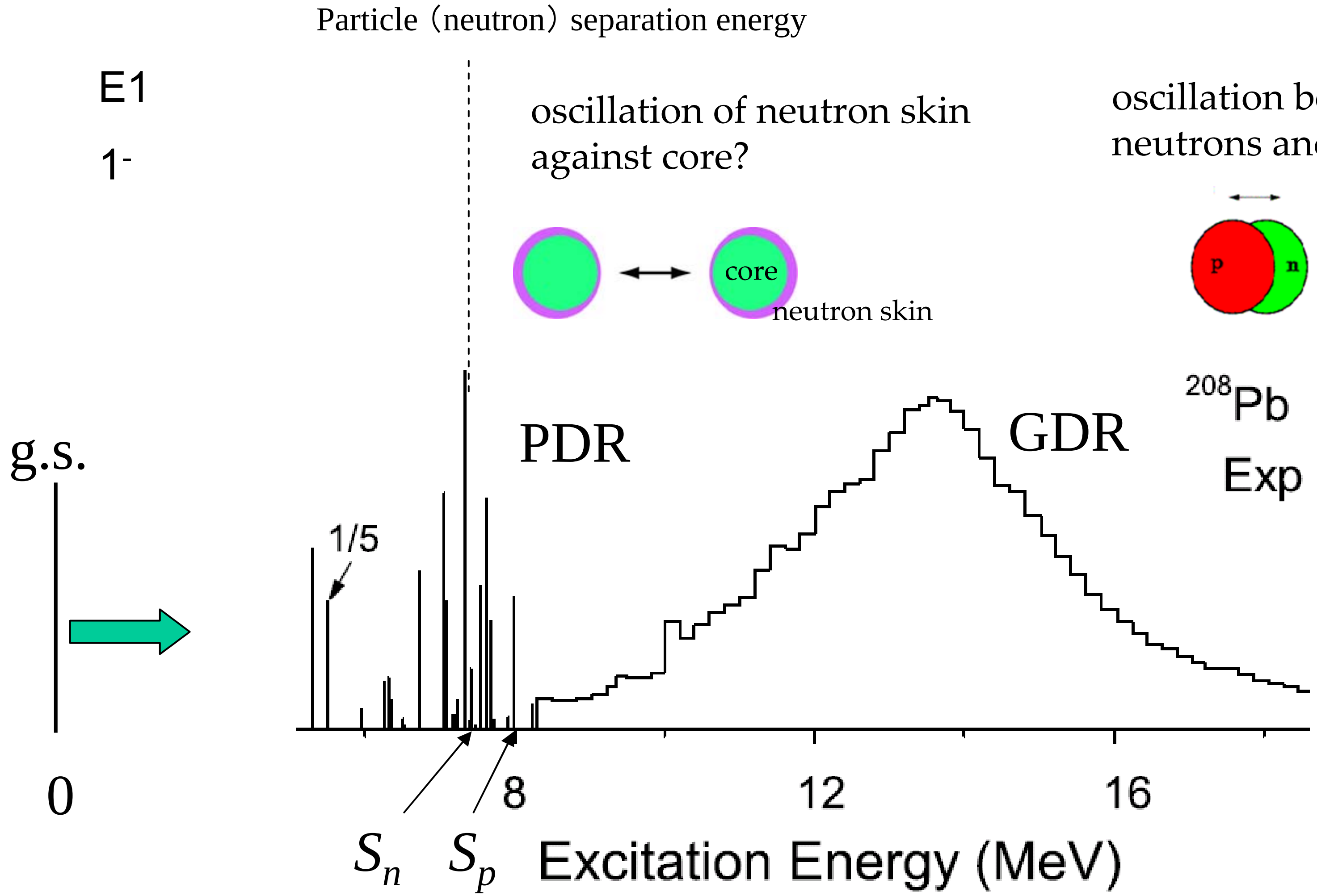

Illustrative View of E1 Strength Distribution and Measurements

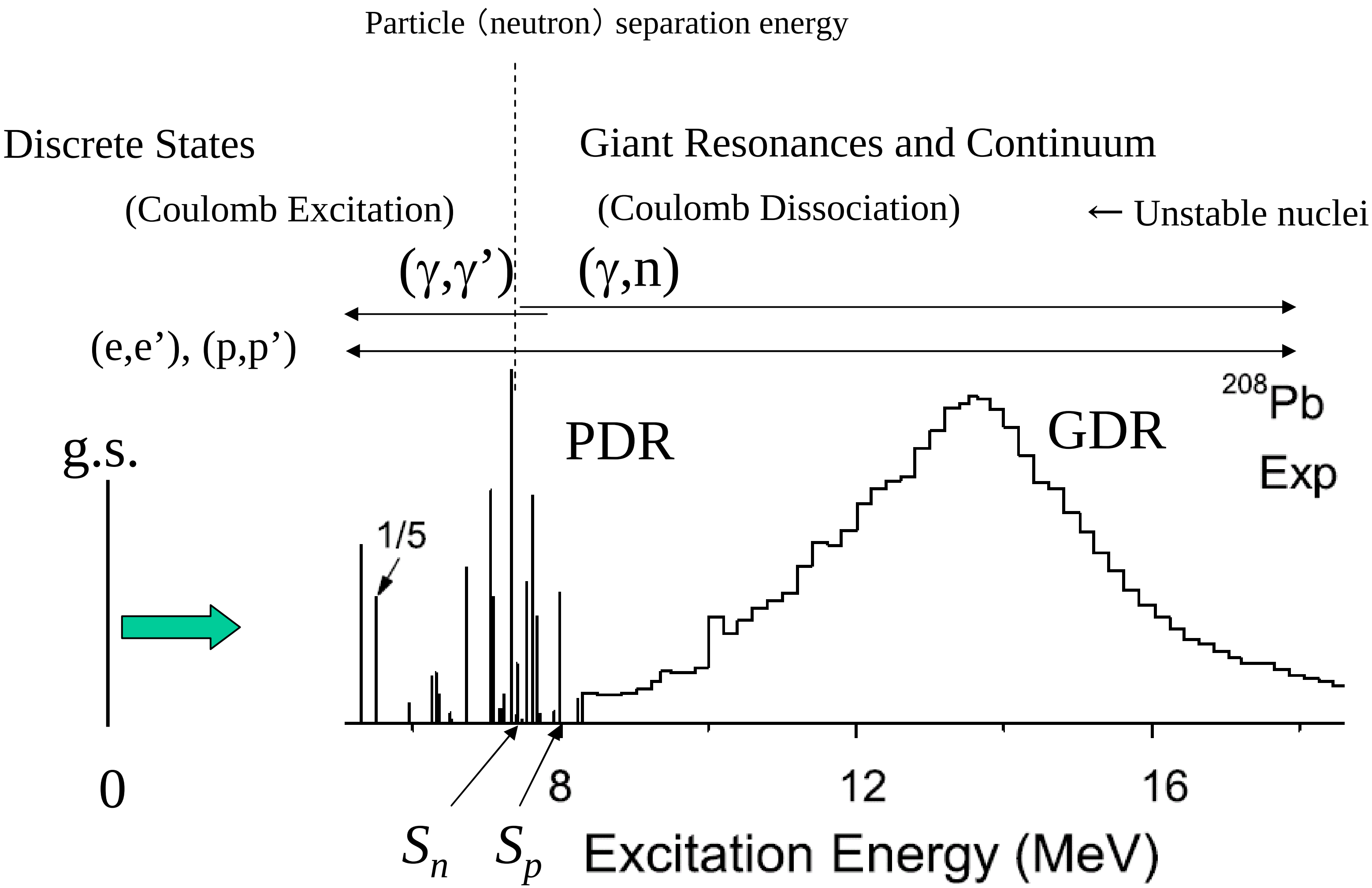

Illustrative View of E1 (M1) Strength Distribution and Measurements

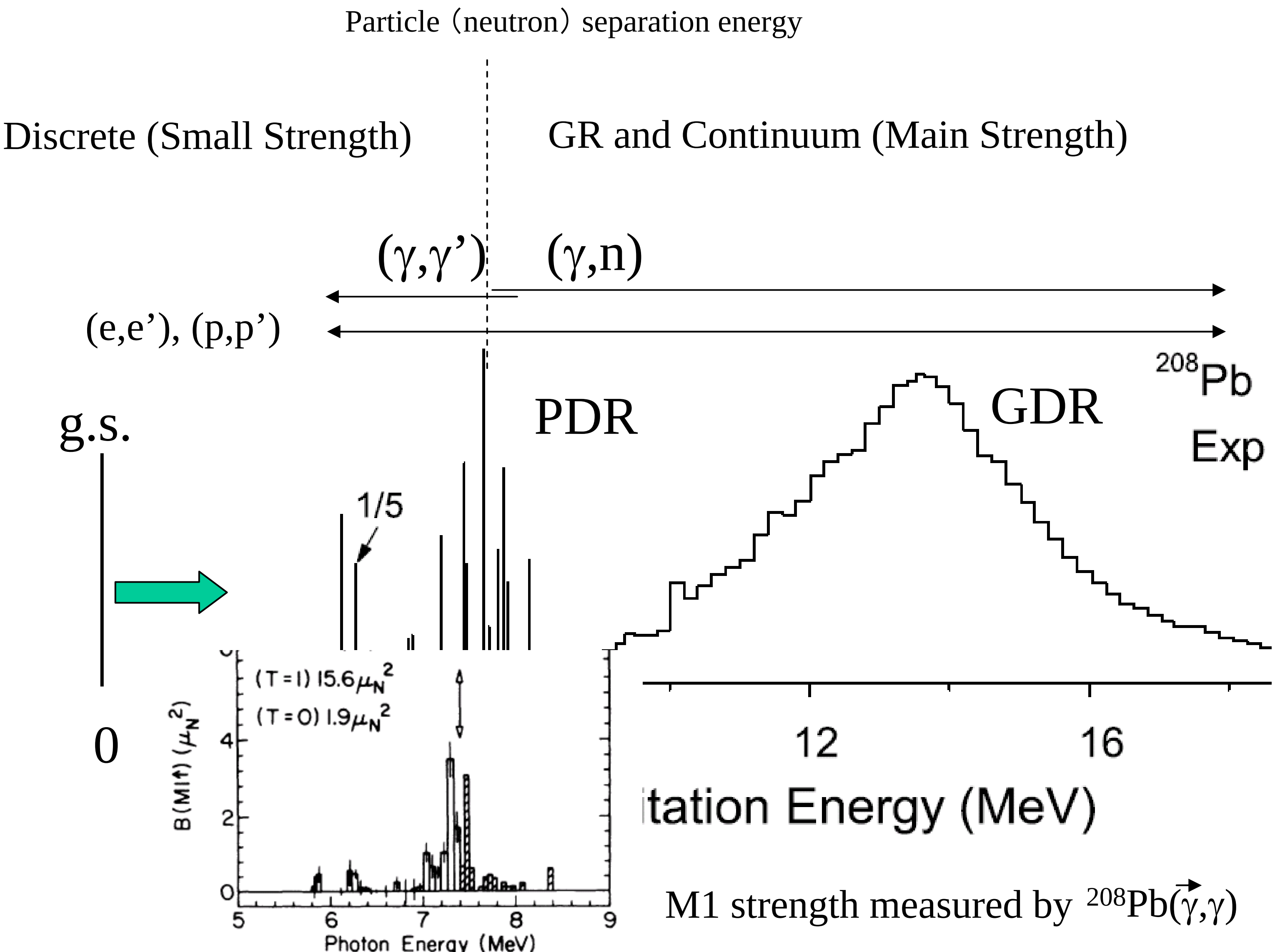

M1 strength measured by $^{208}Pb(\vec{\gamma},\gamma)$

R.M. Laszewski et al, PRL61(1988)1710

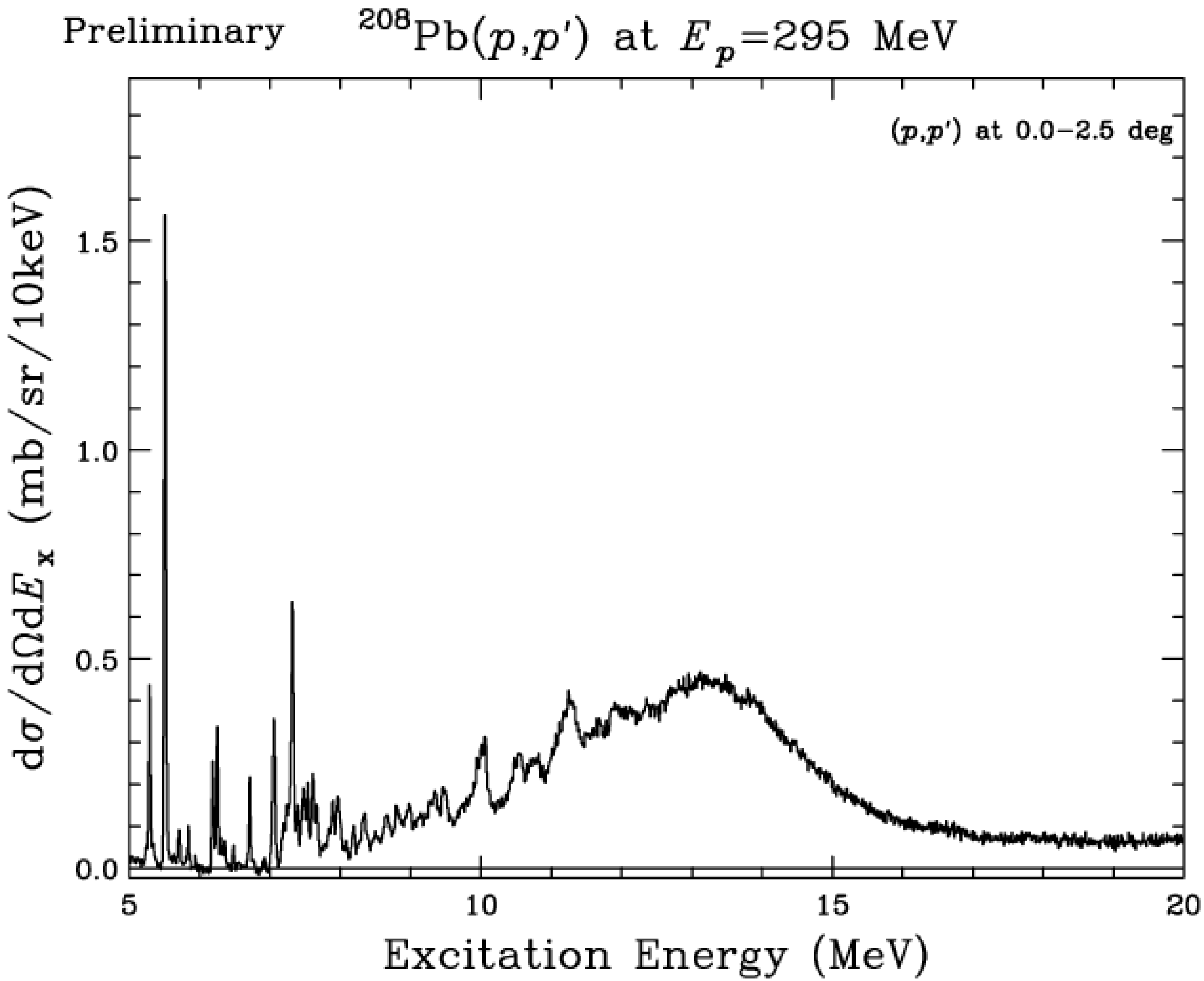
Preliminary
^{208}Pb(p,p') at E_p=295 MeV
(p,p') at 0.0–2.5 deg
dσ/dΩdE_x (mb/sr/10keV)
0.0
0.5
1.0
1.5
5
10
15
20
Excitation Energy (MeV)

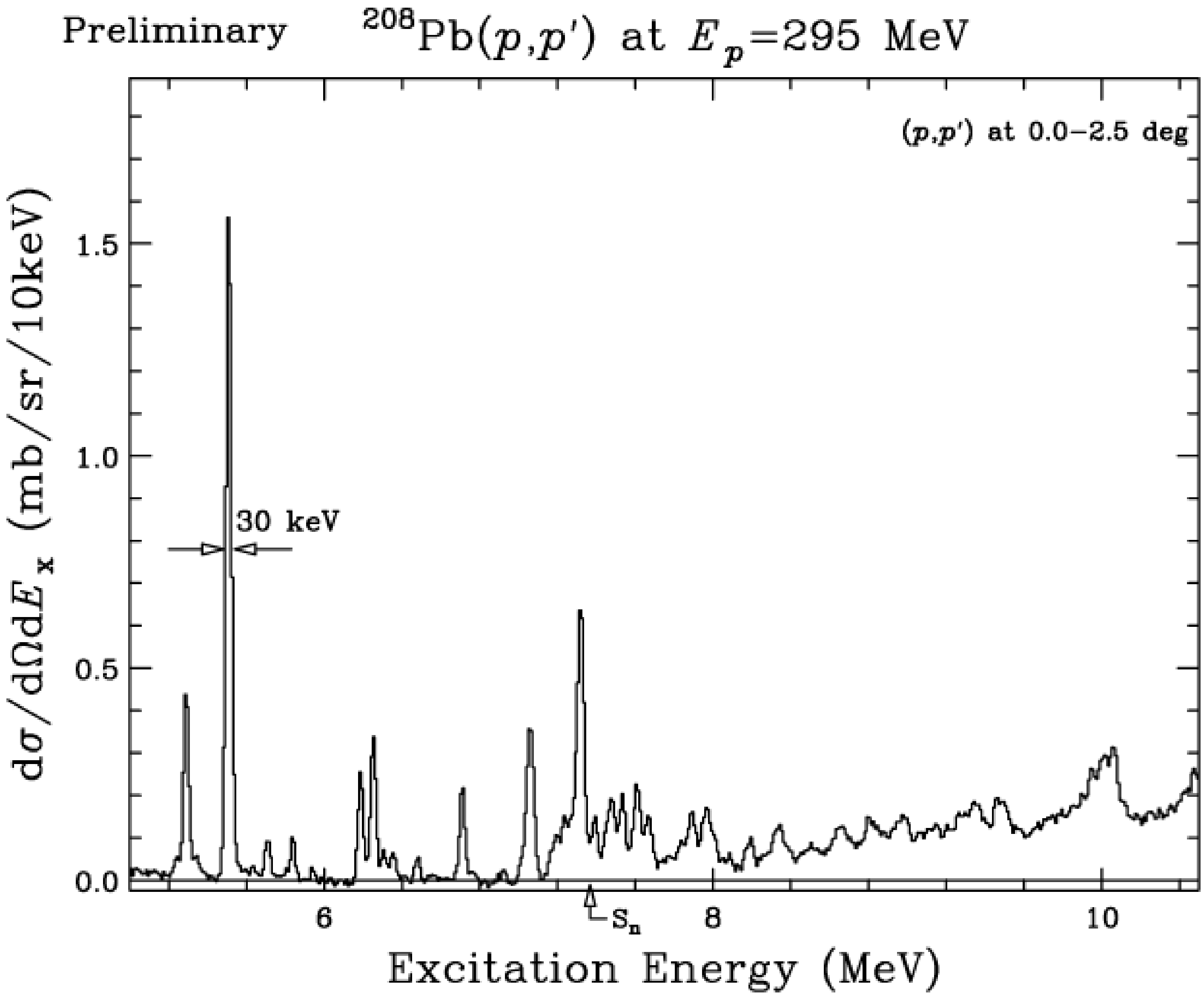

Preliminary
^{208}Pb(p,p') at E_p=295 MeV
(p,p') at 0.0–2.5 deg
30 keV
$d\sigma/d\Omega dE_x$ (mb/sr/10keV)
0.0
0.5
1.0
1.5
6
8
10
S_n
Excitation Energy (MeV)

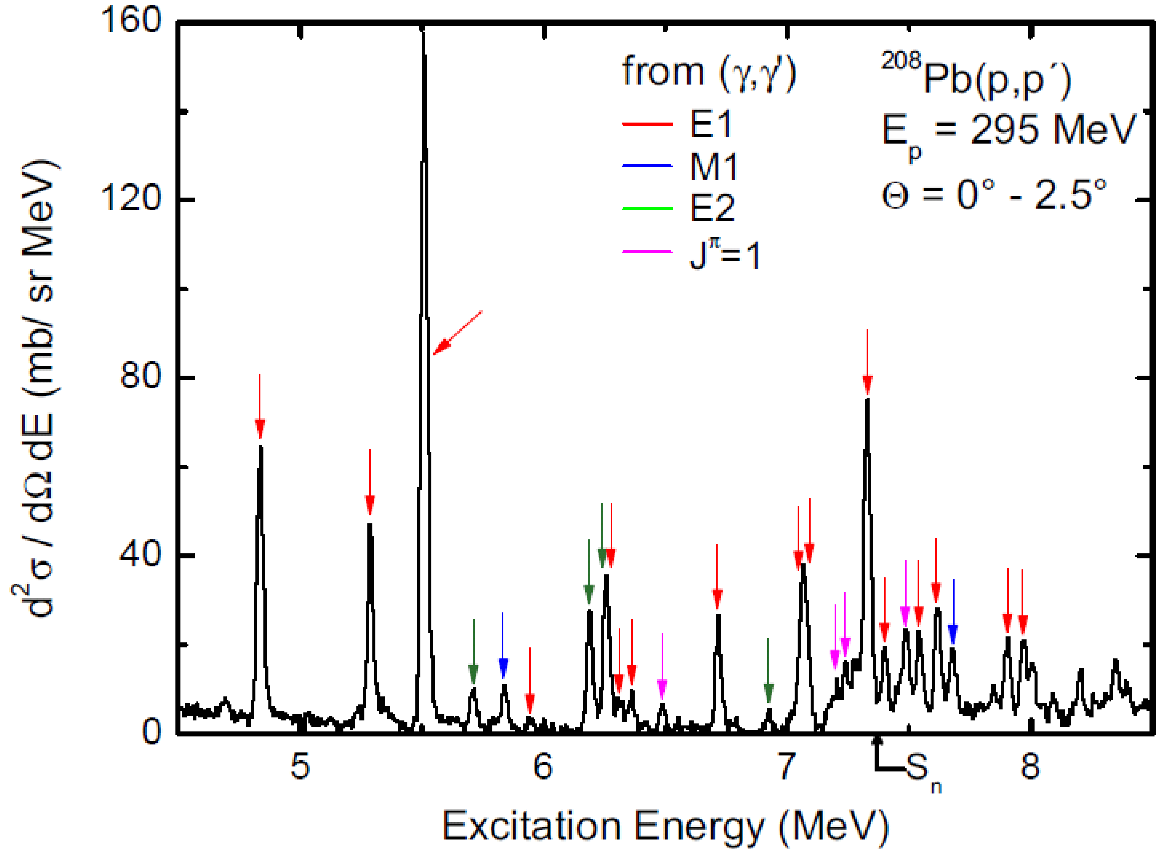

Fig. 5.1: Low-energy part of the spectrum of the ^{208}Pb(p,p') reaction at E_p = 295 MeV and Θ_{lab} = 0°. The arrows indicate transitions which are also observed in the ^{208}Pb(γ,γ') experiment [29].

I. Poltoratska, PhD thesis

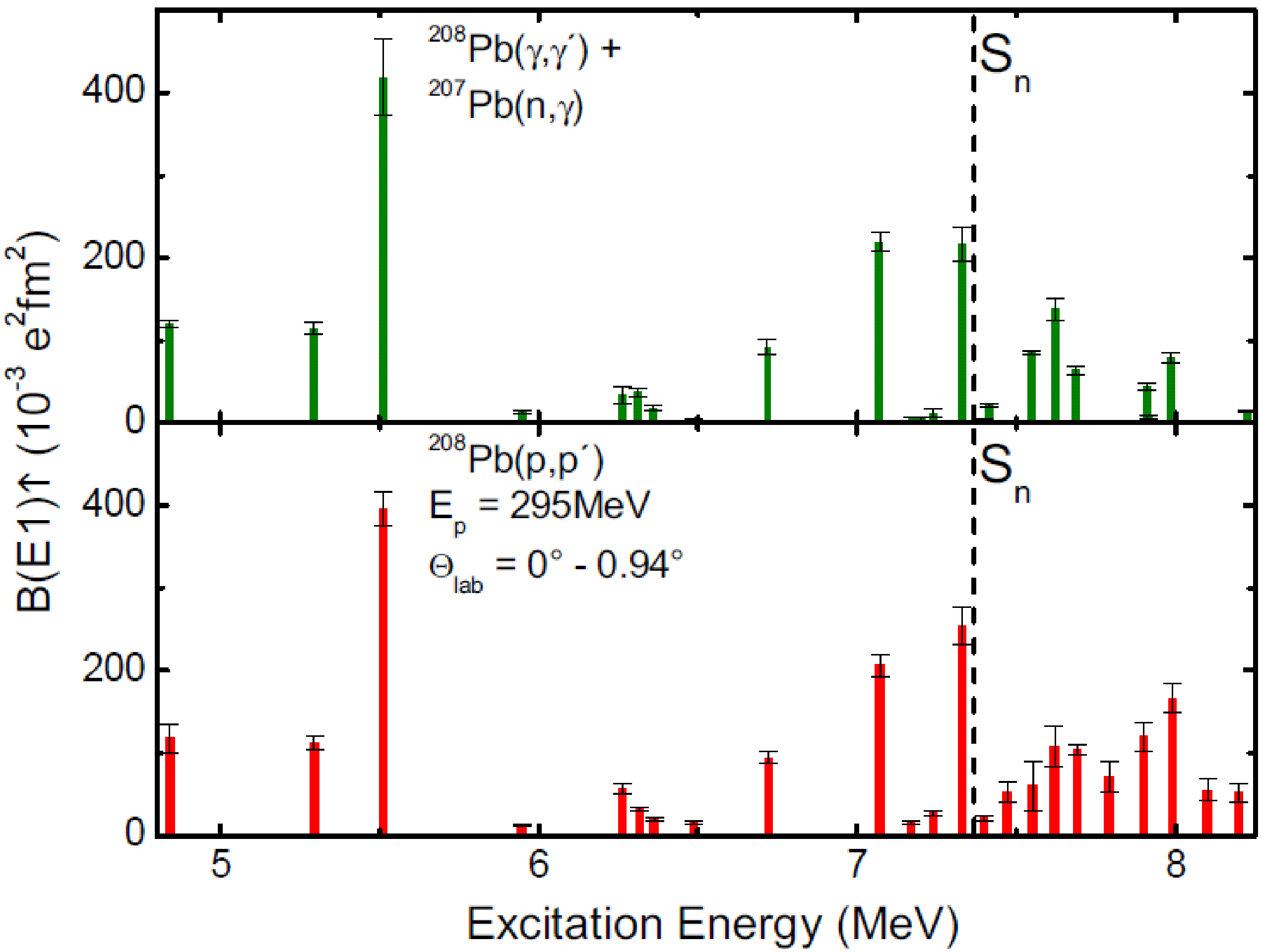

Fig. 5.10: B(E1) strength distribution in ^{208}Pb below the GDR extracted from the present work (bottom) in comparison to the (γ,γ') results from [28, 29, 30, 31] and ^{207}Pb(n,γ) data from [158] (top).

I. Poltoratska, PhD thesis

E1/M1 Decomposition by Spin Observables

- Polarization observables at 0° ➡ spinflip / non-spinflip separation*

  (model-independent)

$$D_{SS} + D_{NN} + D_{LL} = \begin{cases} -1 \text{ for } \Delta S = 1\text{, M1 excitations} \\ 3 \text{ for } \Delta S = 0\text{, E1 excitations} \end{cases}$$

➡ E1 and M1 cross sections can be decomposed

At 0° $D_{SS} = D_{NN}$

$$\text{Total Spin Transfer } \Sigma \equiv \frac{3-(2D_{SS}+D_{LL})}{4} = \begin{cases} 1 \text{ for } \Delta S = 1 \\ 0 \text{ for } \Delta S = 0 \end{cases}$$

T. Suzuki, PTP 103 (2000) 859

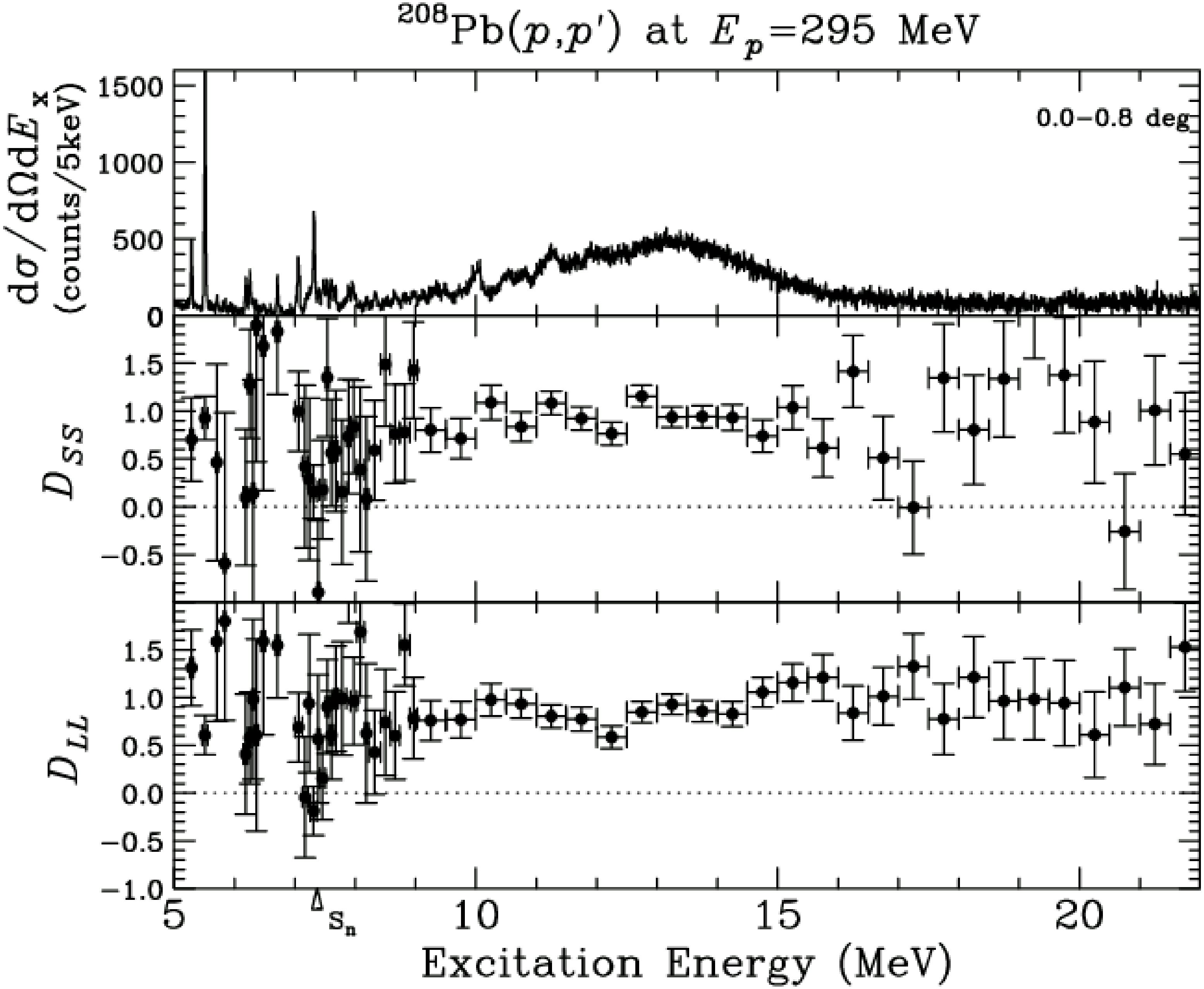

^{208}Pb(p,p') at E_p=295 MeV
dσ/dΩdE_x (counts/5keV)
0.0–0.8 deg
D_{SS}
D_{LL}
S_n
Excitation Energy (MeV)
5
10
15
20

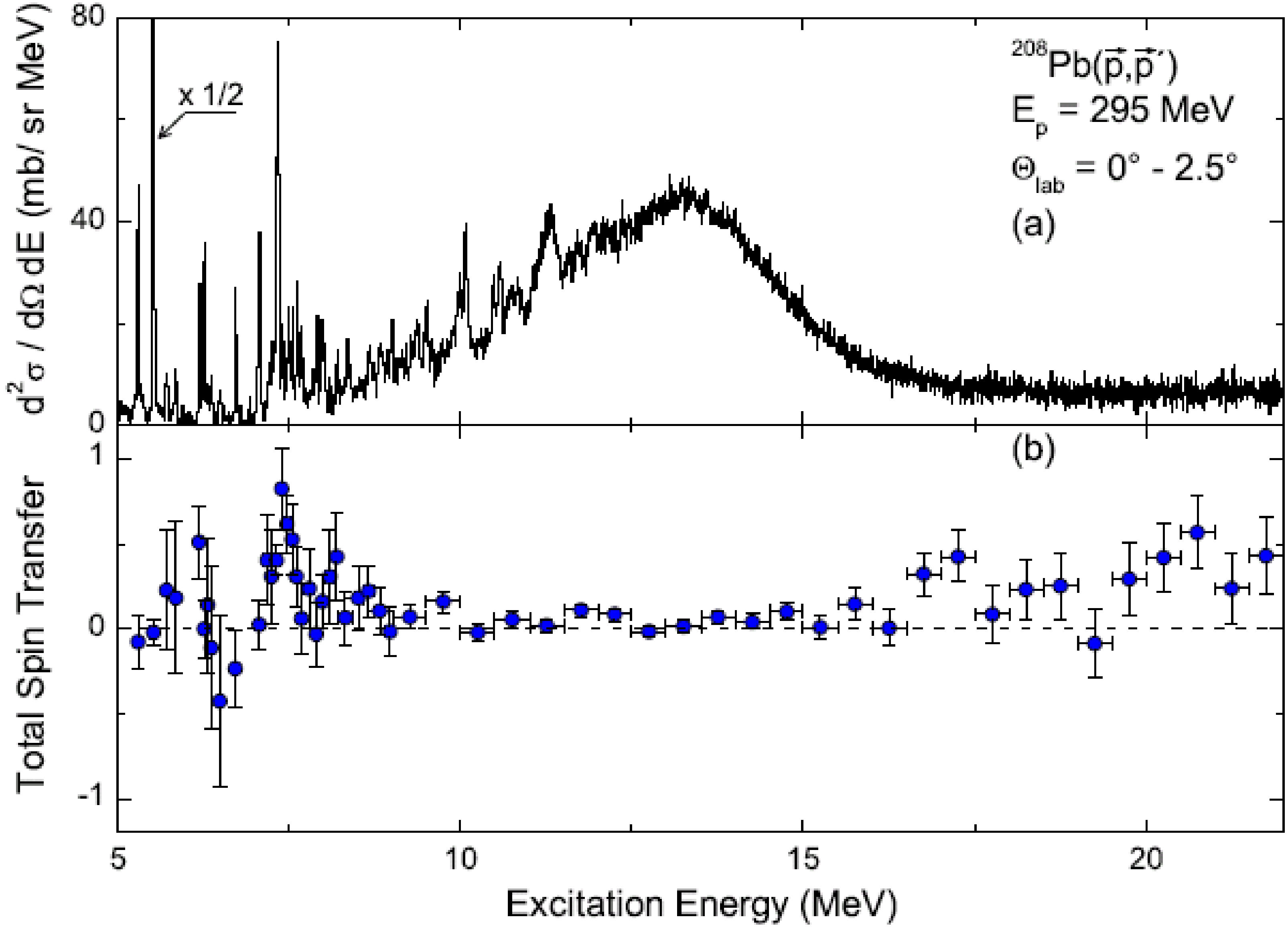

^{208}Pb($\vec{p}$,$\vec{p}'$)
E_p = 295 MeV
Θ_{lab} = 0° - 2.5°
(a)
(b)
x 1/2
$d^2\sigma$ / dΩ dE (mb/ sr MeV)
Total Spin Transfer
Excitation Energy (MeV)
80
40
0
1
0
-1
5
10
15
20

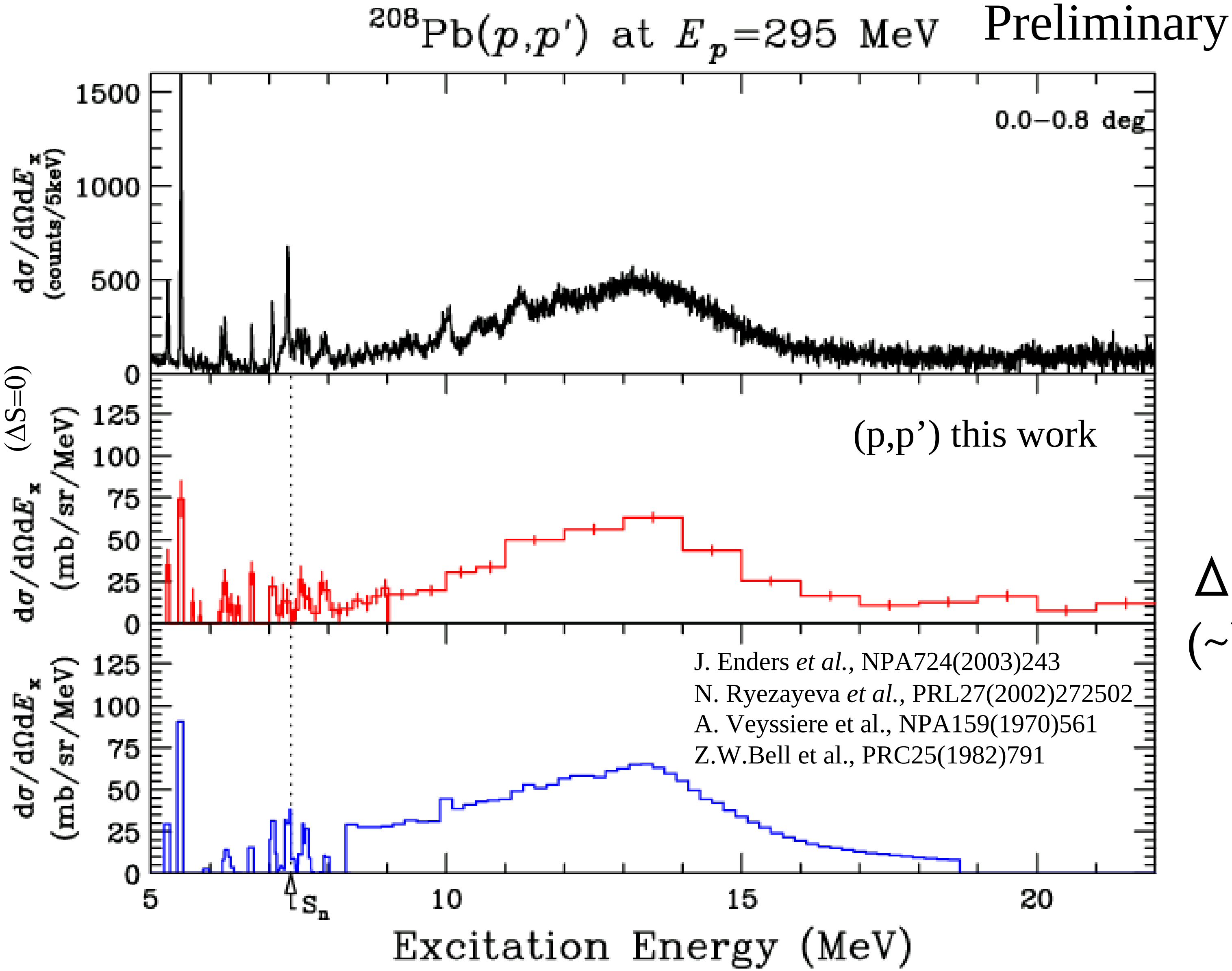

^{208}Pb(p,p') at E_p=295 MeV
Preliminary
0.0–0.8 deg
dσ/dΩdE$_x$ (counts/5keV)
1500
1000
500
0
dσ/dΩdE$_x$ (mb/sr/MeV) (ΔS=0)
125
100
75
50
25
0
(p,p') this work
dσ/dΩdE$_x$ (mb/sr/MeV)
J. Enders et al., NPA724(2003)243
N. Ryezayeva et al., PRL27(2002)272502
A. Veyssiere et al., NPA159(1970)561
Z.W.Bell et al., PRC25(1982)791
5
10
15
20
S$_n$
Excitation Energy (MeV)

ΔS=0
(~E1)

Multipole Decomposition

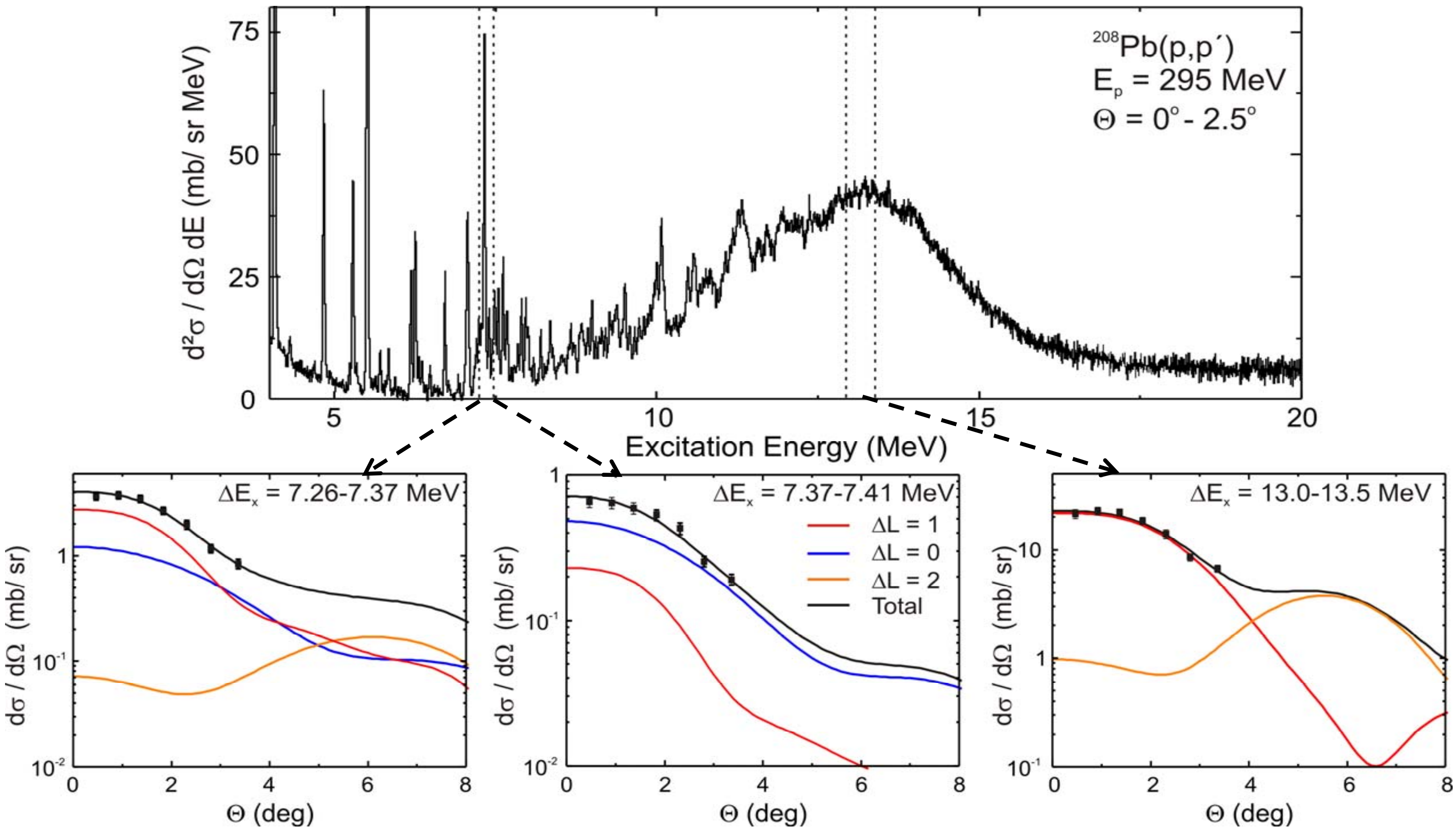

- Neglect of data for Θ>4: (p,p´) response too complex
- Included E1/M1/E2 or E1/M1/E3 (little difference)

Comparison of Both Methods

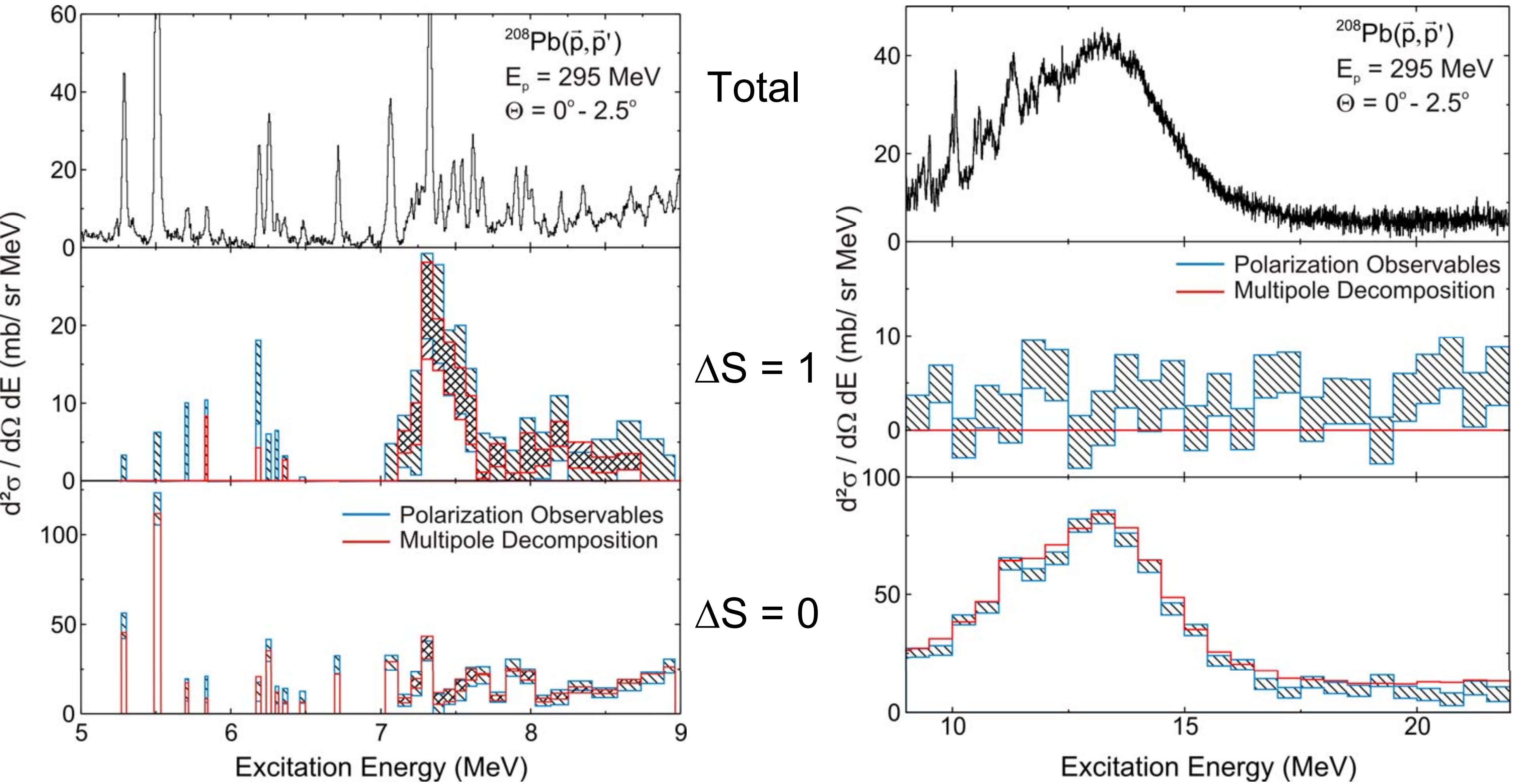

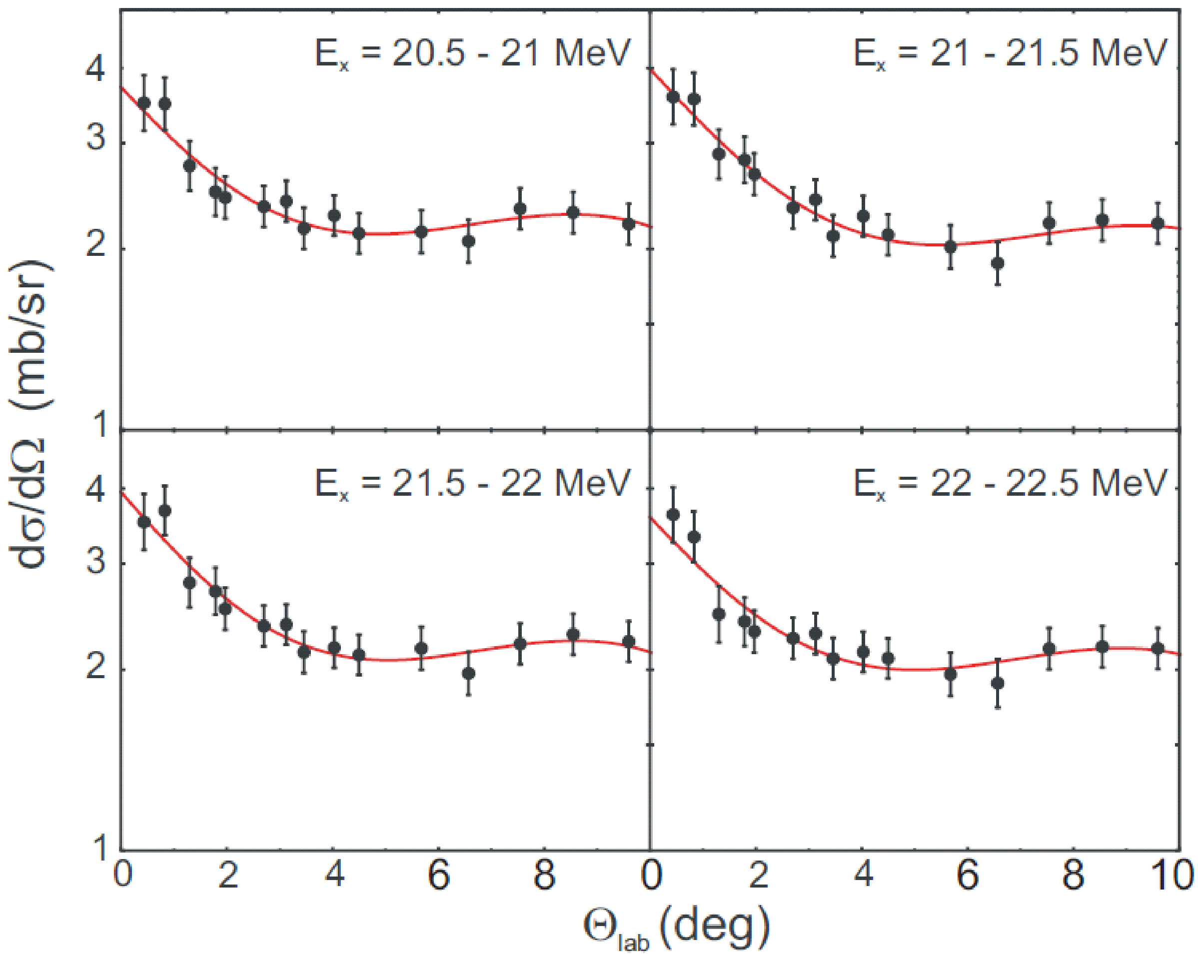

Fig. 5.6: Angular distributions of the cross sections at excitation energies from 20.5 MeV to 22.5 MeV in 500 keV bins fitted by a polynomial function of third order Eq. (5.4).

I. Poltoratska, PhD thesis

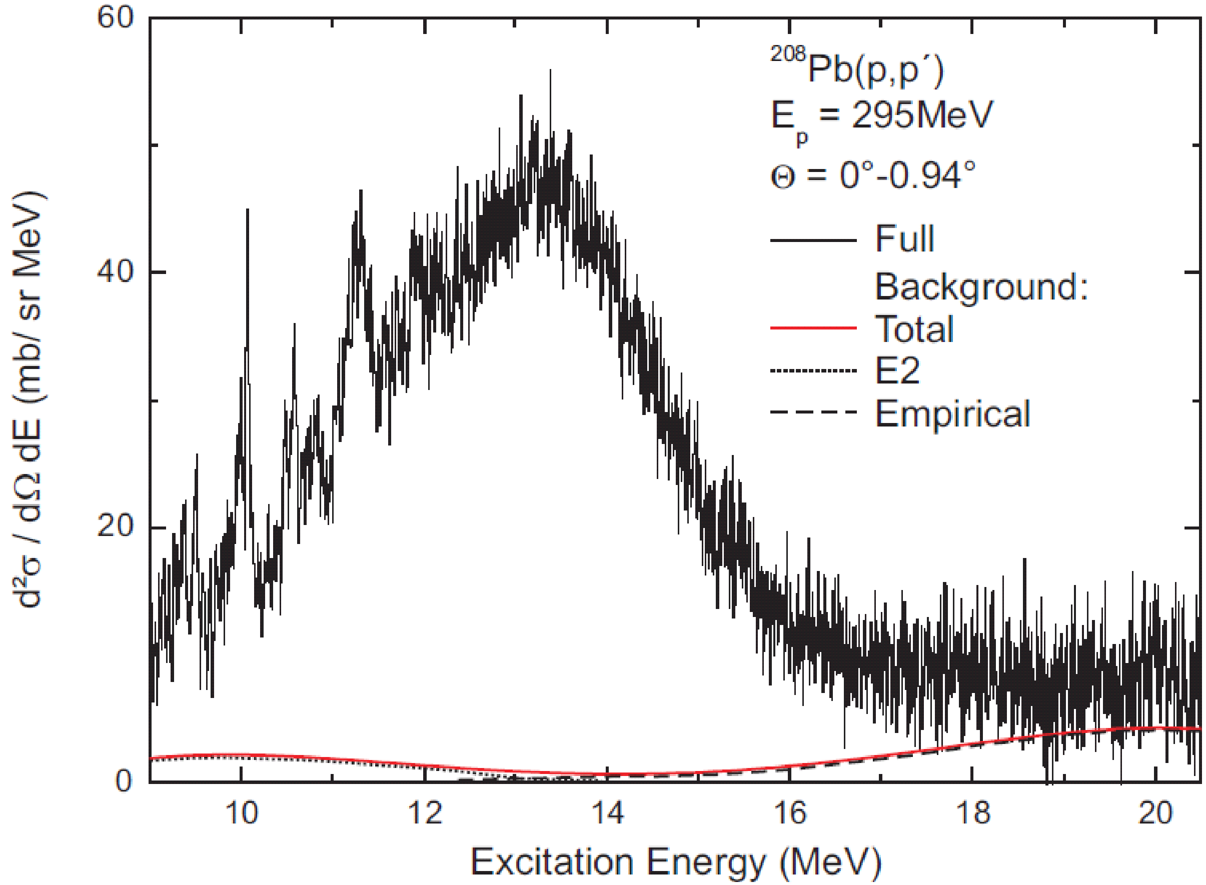

Fig. 5.7: Decomposition of the spectrum in the GDR region on E1, E2 cross sections and a phenomenological background. The solid black histogram shows the excitation energy spectrum from 9 MeV to 21 MeV in a small scattering angle cut Θ_{lab} = 0° - 0.94°. The dotted black curve corresponds to the E2 contribution, while the dashed one shows the phenomenological background, and the red solid curve illustrates the sum of these contributions.

I. Poltoratska, PhD thesis

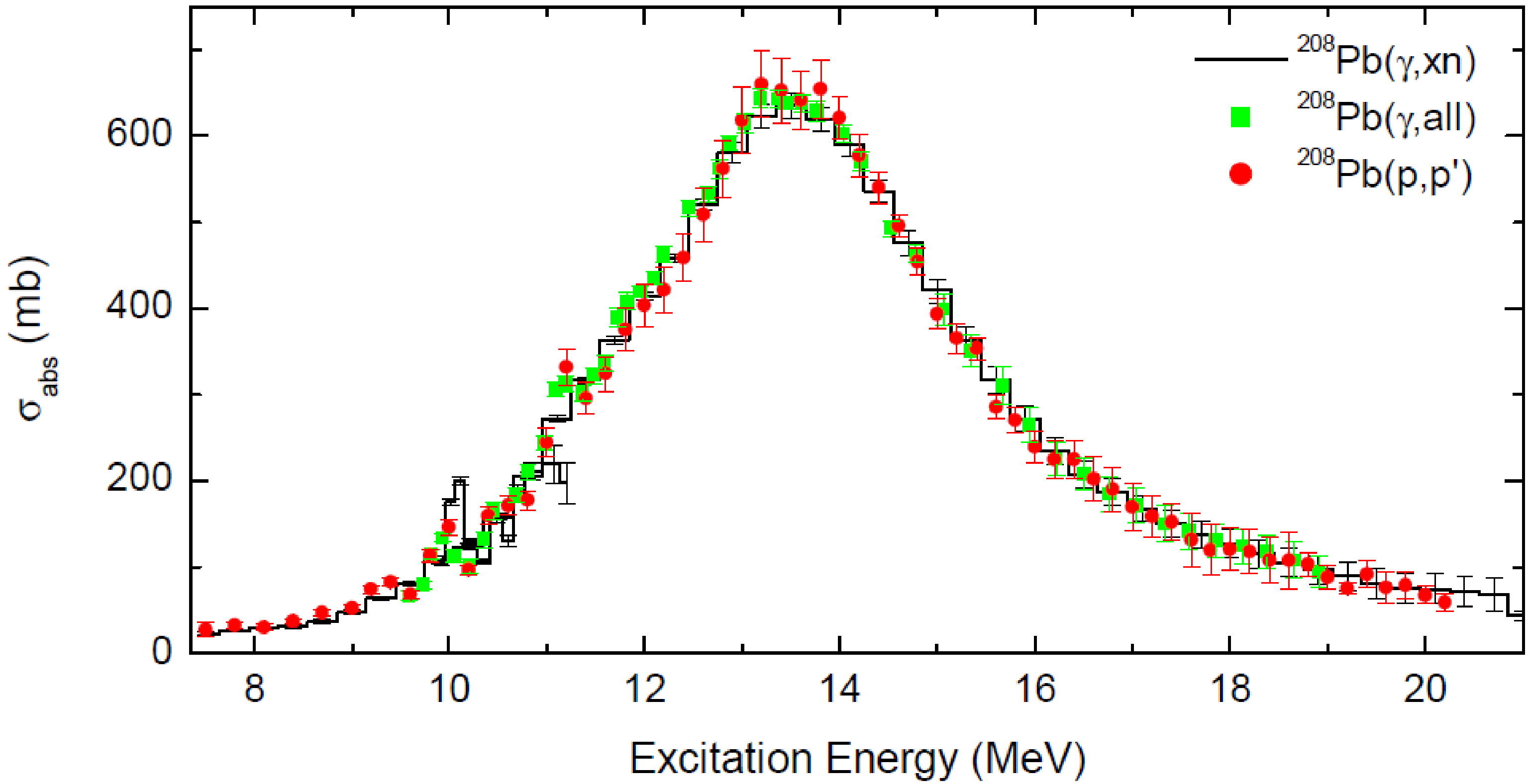

Fig. 5.11: Total absorption cross sections for the GDR region. Red circles denote σ_{abs} obtained in the present work, green squares are the results from [170] and black histogram represents the $(\gamma,$xn) data from [168, 169].

I. Poltoratska, PhD thesis

Electric Dipole Polarizability in ^{208}Pb

励起強度分布のモーメントと和則

オペレータFに対する励起強度関数（Strength Function）

$$S(\omega) \equiv \sum_k \left| \langle k | F | 0 \rangle \right|^2 \delta(\omega - \omega_k)$$

ω: 励起エネルギー

励起強度関数S(ω)のp次のモーメント

$$m_p \equiv \int_0^\infty S(\omega)\omega^p d\omega = \sum_k \left| \langle k | F | 0 \rangle \right|^2 \omega_k^p$$

参考文献[8]

$$S = m_0 = \int_0^{\infty} S(\omega)d\omega = \sum_k \left|\langle k|F|0\rangle\right|^2$$

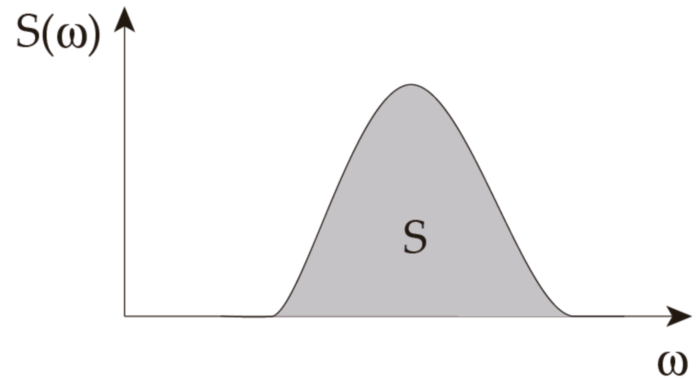

$$\overline{\omega} = \frac{m_1}{m_0} = \frac{\int_0^{\infty} S(\omega)\omega\, d\omega}{\int_0^{\infty} S(\omega)d\omega} = \frac{\sum_k \left|\langle k|F|0\rangle\right|^2 \omega_k}{\sum_k \left|\langle k|F|0\rangle\right|^2}$$

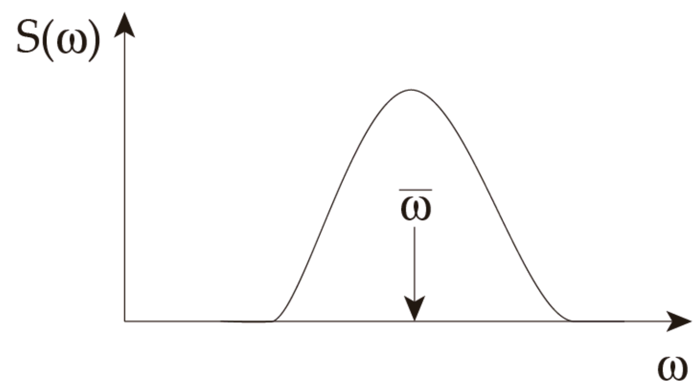

$$\sigma^2 = \frac{m_2}{m_0} - \left(\frac{m_1}{m_0}\right)^2 = \frac{\int_0^{\infty} S(\omega)\omega^2 d\omega}{\int_0^{\infty} S(\omega)d\omega} - \left(\frac{\int_0^{\infty} S(\omega)\omega d\omega}{\int_0^{\infty} S(\omega)d\omega}\right)^2$$

$$= \frac{\int_0^{\infty} S(\omega)(\omega - \overline{\omega})^2 d\omega}{\int_0^{\infty} S(\omega)d\omega}$$

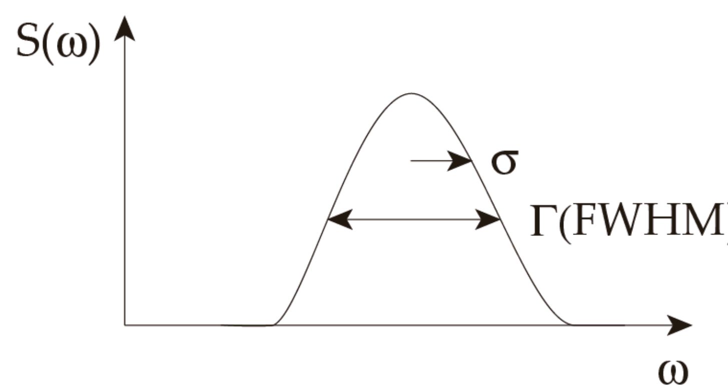

参考文献[8]

全ての励起状態に関する積算値は、
対応するオペレータの
基底状態の期待値を表す。

$$F : Hermitian$$

$$F = F^{\dagger}$$

$$
\begin{aligned}
m_p \equiv \int_0^{\infty} S(\omega)\omega^p d\omega &= \sum_k \left|\langle k|F|0\rangle\right|^2 \omega_k^p \\
&= \sum_k \langle 0|F|k\rangle\langle k|F|0\rangle\omega_k^p \\
&= \langle 0|F\left(\sum_k |k\rangle\langle k|\right)\omega_k^p F|0\rangle \\
&= \langle 0|F(H-E_0)^p F|0\rangle
\end{aligned}
$$

励起状態を全て調べると基底状態の性質が分かる。

参考文献[8]

対応するオペレータは、ハミルトニアンHとの（反）交換関係で表すことができる（ことがある）。

$$m_0 = \frac{1}{2}\langle 0|F^2|0\rangle$$

$$m_1 = \frac{1}{2}\langle 0|[F,[H,F]]|0\rangle$$

$$m_2 = \frac{1}{2}\langle 0|\{[F,H],[H,F]\}|0\rangle$$

$$m_3 = \frac{1}{2}\langle 0|[[F,H],[H,[H,F]]]|0\rangle$$

導出例：

$$\begin{aligned} m_1 &= \frac{1}{2}\langle 0|[F,[H,F]]|0\rangle \\ &= \frac{1}{2}\langle 0|[F,HF-FH]|0\rangle \\ &= \frac{1}{2}\langle 0|FHF-F^2H-HF^2+FHF]|0\rangle \\ &= \frac{1}{2}\langle 0|2FHF-F^2E_0-E_0F^2]|0\rangle \\ &= \langle 0|F(H-E_0)^{1}F|0\rangle \end{aligned}$$

参考文献[8]

Dipole Polarizability

Static Dipole Polarizability
Electric Dipole Polarizability
双極子分極能

E1励起強度に対するm_{-1}和則に対応

参考文献[8]

Dipole Polarizability

$$\alpha_D \equiv \sum_k \frac{\left|\langle k | D | 0 \rangle\right|^2}{\omega_k}$$

Dipole Polarizability

$$D \equiv \frac{1}{2} \sum_{k=1}^{A} \tau_{3,k} r_k Y_{10}(\hat{r}_k)$$

Electric Dipole Operator

$\frac{1}{2}\sum(1-\tau_3) r Y_{10}$ から重心移動項を除いて符号反転したもの

$$\alpha_D = m_{-1} = \frac{1}{2} \langle 0 | [[X^\dagger, H], X] | 0 \rangle$$

X: solution of $[H, X] = D$

参考文献[8]

Dipole Polarizability

Dipole Polarizability は、外部電場に対する誘電分極に対応する。

E1 Field（振動電場）

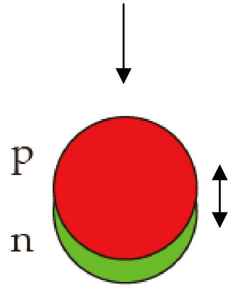

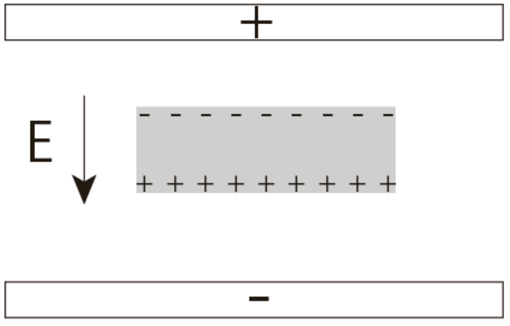

E1 response of a nucleus

誘電分極

E1励起強度と和則

A. Migdal (1944)

1-(および2+)の平均励起エネルギーを和則により求めようとした。

$$\overline{\omega}^{E1} \equiv \sqrt{\frac{m_1^{E1}}{m_{-1}^{E1}}}$$

$$m_1^{E1} \equiv \sum_k \left| \left\langle k \middle| D \middle| 0 \right\rangle \right|^2 \omega_k$$

$$m_{-1}^{E1} \equiv \sum_k \frac{\left| \left\langle k \middle| D \middle| 0 \right\rangle \right|^2}{\omega_k}$$

参考文献[5]

E1励起強度と和則

1次のモーメント

$$m_1^{E1} = \frac{1}{2} \langle 0 | [D,[H,D]] | 0 \rangle$$

$$H = \sum_{k=1}^{A} \frac{p_k^2}{2M} + V(r_1, r_2, \ldots, r_A)$$

$$[D,V] = 0$$

$$m_1^{E1} = \frac{3A}{32\pi M}$$

Thomas-Reich-Kuhn (TRK) Sum-Rule

参考文献[5]

E1励起強度と和則

-1次のモーメント

原子核を外場 H_{ext} = D の中に置く。全系のハミルトニアンHは

$$H = H_0 + D$$

無摂動のハミルトニアンH_0に対する波動関数をΦ_0と置くと、Hに対する波動関数Φは1次の摂動で、

$$\Phi = \Phi_0 - \sum_n \frac{\langle n|D|0\rangle}{E_n - E_0}|n\rangle$$

これを用いるとDの期待値は、2次の項を無視して

$$\langle\Phi|D|\Phi\rangle = -2\sum_n \frac{|\langle n|D|0\rangle|^2}{E_n - E_0} = -2m_{-1}^{E1}$$

左辺は、E1外場中での陽子と中性子の密度分布差で記述でき

$$\langle\Phi|D|\Phi\rangle = -\frac{1}{2}\int\left(\rho_n(r) - \rho_p(r)\right)rY_{10}d\mathbf{r}$$

参考文献[5]

E1励起強度と和則

-1次のモーメント

$$m_{-1}^{E1} = \frac{1}{4}\int \left(\rho_n(r) - \rho_p(r)\right) r Y_{10} d\mathbf{r}$$

Weizsaecker-Bete の質量公式

$$E_0 = AM + \alpha A + \gamma A^{2/3} + \beta \frac{(N-Z)^2}{A} + \frac{3}{5}\frac{Z^2 e^2}{R_c}$$

の対称エネルギー(Symmetry Energy)項 β と関連付ける。

Migdalは、pとnの分布を同じ半径Rの球とし、外場中での平衡状態のエネルギーを最低とする変分条件から、1次のモーメントを求めた

$$m_{-1}^{E1} = \frac{3AR^2}{320\pi\beta}$$

$$\frac{3}{5}R^2 = \frac{1}{A}\int r^2(\rho_n + \rho_p) d\mathbf{r}$$:平均自乗半径

m.s. radius

$$\overline{\omega}^{E1} \equiv \sqrt{\frac{m_1^{E1}}{m_{-1}^{E1}}} = \frac{1}{R}\sqrt{\frac{10\beta}{M}} \approx 85A^{-1/3}\ (\mathrm{MeV})$$ **核全体の効果(Volume)**

参考文献[5]

E1励起強度と和則

Goldhaber-Teller(1948)

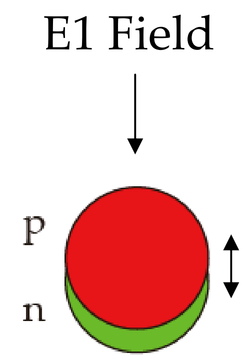

原子核を陽子と中性子からなる非圧縮性の流体とし、E1励起状態は陽子と中性子の流体が逆位相に振動する状態であるとし、調和振動しとして近似した。

$$H = \frac{1}{2B}\Pi_{\nu}^{2} + \frac{C}{2}\nu^{2}$$

Bは陽子流体と中性子流体の換算質量でN=Zの場合B=AM/4。

Cは復元力で表面積$4\pi R^2$に比例すると考えられる。

E1の平均励起エネルギーは、

$$\overline{\omega}^{E1} \equiv \sqrt{\frac{C}{B}} \propto \sqrt{\frac{R^2}{A}} \propto A^{-1/6}$$

核表面の効果(Surface)

参考文献[5]

参考文献[5]

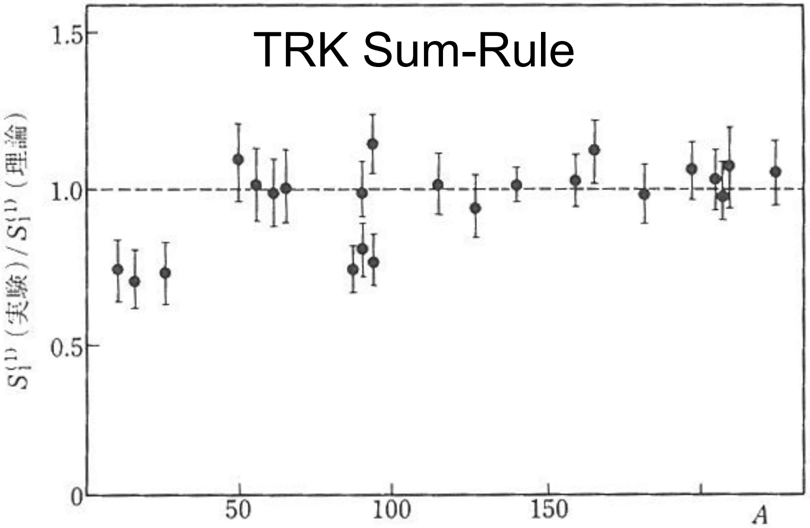

図 3.1　1⁻ 状態励起に対する和則値の理論値と実験値の比[8)] 実験値は励起エネルギー30 MeV までの和．A は原子核の質量数

参考文献[5]

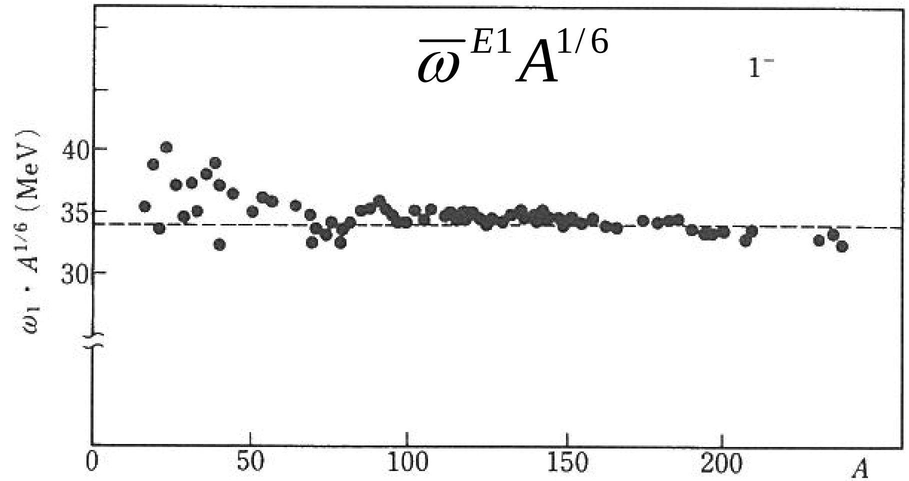

図 3.3　1⁻ 巨大共鳴状態のエネルギー ω_1 の質量数(A)依存[9)](実験値(●)は $\omega_1 = 34/A^{1/6}$(MeV)でよく再現される)

参考文献[6]

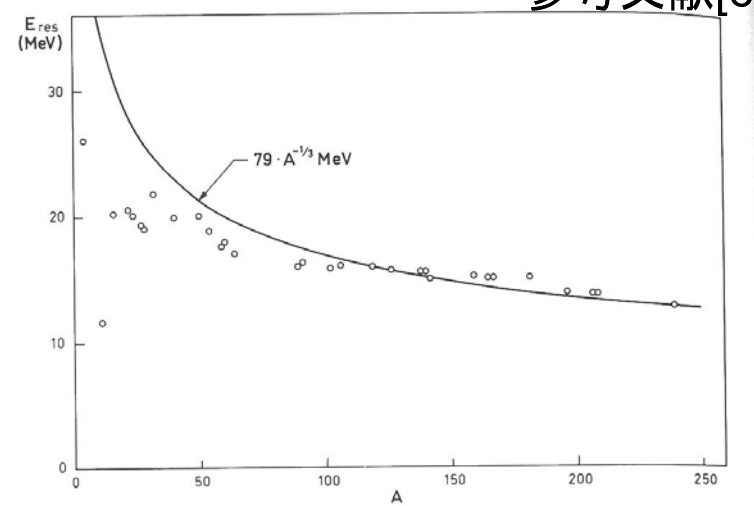

Figure 6-19 Systematics of dipole resonance frequency. The experimental data are taken from the review article by E. Hayward (*Nuclear Structure and Electromagnetic Interactions*, p. 141, ed. N. MacDonald, Oliver and Boyd, Edinburgh and London, 1965), except for ^{4}He, for which the resonance frequency is that given in the survey article by W. E. Meyerhof and T. A. Tombrello, *Nuclear Phys.* **A109**, 1 (1968). In the case of the deformed nuclei, which exhibit two resonance maxima, the energy represents a weighted mean of the two resonance energies. The solid curve represents the estimate based on the liquid-drop model (see Eq. (6A-65)).

Symmetry Energy に、**Volumeの効果とSurfaceの効果を両方とりいれる必要**がある。

Surface効果には中性子スキンが大きく寄与する。

Hydro-dynamical Approach

- E. Lipparini and s. Stringari, Phys. Lett. 112B, 421 (1982).

$$E_{sym} = \frac{1}{2}\frac{(N-Z)^2}{A^2}(b_{vol} - b_{surf}A^{-1/3})$$

$$\alpha_D = \alpha_D^M\left(1 + \frac{5}{3}\frac{b_{surf}}{b_{vol}}A^{-1/3}\right)$$

$$\alpha_D^M = \frac{1}{12}\frac{A\langle r^2\rangle}{b_{vol}}$$

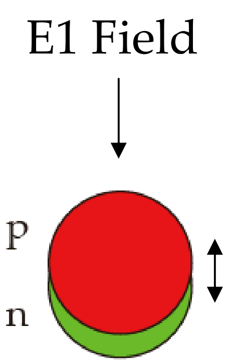

Symmetry Energy に、**Volumeの効果とSurfaceの効果を両方とりいれる必要**がある。

Surface効果には中性子スキンが大きく寄与する。

$$\alpha_{\mathrm{D}} \equiv \frac{\sigma_{-2}}{2\pi^2} \cdot \frac{\hbar c}{e^2} = \sum \frac{\sigma_{\mathrm{abs}}(E_x)}{E_x^2} \cdot \frac{\hbar c}{2\pi^2 e^2}$$

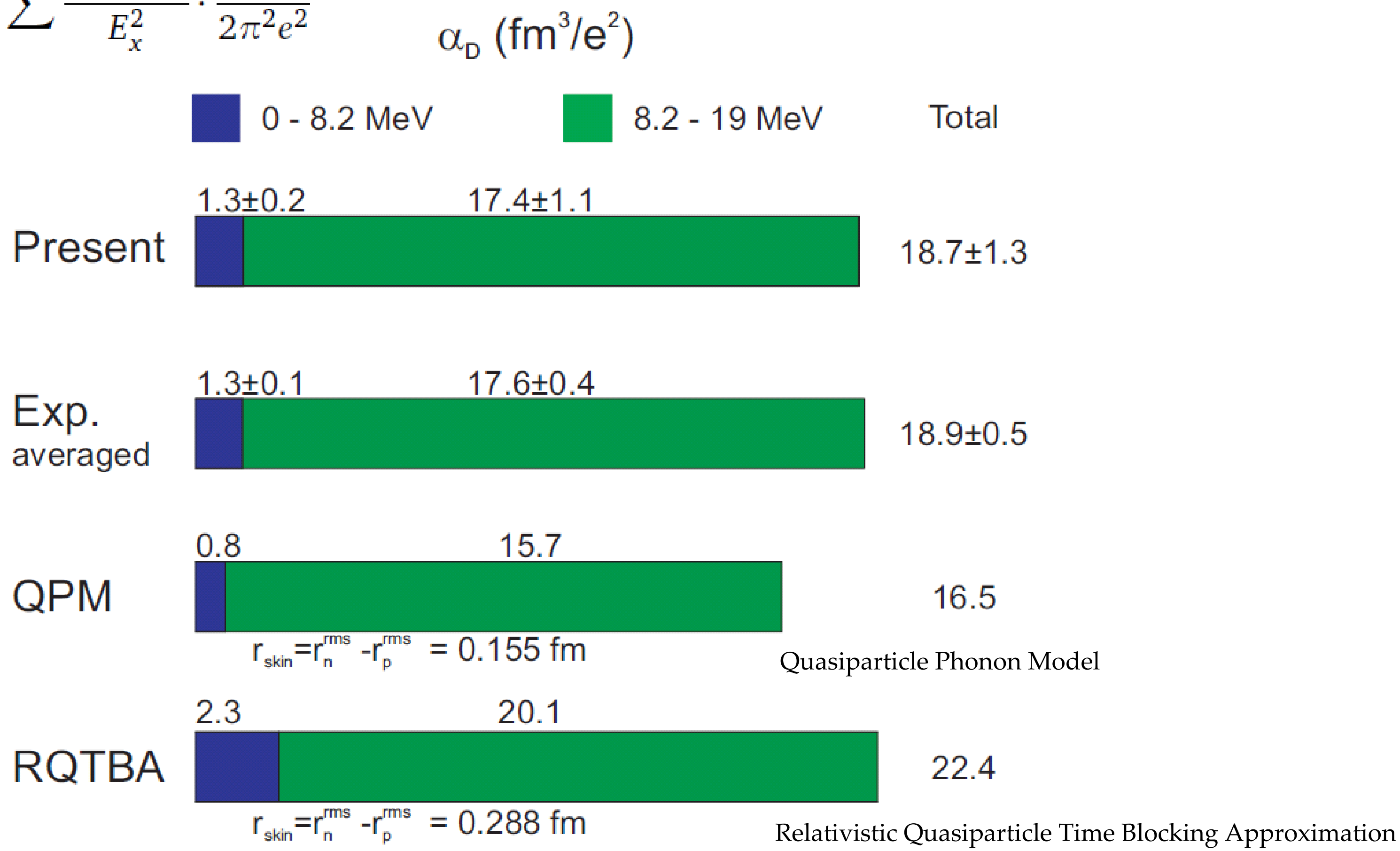

Fig. 5.13: Static dipole polarizability of ^{208}Pb. From top to bottom: α_D extracted in the present thesis; average value for α_D from the available experimental data (see text for details); polarizability and neutron skin radius extracted from the QPM calculations. Bottom: the same for RQTBA predictions. All numerical values for α_D are given in the fm^3/e^2 units. Blue bars correspond to the dipole polarizability in the pygmy dipole resonance region, green ones to the giant resonance region, from 8.2 MeV to 19 MeV.

I. Poltoratska, PhD thesis

P.-G. Reinhard and W. Nazarewicz, Phys. Rev. C 81, 051303(R) (2010).

Self-Consistent Mean Field Theory

平均場計算の入力として用いる軌道(Single Particle Orbit)と、
計算によって得られた平均場の作る軌道がConsistentである
平均場計算

(Nuclear) Energy Density Functional Theory: エネルギー密度汎関数理論

原子核の全ての物理量を、エネルギー密度分布関数の関数として
記述しようとする理論的試み。

Skyrm Force

主に重い原子核を中心として、原子核の平均場的性質をうまく記述
する核内有効相互作用を、使いやすい形にパラメータ化して現象論
的に決めたもの。
δ 型の相互作用で密度依存性があり、2体力と3体力を含む。
数多くの種類がある。

$$\alpha_D = \frac{\hbar c}{2\pi^2 e^2} \int \frac{\sigma_{abs}}{\omega^2}\, d\omega,$$

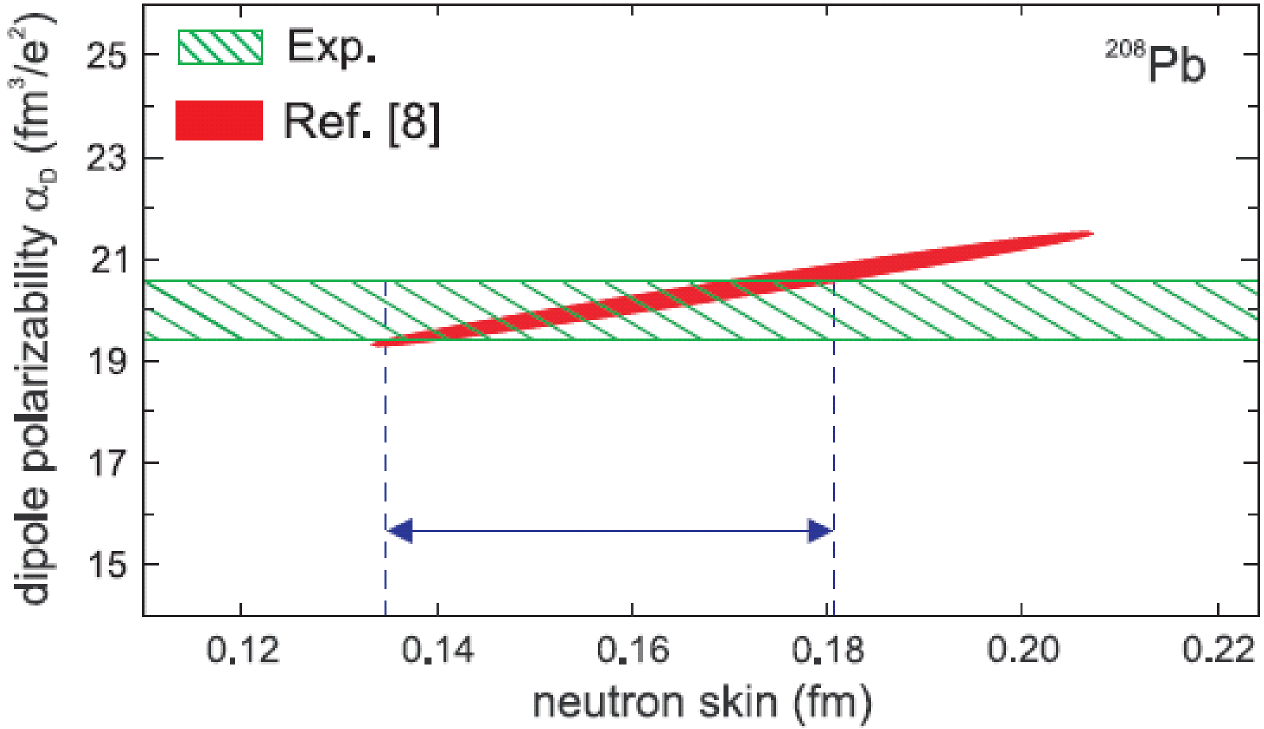

FIG. 5: (Color online) Extraction of the neutron skin in ^{208}Pb based on the correlation between $r_{\rm skin}$ and the dipole polarizability α_D established in Ref. [8].

[8] P.-G. Reinhard and W. Nazarewicz, PRC81, 051303(R) (2010).

submitted

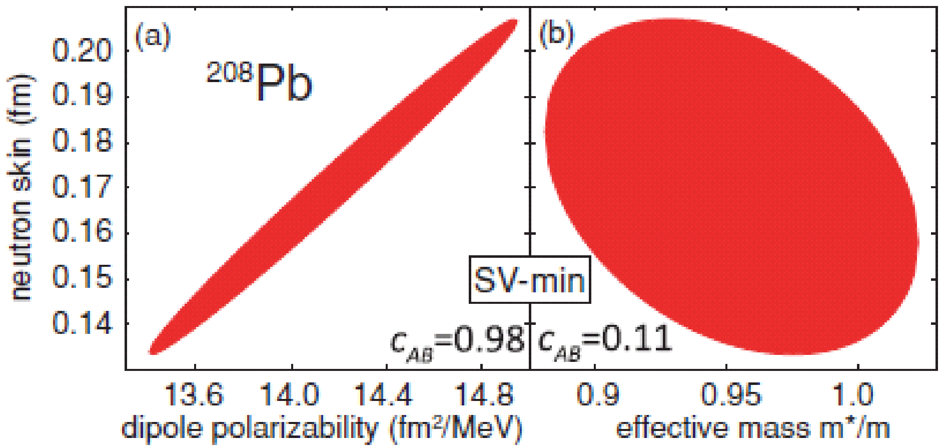

FIG. 1. (Color online) The covariance ellipsoids for two pairs of observables as indicated. The filled area shows the region of reasonable domain **p**. (Left) Neutron skin and isovector dipole polarizability in ^{208}Pb. (Right) Neutron skin in ^{208}Pb and effective nucleon mass m^*/m in symmetric nuclear matter.

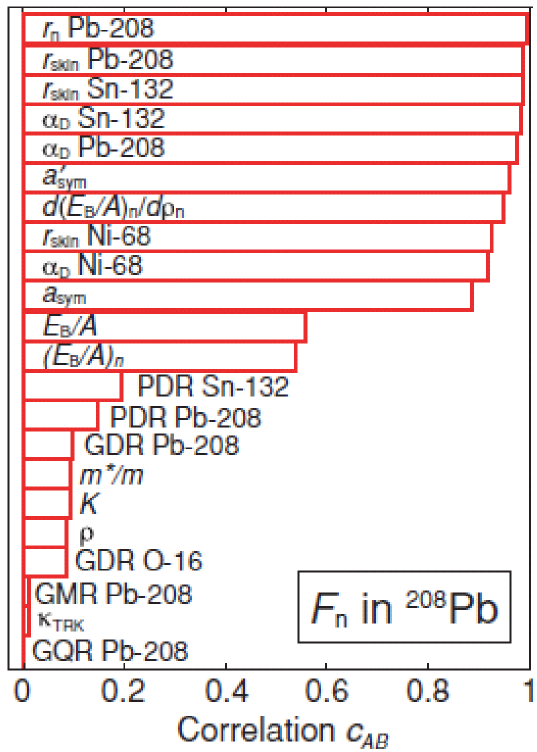

FIG. 2. (Color online) Correlation (6) of various observables with the neutron form factor F_n ($q = 0.45$ fm^{-1}) in ^{208}Pb.

P.-G. Reinhard and W. Nazarewicz,
Phys. Rev. C 81, 051303(R) (2010).

TABLE VI. Obtained values of r_n, r_p, and Δr_{np} for ^{208}Pb compared with several experimental and theoretical results (all in fm). Except for this work, the errors are statistical only.

	Model					Experiment					
	SkM*	SkX	NL3	DD-ME2	FSUGold	GDR[a]	PDR[b]	antiproton[c]	(p, p) at 800 MeV[d]	(p, p) at 650 MeV[e]	This work
r_p	5.45	5.44	5.46	–	–	–	–	5.44	5.45	5.46	5.442(2)
r_n	5.62	5.60	5.74	–	–	–	–	5.60	5.59(4)	5.66(4)	$5.653^{+0.054}_{-0.063}$
Δr_{np}	0.17	0.16	0.28	0.19	0.21	0.19(9)	0.18(4)	0.16(2)	0.14(4)	0.20(4)	$0.211^{+0.054}_{-0.063}$

[a]The isovector giant dipole resonance (GDR) from ^{208}Pb(α, α') at $E_\alpha = 120$ MeV [12].
[b]The measurement of "pigmy" dipole resonance (PDR) strength from ^{208}Pb(γ, γ') [19].
[c]The analysis of the x-ray cascade from antiprotonic atoms assuming two-parameter-Fermi distribution for both ρ_p and ρ_n [18].
[d]Ref. [9].
[e]Ref. [13].

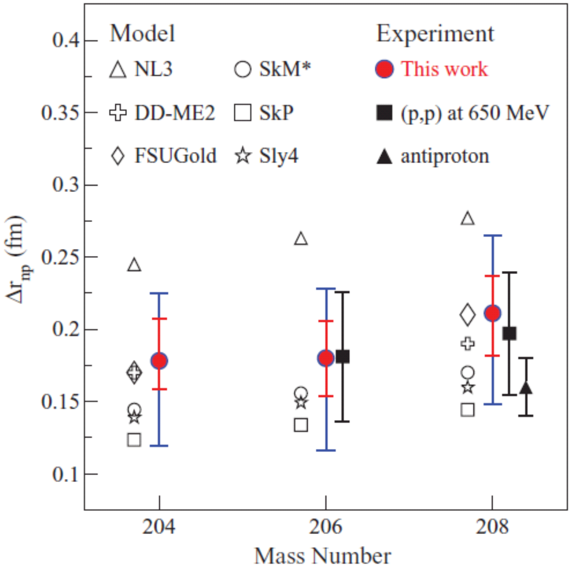

FIG. 8. (Color online) Systematic behavior of the neutron skin thicknesses for ^{204,206,208}Pb. The filled circles are the results of this work with the two types of error bars. The filled squares and triangle are from the analysis of proton elastic scattering at 650 MeV [13] and x rays from antiprotonic atoms [18], respectively, with statistical errors only. The open triangles, crosses, and diamonds show the calculations of relativistic mean-field models with NL3 [45], DD-ME2 [46], and FSUGold [47] parametrization and the open circles, squares, and stars are from nonrelativistic mean-field models with SkM* [43], SkP [44], and Sly4 [48] parametrization.

proton elastic scattering

J. Zenihiro et al., PRC82, 044611 (2010).

spin-M1 Strength Distribution in ^{208}Pb

Extraction of spin-M1 strengh (B(σ))

After making extrapolation to q=0, with a help of DWBA calc.

M. Sasano et al., PRC79, 024602(2009).

Gamow-Teller unit cross section of (p,n) reactions at 297 MeV,

extrapolated to A=208:

$$\hat{\sigma}_{\mathrm{GT}}(A=208)=1.9\,\mathrm{mb/sr}$$

Converted to B(σ) unit cross section of (p,p') reactions for A=208.

$$\hat{\sigma}_{\sigma}(A=208)=0.72\,\mathrm{mb/sr}/\mu_{\mathrm{N}}^{2}$$

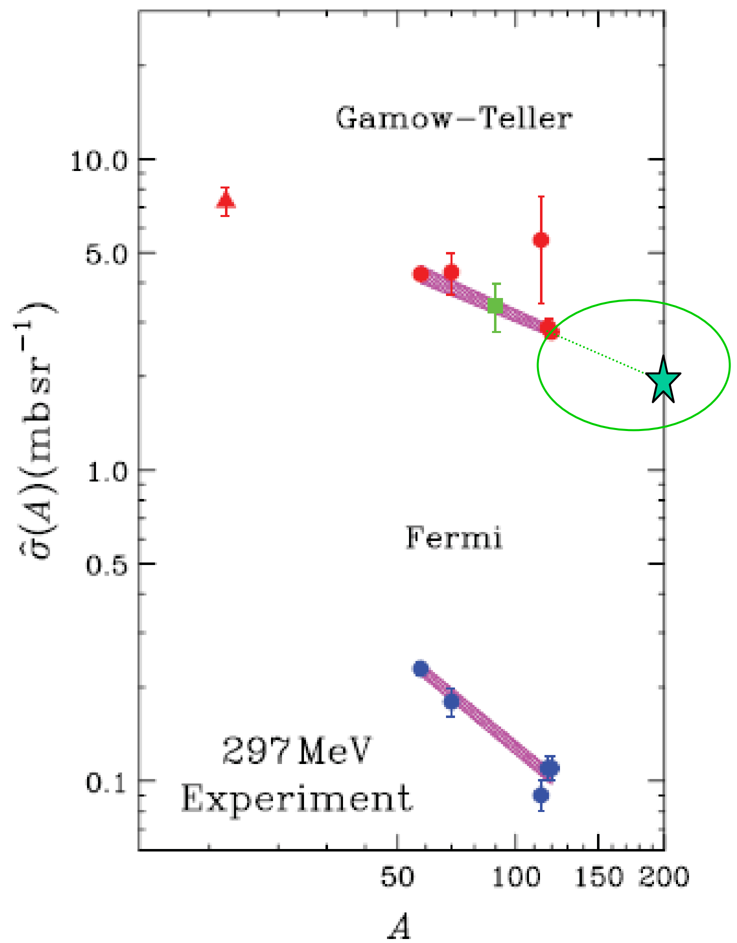

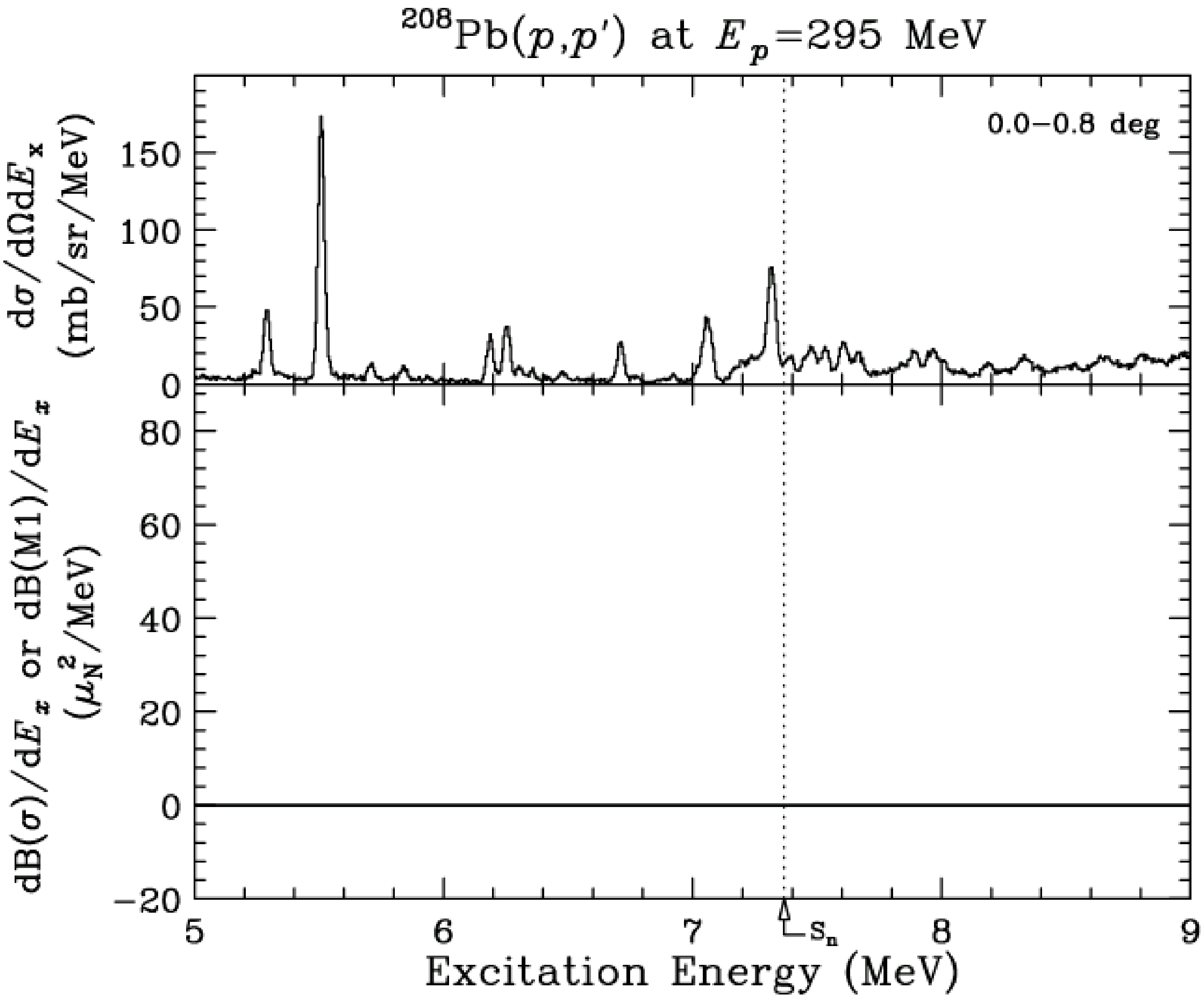

^{208}Pb(p,p') at E_p=295 MeV
0.0–0.8 deg
dσ/dΩdE_x (mb/sr/MeV)
dB(σ)/dE_x or dB(M1)/dE_x (μ_N^2/MeV)
150
100
50
0
80
60
40
20
0
−20
5
6
7
8
9
S_n
Excitation Energy (MeV)

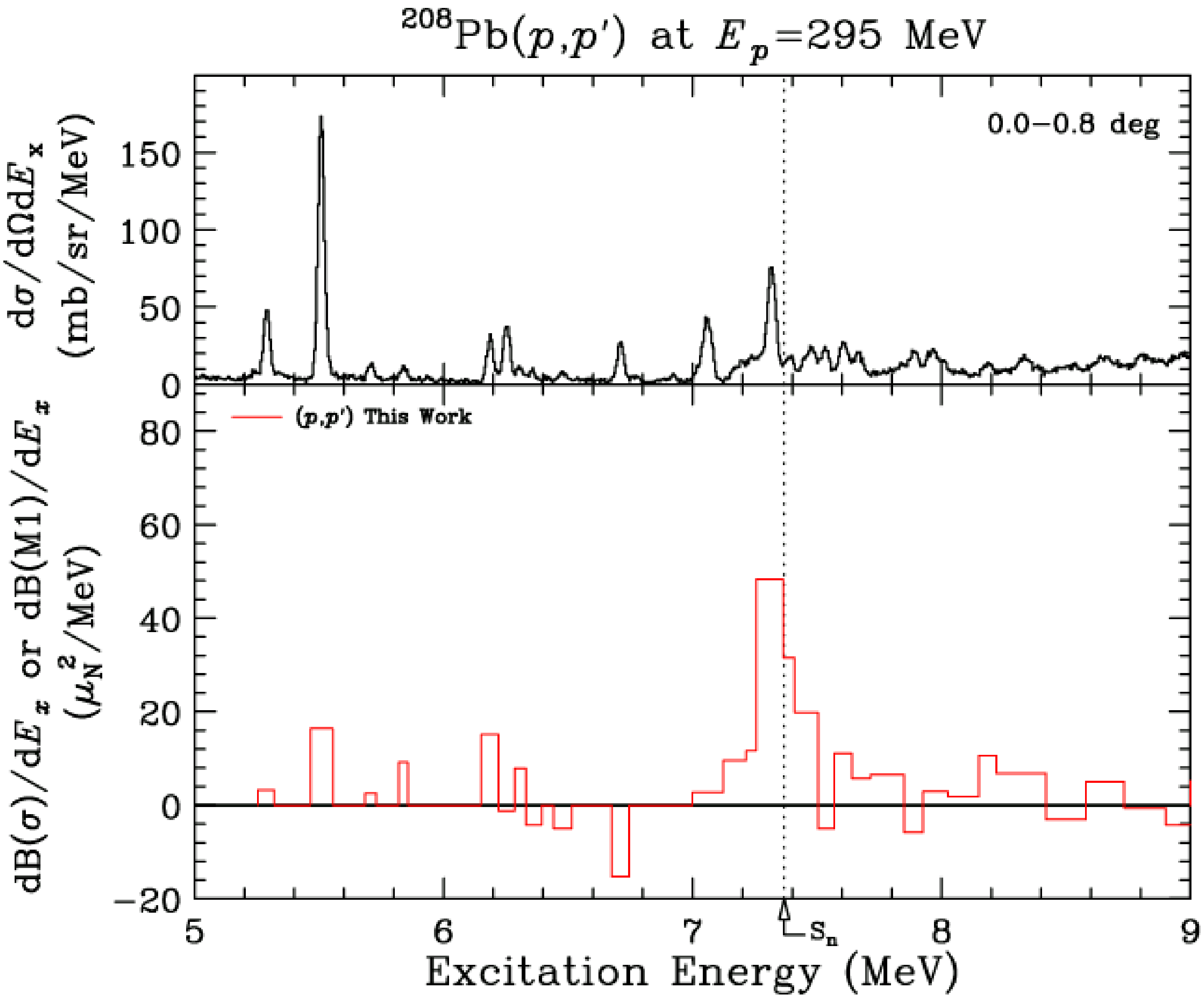

^{208}Pb(p,p') at E_p=295 MeV
0.0–0.8 deg
dσ/dΩdE$_x$ (mb/sr/MeV)
150
100
50
0
(p,p') This Work
dB(σ)/dE$_x$ or dB(M1)/dE$_x$ (μ_N^2/MeV)
80
60
40
20
0
−20
5
6
7
8
9
S$_n$
Excitation Energy (MeV)

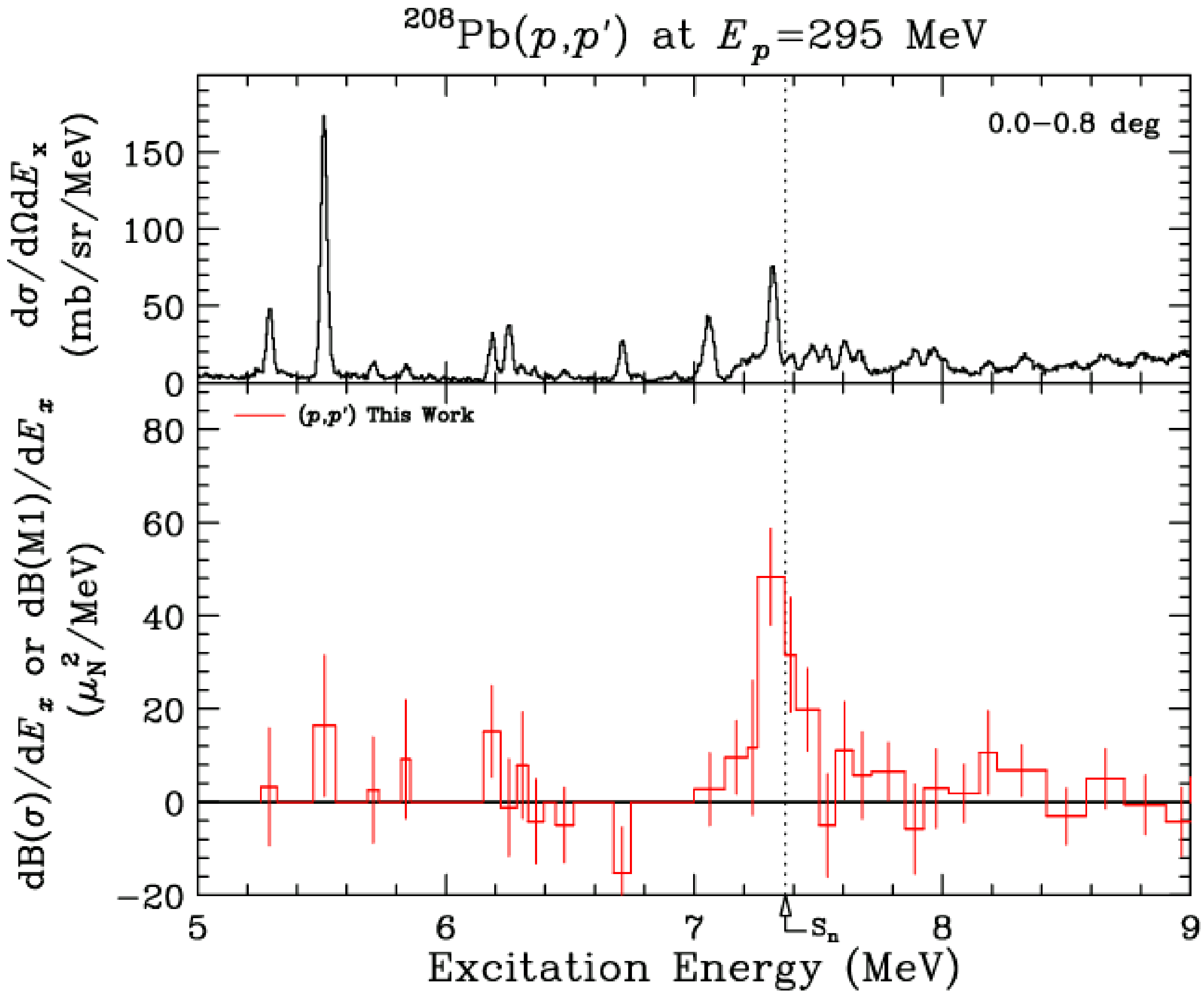

^{208}Pb(p,p') at E_p=295 MeV
0.0−0.8 deg
$d\sigma/d\Omega dE_x$ (mb/sr/MeV)
(p,p') This Work
$dB(\sigma)/dE_x$ or dB(M1)/dE_x (μ_N^2/MeV)
S_n
Excitation Energy (MeV)

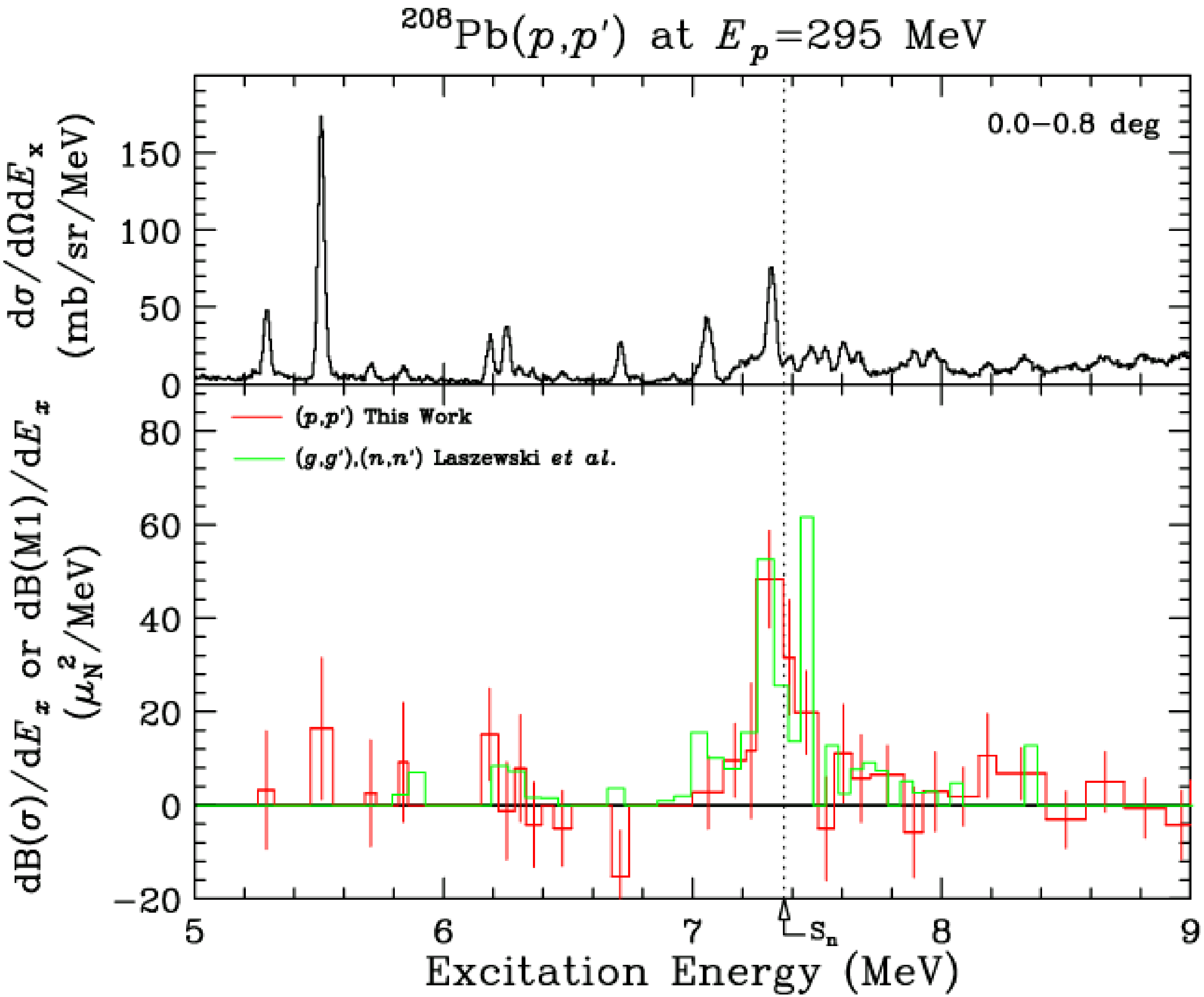

^{208}Pb(p,p') at E_p=295 MeV
0.0–0.8 deg
dσ/dΩdE_x (mb/sr/MeV)
150
100
50
0
(p,p') This Work
(g,g'),(n,n') Laszewski et al.
dB(σ)/dE_x or dB(M1)/dE_x (μ_N^2/MeV)
80
60
40
20
0
−20
5
6
7
8
9
S_n
Excitation Energy (MeV)

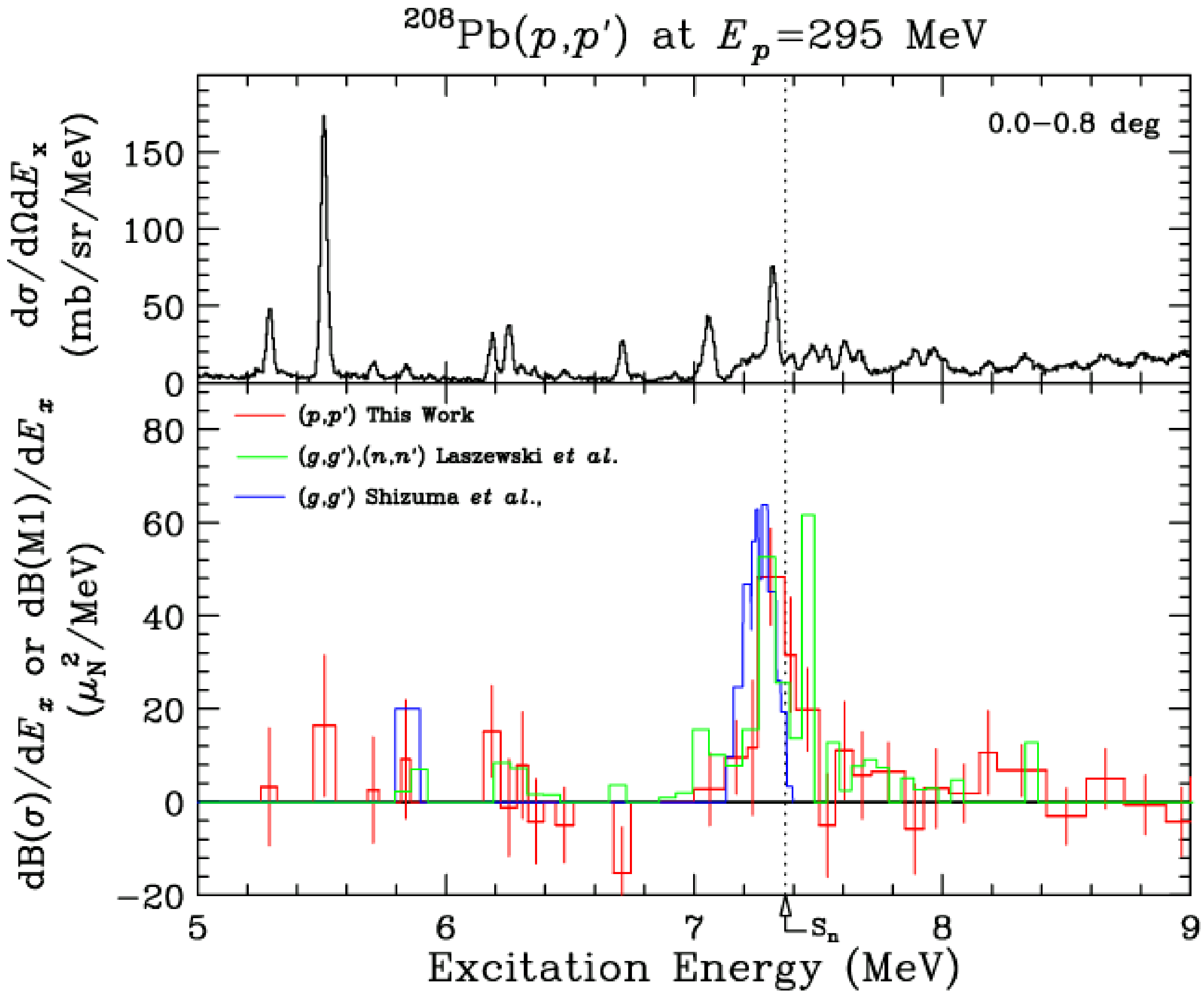

^{208}Pb(p,p') at E_p=295 MeV
0.0–0.8 deg
dσ/dΩdE_x (mb/sr/MeV)
(p,p') This Work
(g,g'),(n,n') Laszewski et al.
(g,g') Shizuma et al.,
dB(σ)/dE_x or dB(M1)/dE_x (μ_N^2/MeV)
S_n
Excitation Energy (MeV)

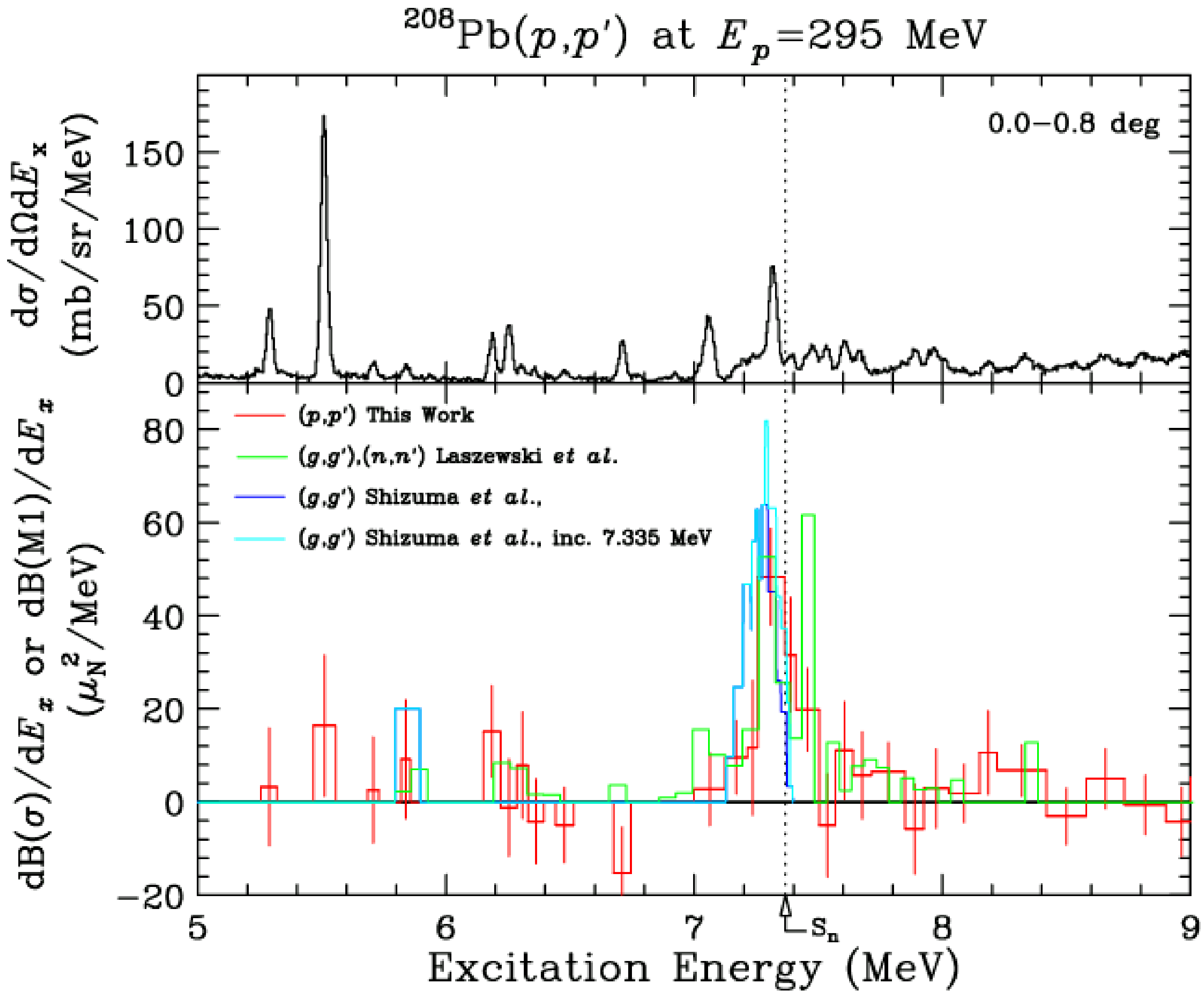

^{208}Pb(p,p') at E_p=295 MeV
0.0−0.8 deg
dσ/dΩdE_x (mb/sr/MeV)
150
100
50
0
(p,p') This Work
(g,g'),(n,n') Laszewski et al.
(g,g') Shizuma et al.,
(g,g') Shizuma et al., inc. 7.335 MeV
dB(σ)/dE_x or dB(M1)/dE_x (μ_N^2/MeV)
80
60
40
20
0
−20
5
6
7
8
9
S_n
Excitation Energy (MeV)

Preliminary

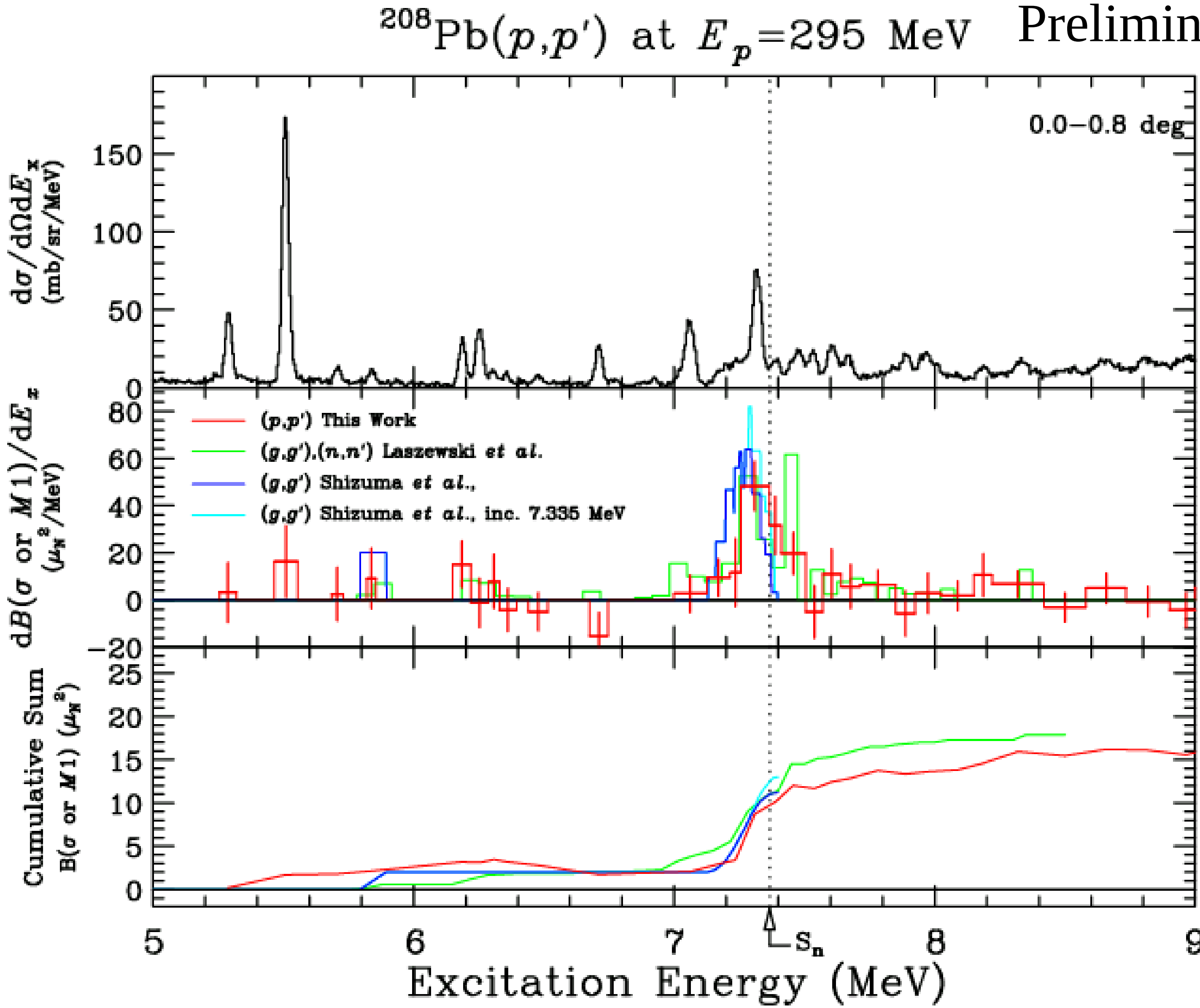

$15\,\mu_N^2$

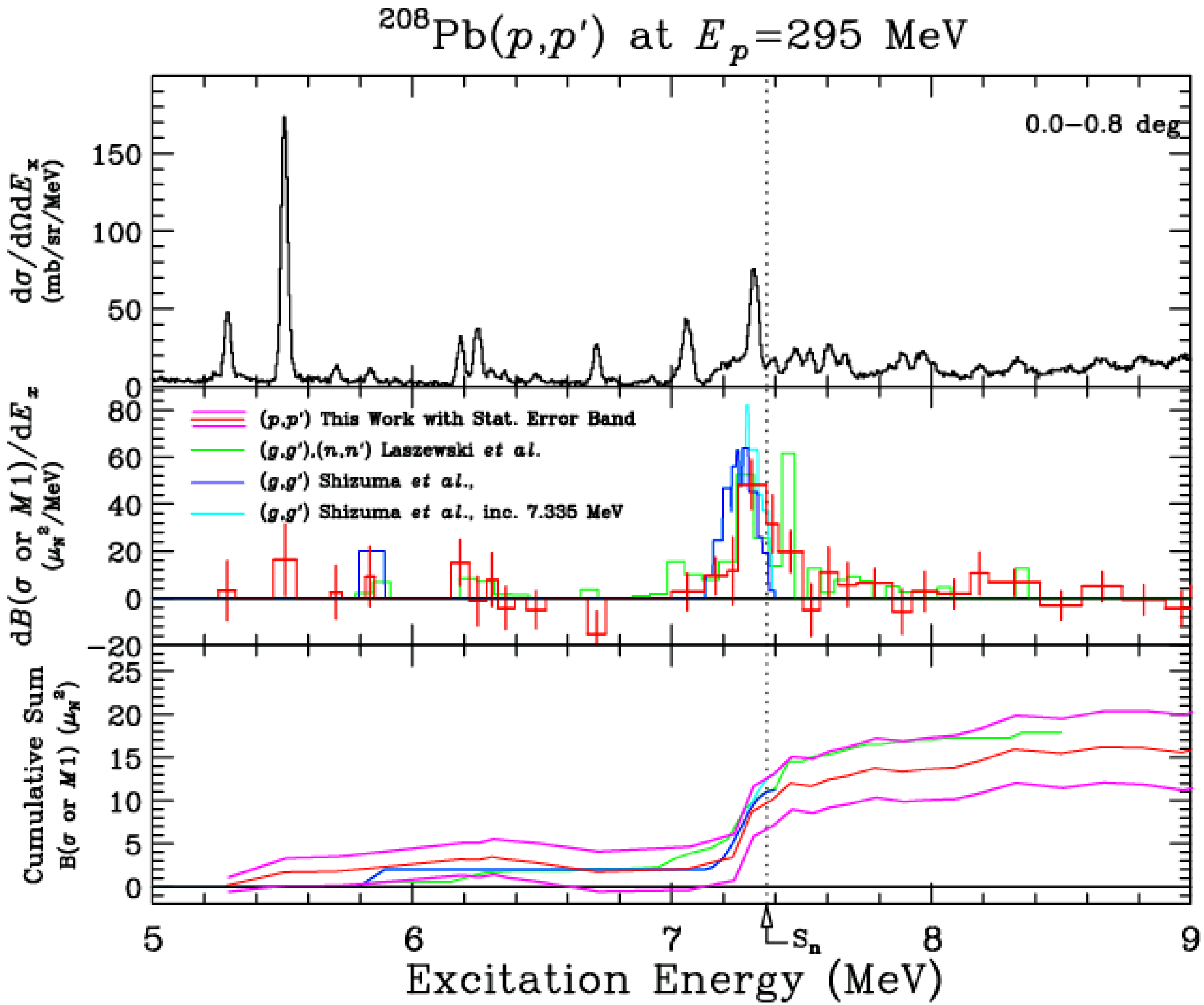

^{208}Pb(p,p') at E_p=295 MeV
0.0–0.8 deg
dσ/dΩdE_x (mb/sr/MeV)
dB(σ or M1)/dE_x (μ_N^2/MeV)
(p,p') This Work with Stat. Error Band
(g,g'),(n,n') Laszewski et al.
(g,g') Shizuma et al.,
(g,g') Shizuma et al., inc. 7.335 MeV
Cumulative Sum B(σ or M1) (μ_N^2)
S_n
Excitation Energy (MeV)

^{120}Sn

Very Preliminary

P. von Neumann-Cosel,
A. T. et al.,

^{120}Sn(p,p’) at 295 MeV, θ=0-0.8°

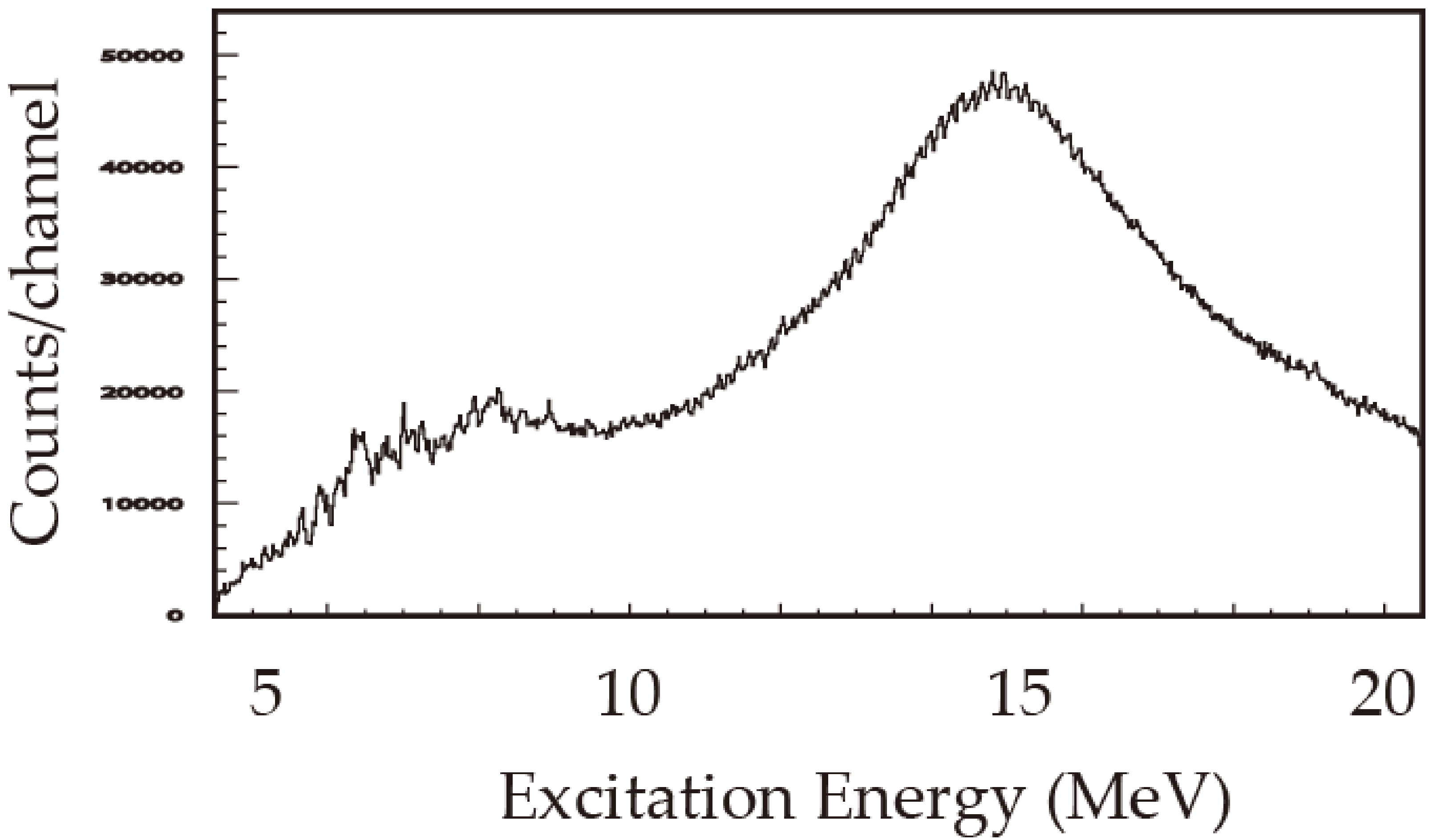

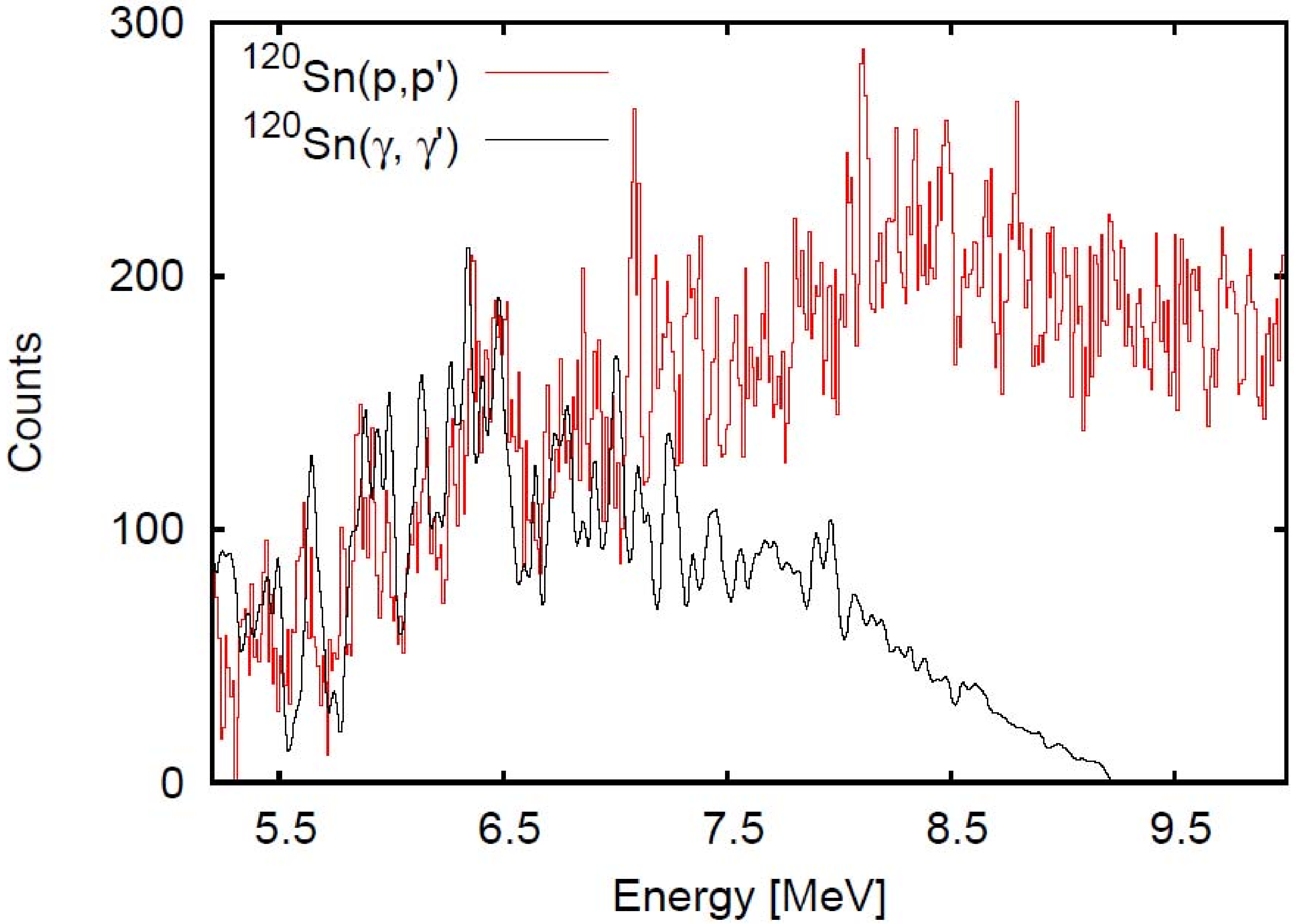

Figure 4.6: Comparison of the excitation energy spectra with (γ,γ') experiment.

A.M. Heilmann, master thesis

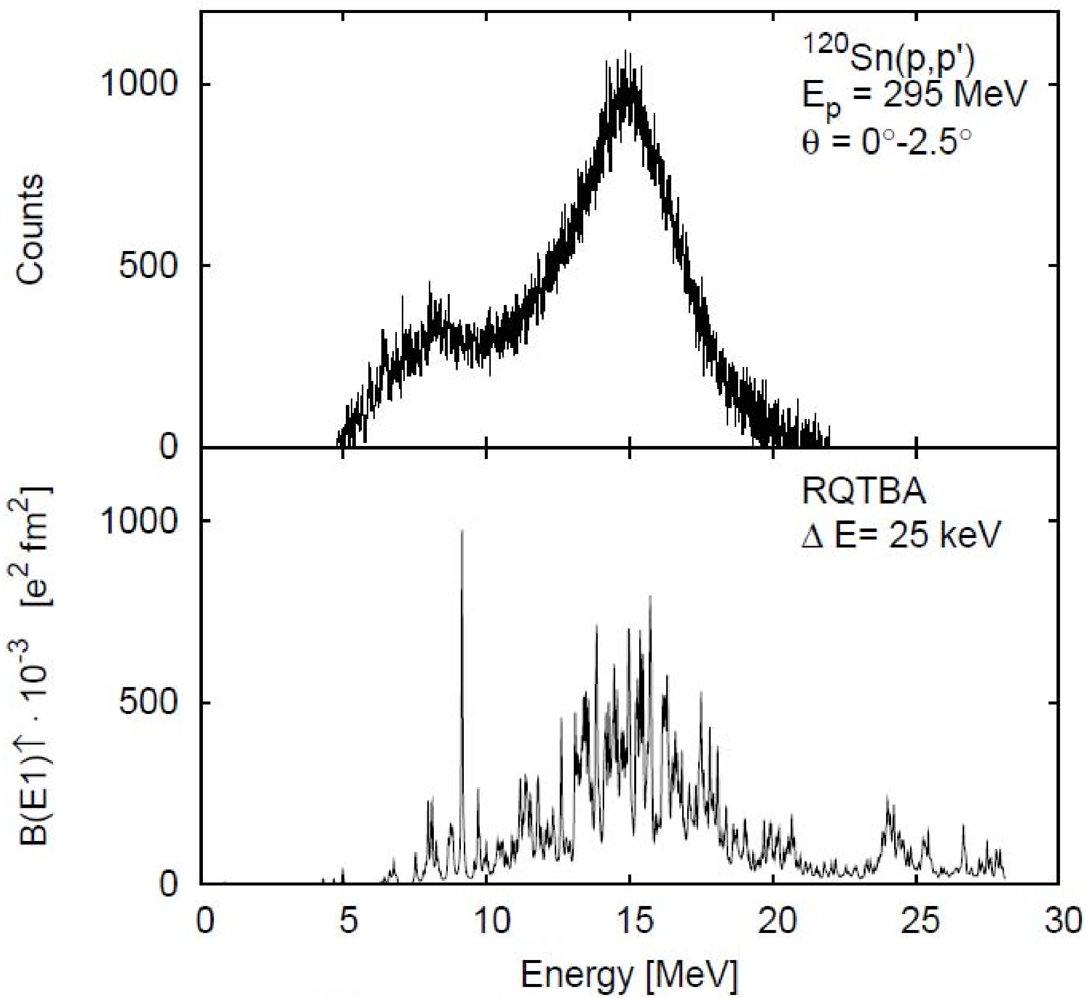

Figure 4.7: Comparision of the ^{120}Sn$(\vec{p},\vec{p}')$ excitation spectrum with RQTBA calculations.

A.M. Heilmann, master thesis

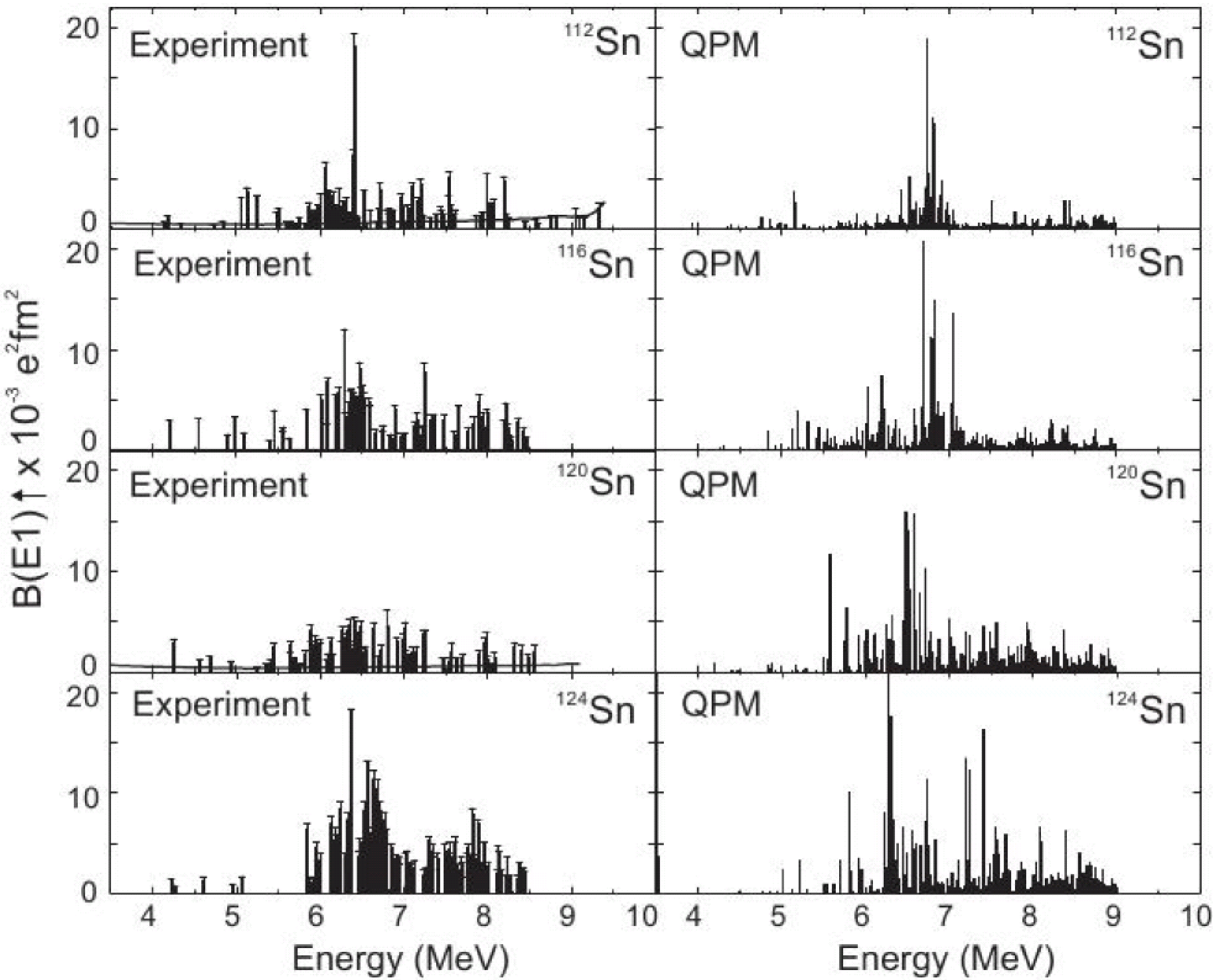

A.M. Heilmann, master thesis

^{154}Sm

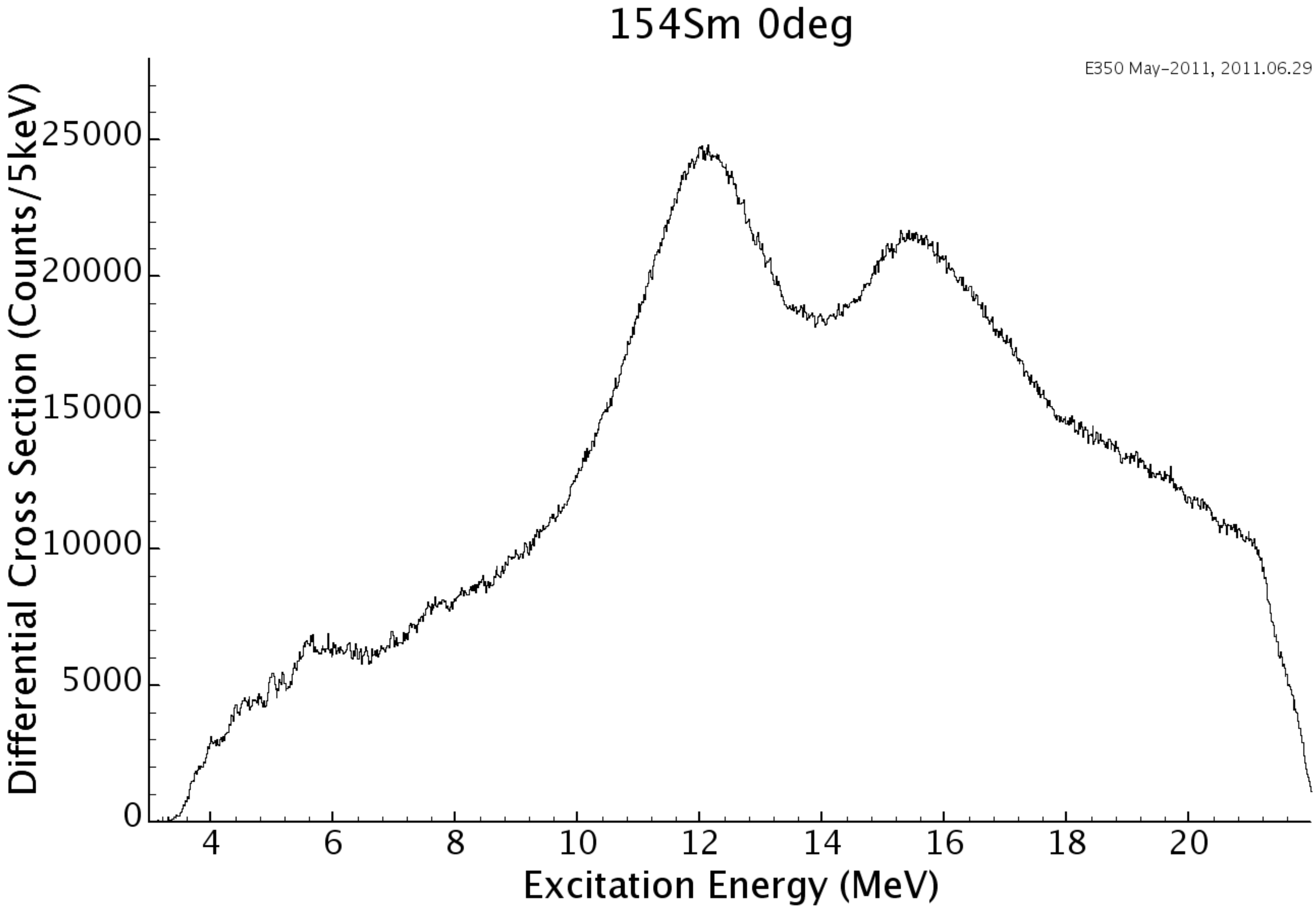
154Sm 0deg
E350 May-2011, 2011.06.29
Differential Cross Section (Counts/5keV)
0
5000
10000
15000
20000
25000
4
6
8
10
12
14
16
18
20
Excitation Energy (MeV)

^{154}Sm spin-M1 Resonance?

E350, June 2011

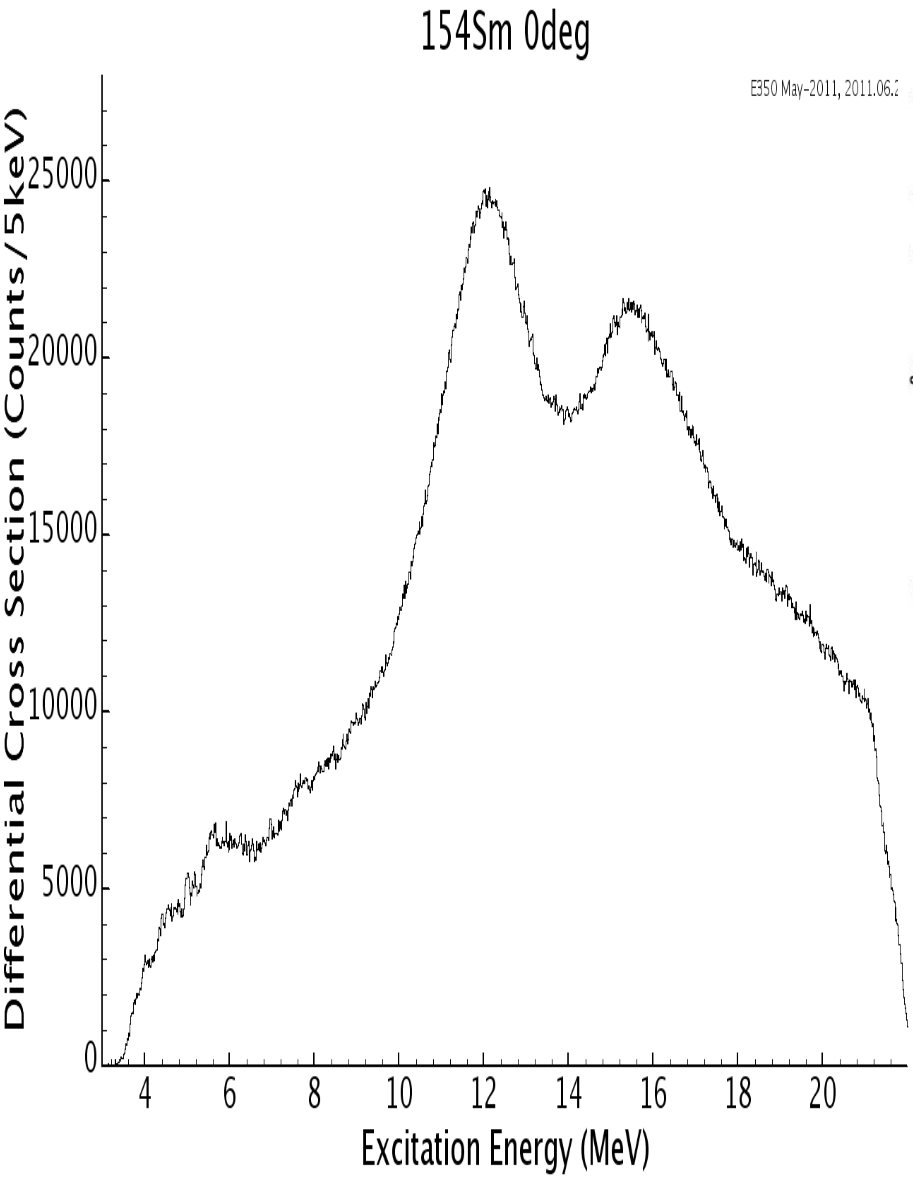

H. Woertche, D. Frekers et al.,

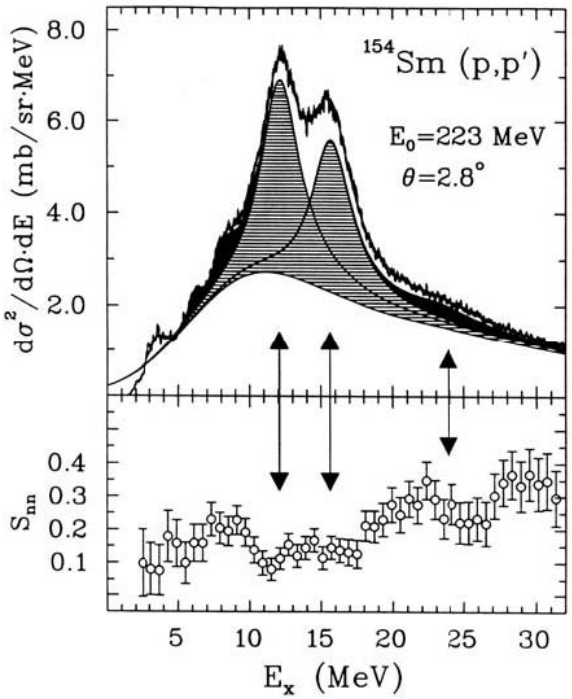

D. Frekers et al, PLB244, 178(1990).

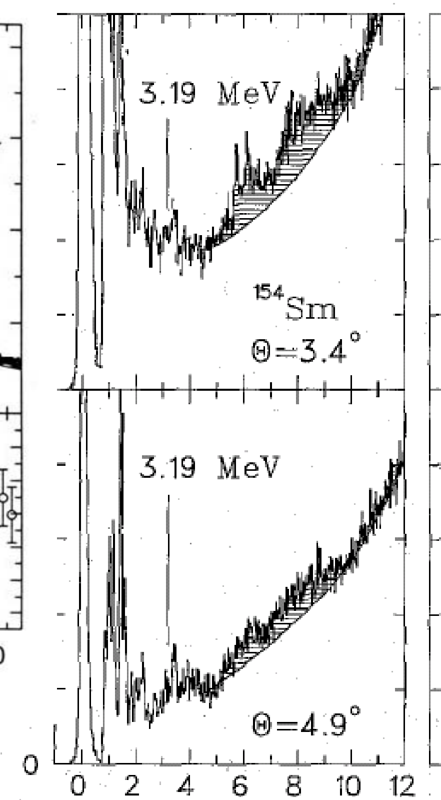

Fig. 1. Proton spectra taken at 200 MeV incident energ

^{154}Sm

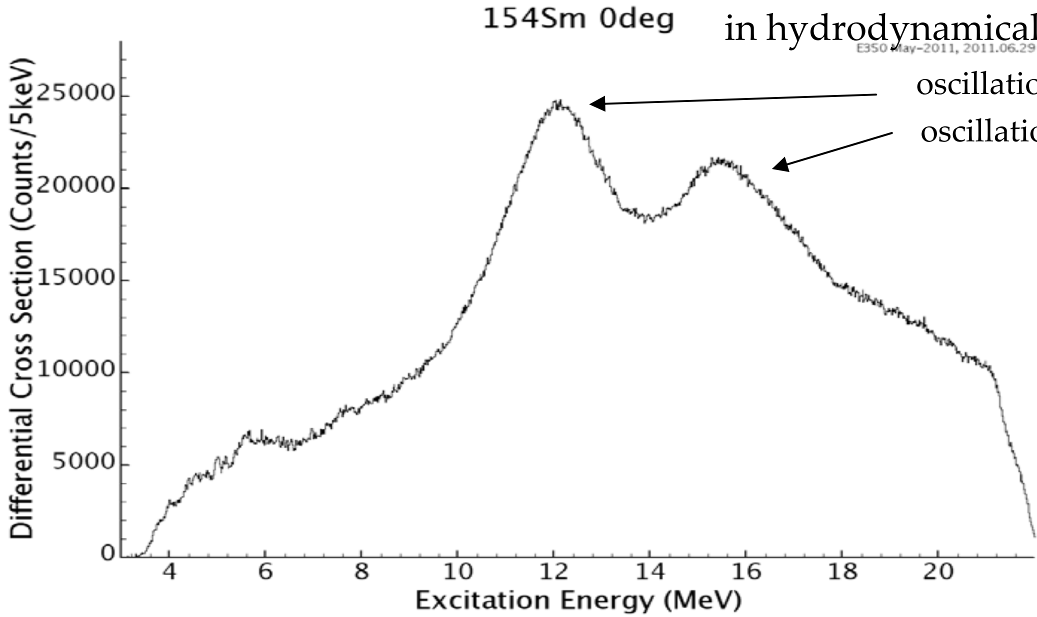

in hydrodynamical model

oscillation along the major deformation axis

oscillation along the minor deformation axis

area
2:1 oblate
1:2 prolate

^{144}Sm

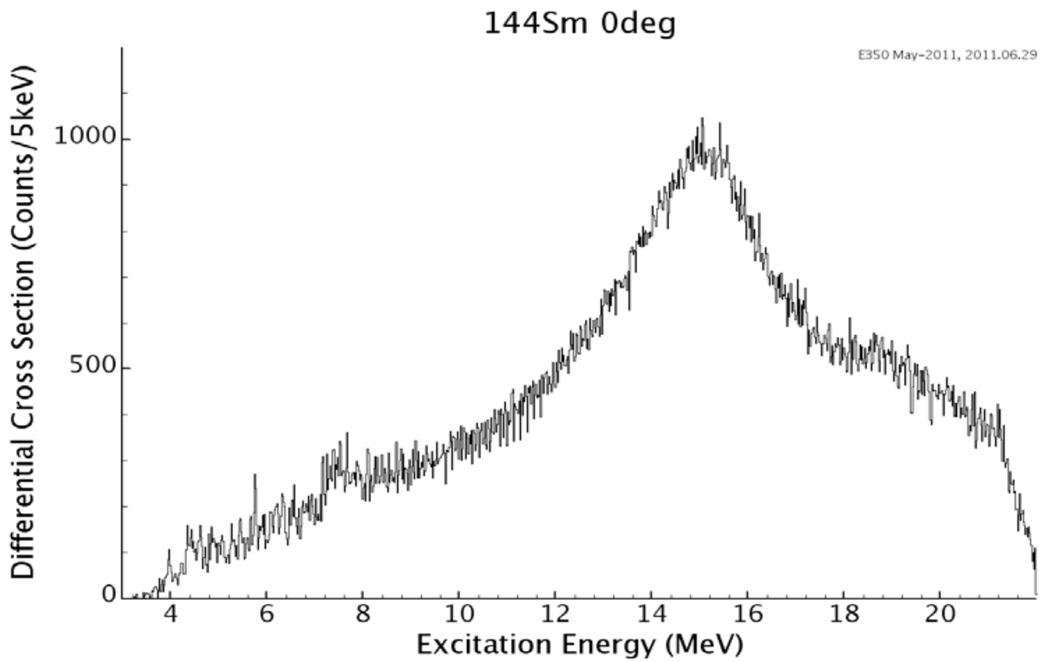

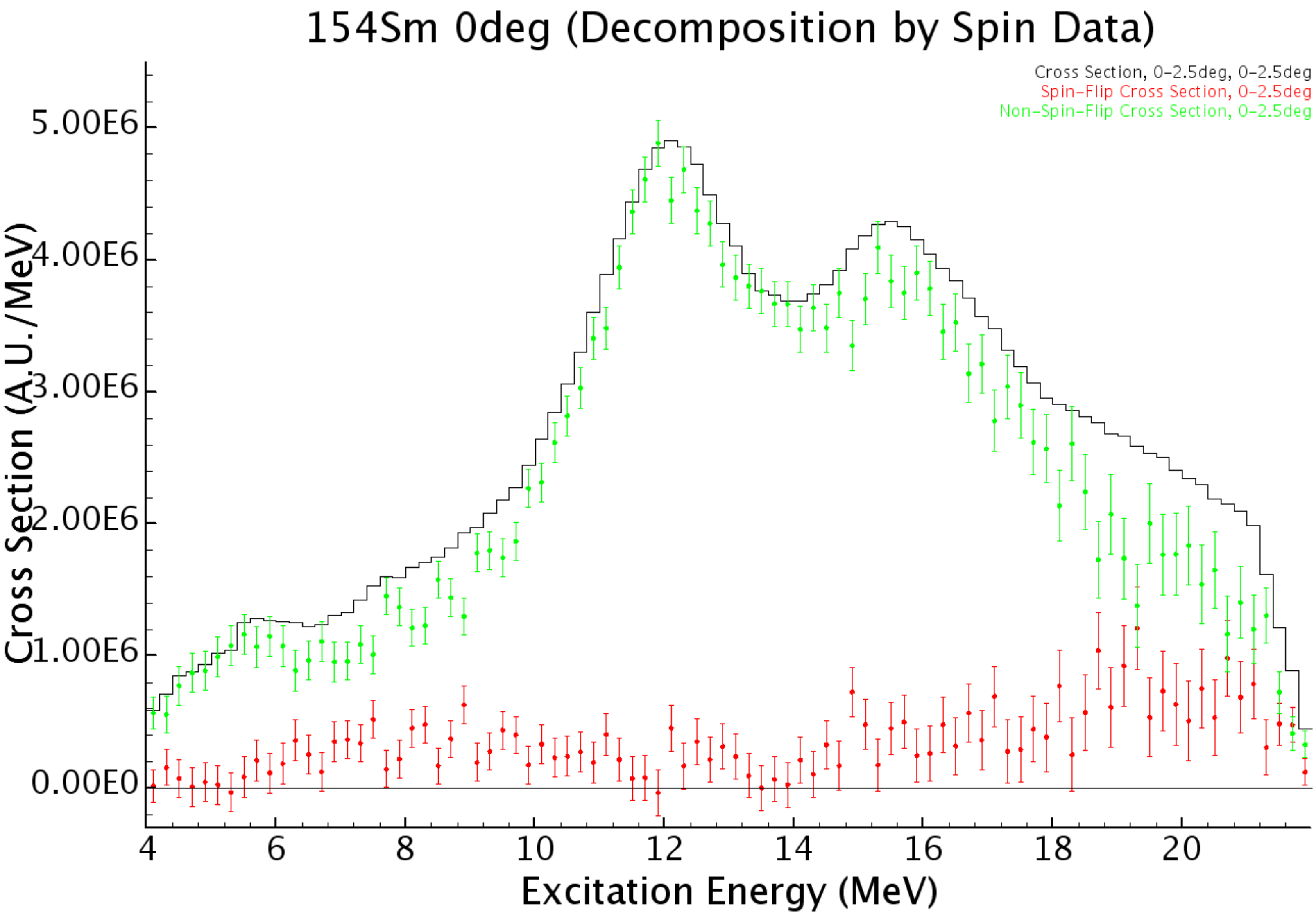

154Sm 0deg (Decomposition by Spin Data)
Cross Section, 0-2.5deg, 0-2.5deg
Spin-Flip Cross Section, 0-2.5deg
Non-Spin-Flip Cross Section, 0-2.5deg
5.00E6
4.00E6
3.00E6
2.00E6
1.00E6
0.00E0
Cross Section (A.U./MeV)
4
6
8
10
12
14
16
18
20
Excitation Energy (MeV)

Ground State の Core-Polarization のスピン構造

<u>松原</u>、中田、民井 et al.

対象核：N=Z, even-even nuclei in sd-shell region
16O, 20Ne, 24Mg, 28Si, 32S, 36Ar, 40Ca

(p,p′) Spectra at E_p=295 MeV

measured at 0-15 deg.

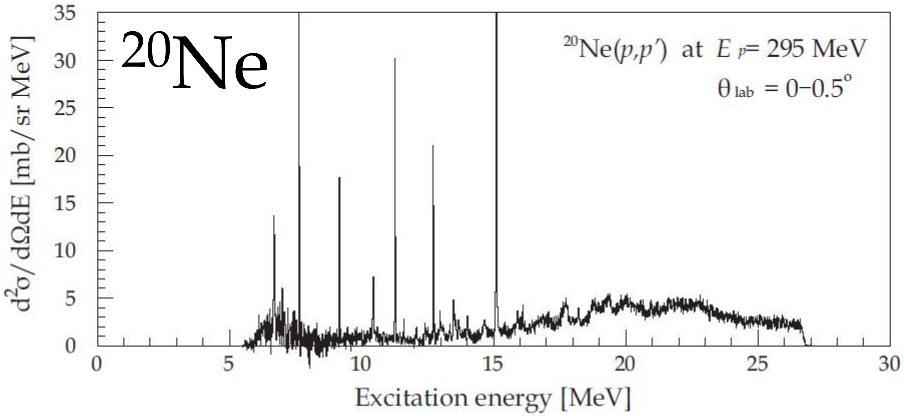

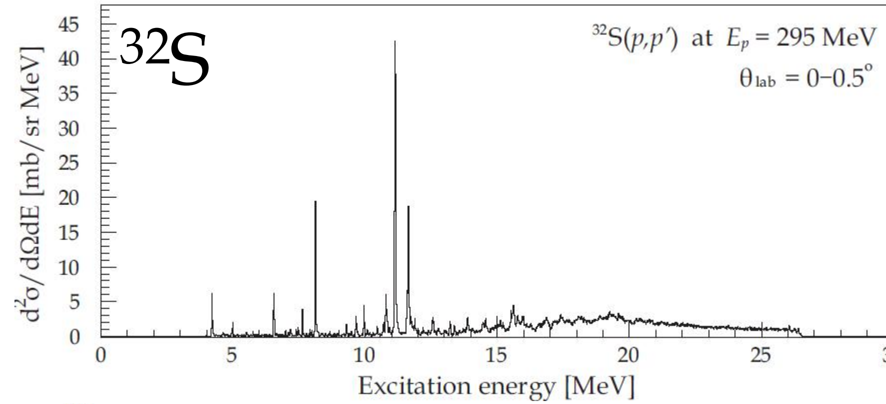

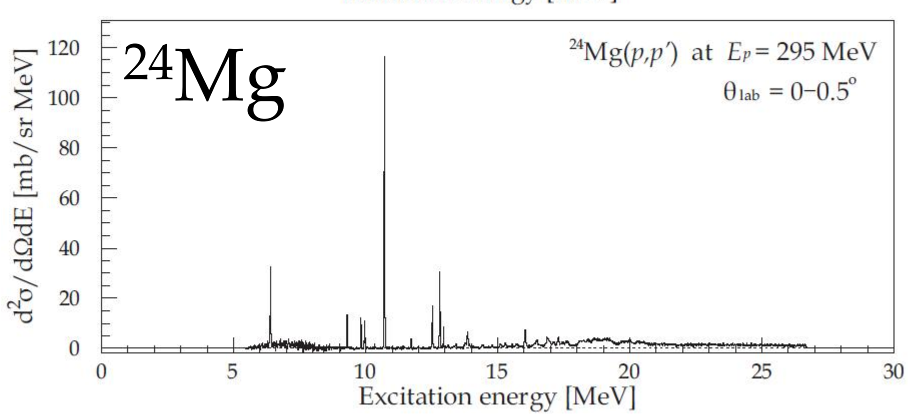

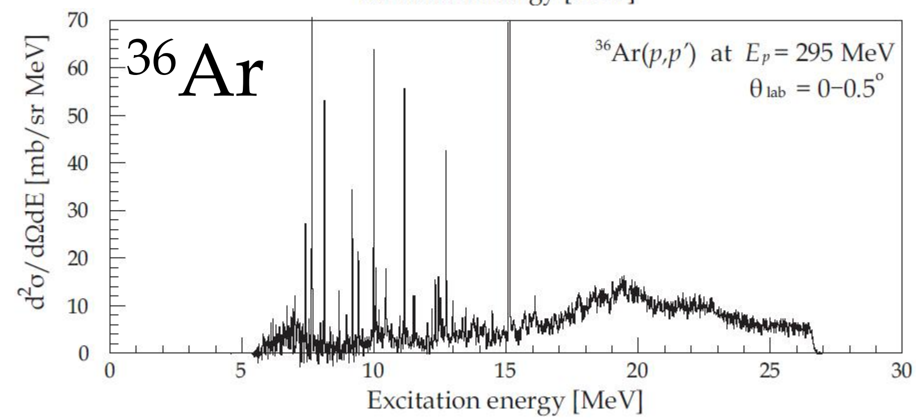

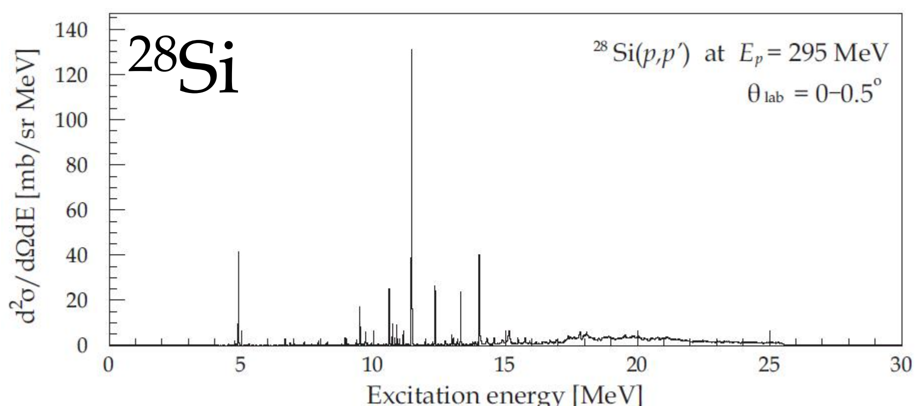

1^+ states were identified from angular distribution for each of IS and IV transitions.

The cross sections at the most forward angles have were converted to the spin-M1 strengths.

sd-shell 核 (N=Z, even-even) ΣB(σ)

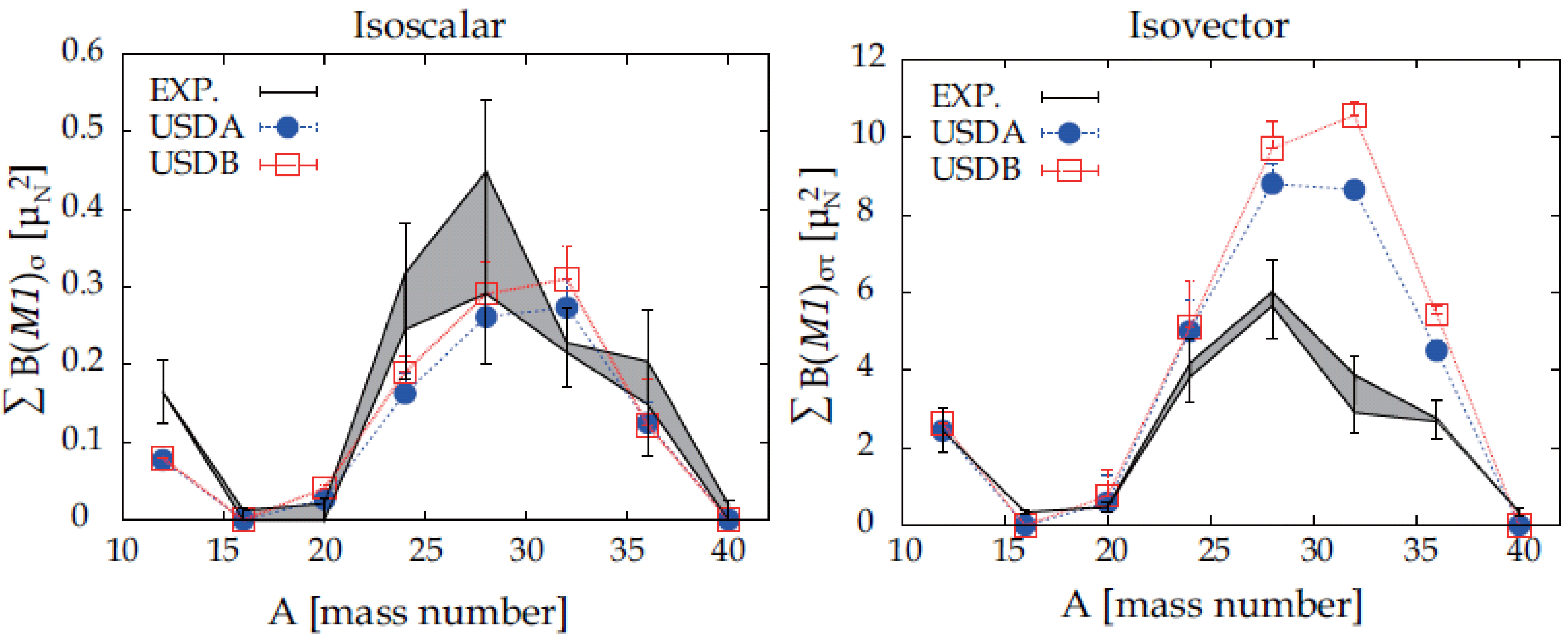

sd-shell 核 (N=Z, even-even) ΣB(σ)のIS/IV比

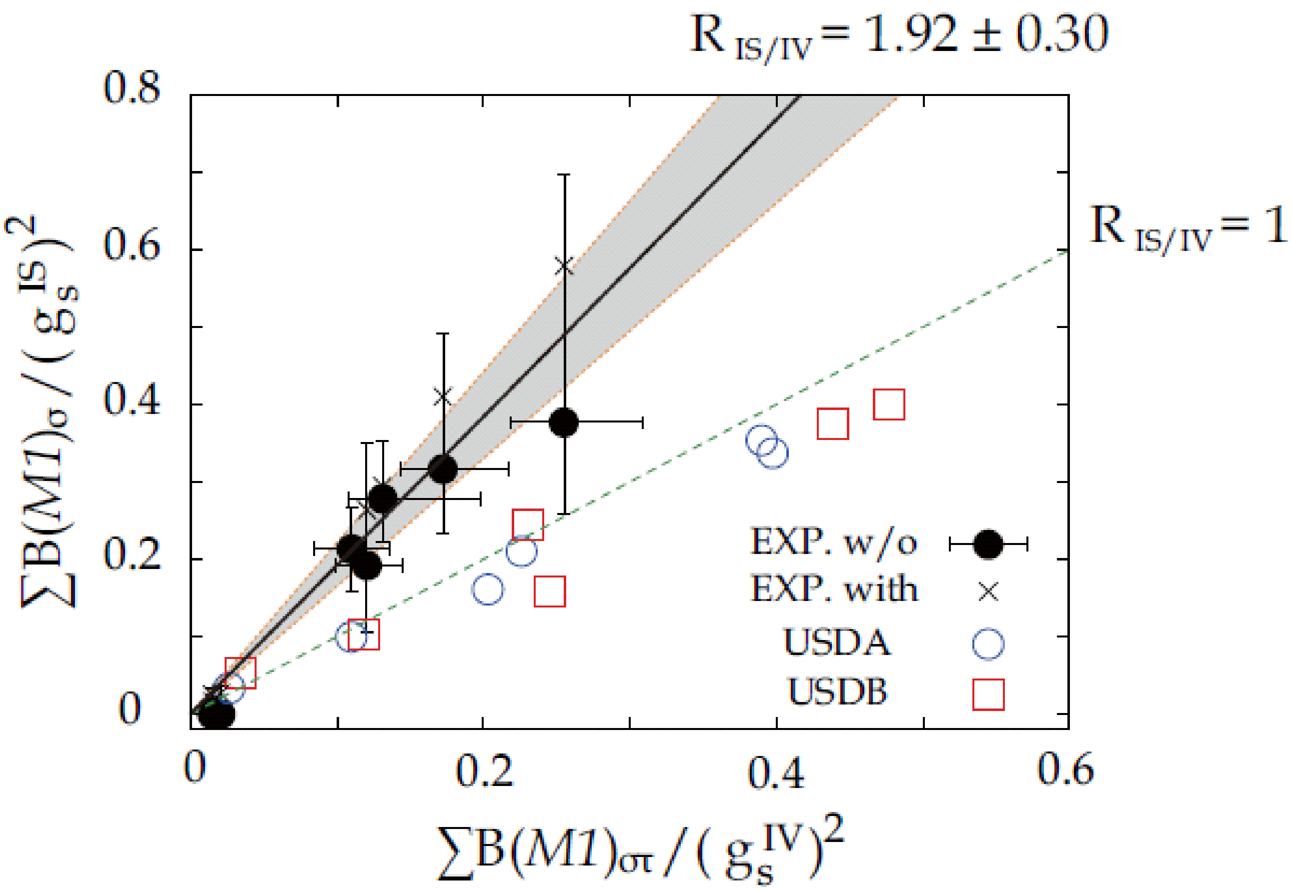

・何故直線上に乗るのか？

・Shell-Model の傾き~1と実験の傾き~2の違いは何を表しているのか？

$$R_{IS/IV} = \frac{\sum |M(\sigma)|^2}{\sum |M(\sigma\tau)|^2} = \frac{\sum B(M1)_\sigma/(g_s^{IS})^2}{\sum B(M1)_{\sigma\tau}/(g_s^{IV})^2},$$

$$\mathbf{S}_p = \sum_{k=1}^{Z} \mathbf{s}_k, \quad \mathbf{S}_n = \sum_{k=Z+1}^{A} \mathbf{s}_k,$$

$$R_{IS/IV} = \frac{\sum |M(\sigma)|^2}{\sum |M(\sigma\tau)|^2} = \frac{\sum B(M1)_\sigma/(g_s^{IS})^2}{\sum B(M1)_{\sigma\tau}/(g_s^{IV})^2},$$

, 2011

IS

$$\sum B(M1)_\sigma = \frac{1}{2J_i+1}\frac{3}{4\pi}\sum_f \left|\left\langle 1_f^+\right| \frac{g_s^{IS}}{2}(\mathbf{S}_p+\mathbf{S}_n)\left|0^+\right\rangle\right|^2 \mu_N^2$$

$$= \frac{1}{2J_i+1}\frac{3}{4\pi}\left(\frac{g_s^{IS}}{2}\right)^2 \left\langle 0^+\right|(\mathbf{S}_p+\mathbf{S}_n)^2\left|0^+\right\rangle,$$

IV

$$\sum B(M1)_{\sigma\tau} = \frac{1}{2J_i+1}\frac{3}{4\pi}\left(\frac{g_s^{IV}}{2}\right)^2 \left\langle 0^+\right|(\mathbf{S}_p-\mathbf{S}_n)^2\left|0^+\right\rangle.$$

$$R_{IS/IV} = \frac{\langle|\,(\mathbf{S}_p+\mathbf{S}_n)^2\,|\rangle}{\langle|\,(\mathbf{S}_p-\mathbf{S}_n)^2\,|\rangle}.$$

(g.s.で挟む)

$$= \frac{\langle|\left(\mathbf{S}_p^2+\mathbf{S}_n^2+2\mathbf{S}_p\cdot\mathbf{S}_n\right)|\rangle}{\langle|\left(\mathbf{S}_p^2+\mathbf{S}_n^2-2\mathbf{S}_p\cdot\mathbf{S}_n\right)|\rangle}.$$

$$\frac{R_{IS/IV}-1}{R_{IS/IV}+1} = \frac{2\langle|\,\mathbf{S}_p\cdot\mathbf{S}_n\,|\rangle}{\langle|\,\mathbf{S}_p{}^2+\mathbf{S}_n{}^2\,|\rangle}$$

~ 0 shell-model (in sd-shell)
~ +1/3>0 exp.

$$\frac{R_{IS/IV}-1}{R_{IS/IV}+1} = \frac{2\langle|\mathbf{S}_p\cdot\mathbf{S}_n|\rangle}{\langle|\mathbf{S}_p{}^2+\mathbf{S}_n{}^2|\rangle}$$

~ 0 shell-model (in sd-shell)
~ +1/3>0 exp.

・sd-shell空間内のshell-modelでは、0で一定値に近い。

・実験値は正で、一定値に近い

ground state のテンソル相関のスピン構造が見えているのではないか？

shell-model に入っていない効果か、major-shellを跨ぐような効果が見えている？

Possible configuration to have a positive C_S value?

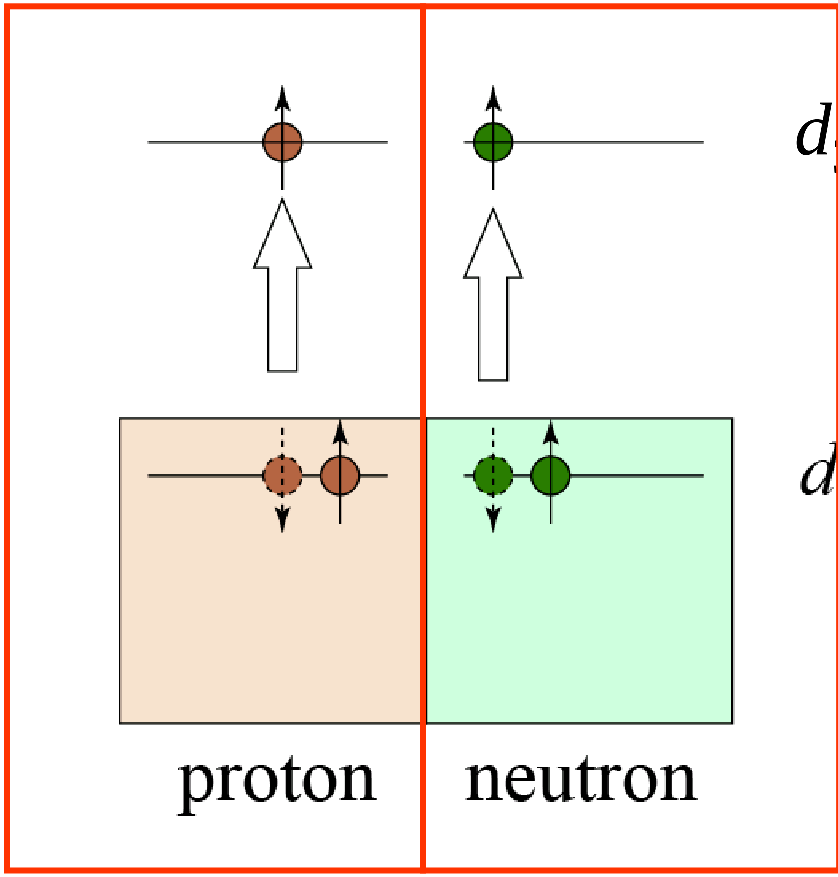

$d_{3/2}$, $f_{7/2}$, or ….

$d_{5/2}$

S_p S_n

$$\Psi = C_0|0\rangle + \sum_i C_i|2p-2h:i\rangle$$

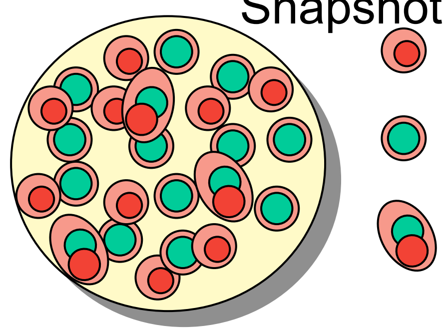

tensor correlation
tensor condensation?

H. Toki *et al.*,

This kind of configuration is mixing in the ground state.

例えば、こんなConfigurationがGround-Stateに混ざっているのが見えているのではないか？

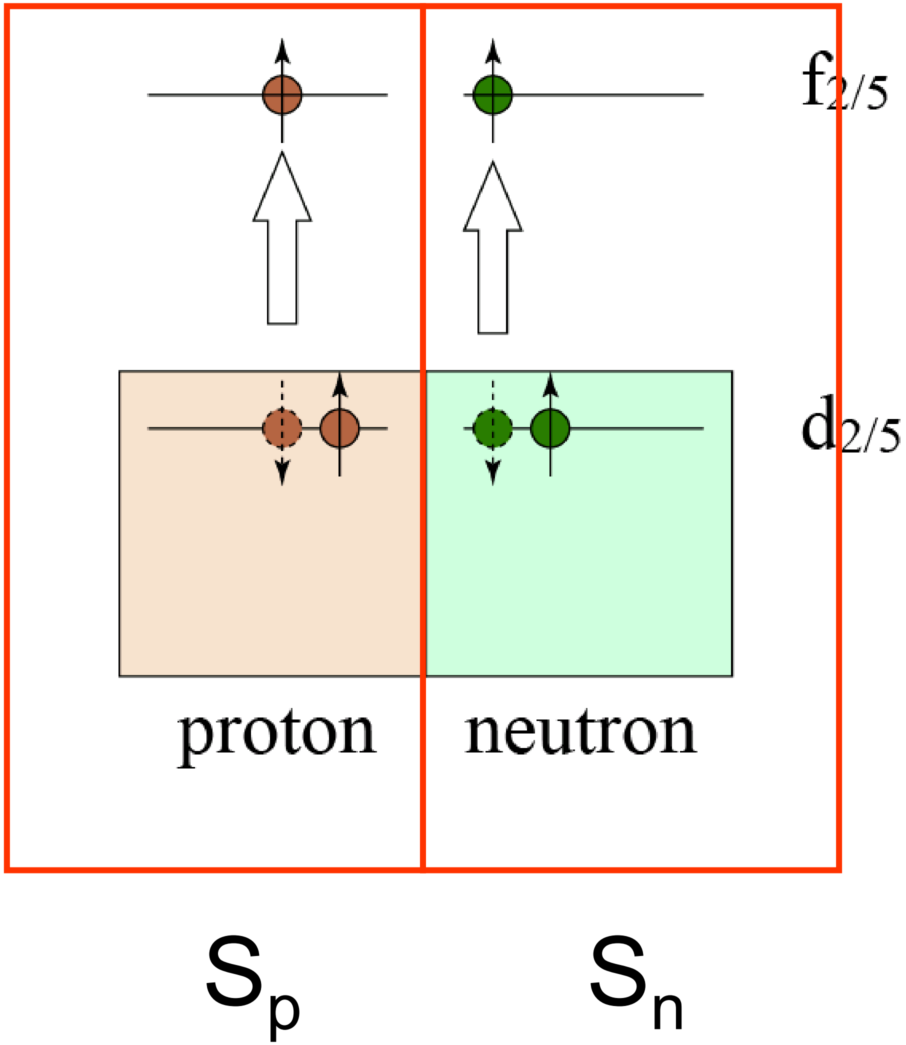

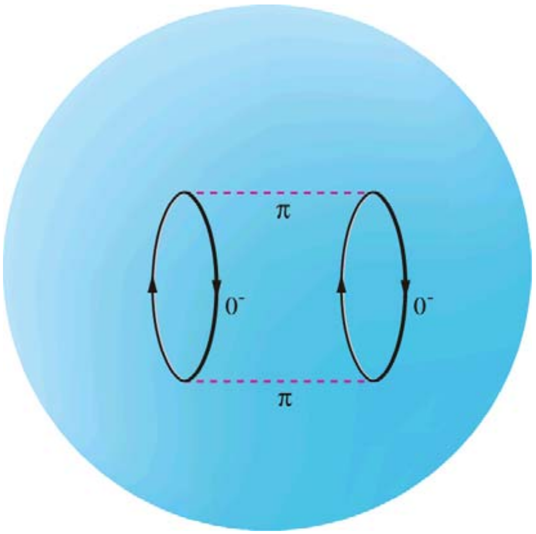

Photon Strength Function, Axel-Brink Hypothesis, and Level Densities

Photon Strength Function (PSF)

$$\langle \Gamma(E_i) \rangle = \frac{1}{\rho(E_i)} \cdot \int_0^{E_i} E_\gamma^3 f^{E1}(E_\gamma) \rho(E_i - E_\gamma)\, dE_\gamma$$

$$\langle \Gamma_{i \to g.s.} \rangle = \frac{f^{E1}(E_\gamma) \cdot E_\gamma^3}{\rho(E_i)}$$

$$f^{E1}(E_\gamma) = \frac{\sigma_{abs}(E_i)}{3(\pi\hbar c)^2 \cdot E_\gamma}$$

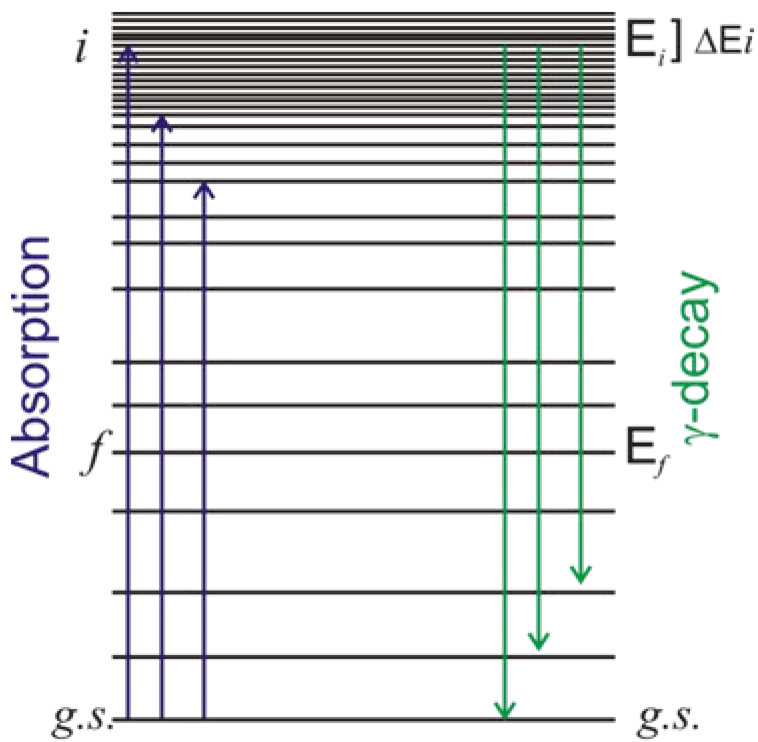

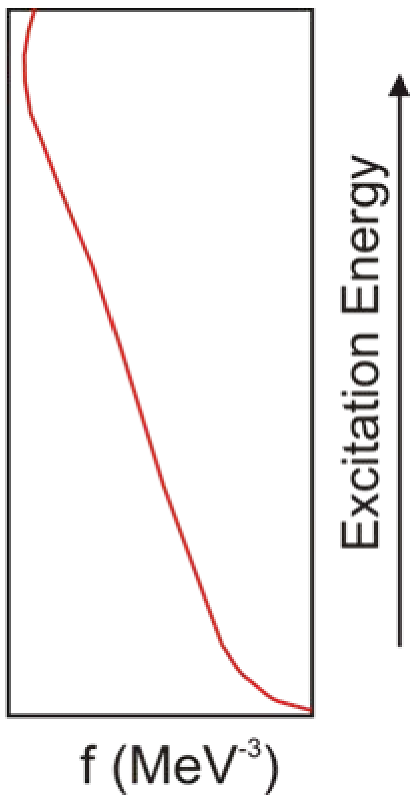

Axel-Brink Hypothesis

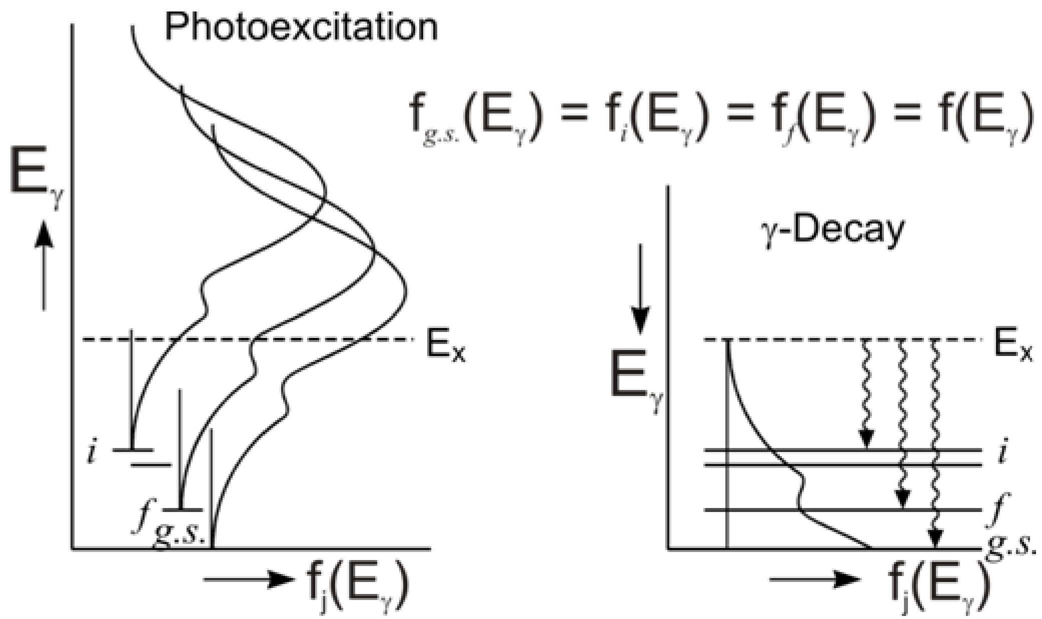

- Strength
  - depends only on E_γ
  - is independent of the initial state structure: E_x, J^π,…

- Same PSF for γ absorption and emission

Experimental Discrepancies in PSF

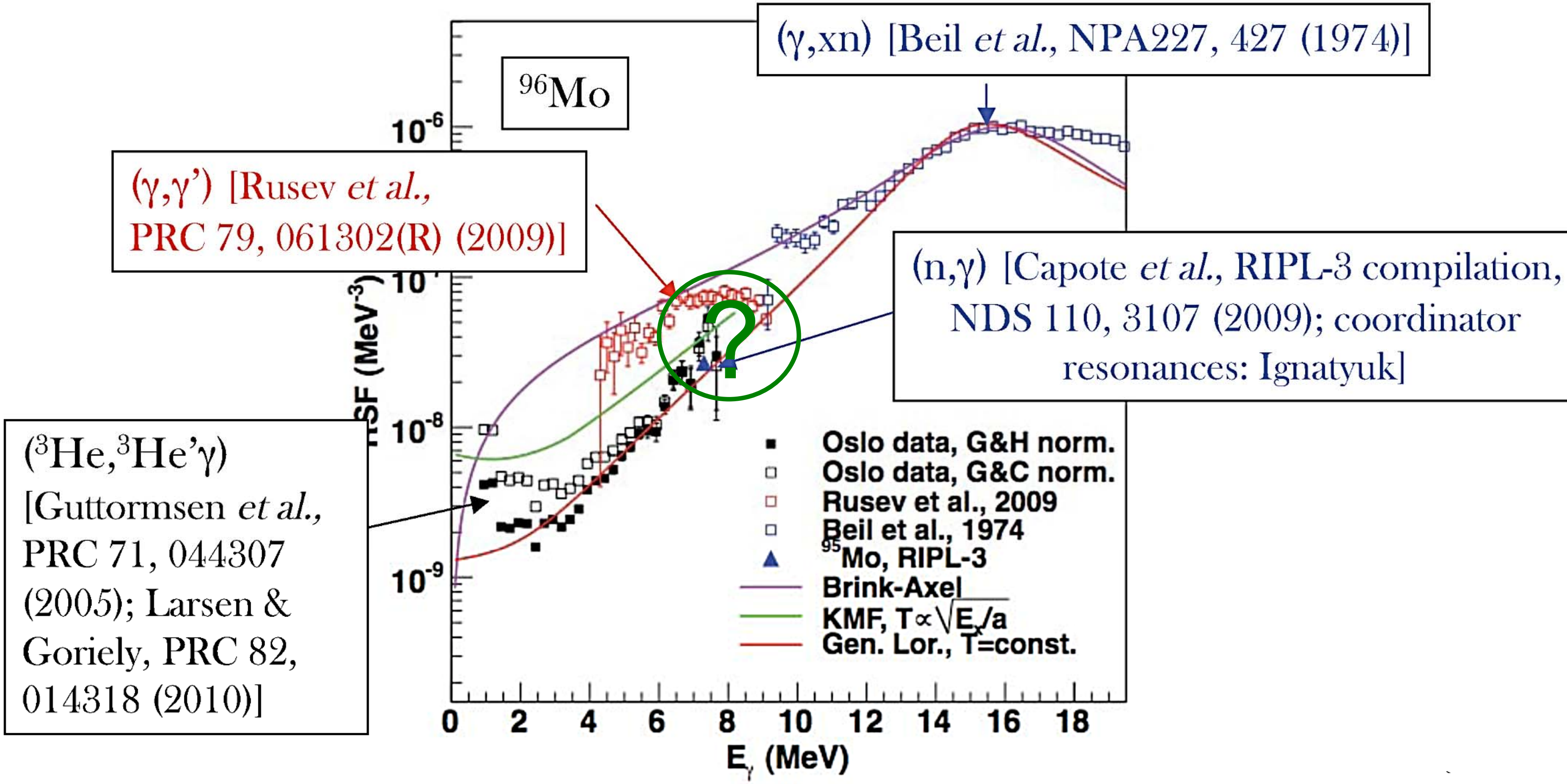

Ann-Cecilie Larsen, Workshop on Gamma Strength and Level Density, Dresden-Rossendorf, August 2010

Problems

- Experimental:
  - (γ,γ') reaction measures strength (roughly) up to threshold only
  - Experimental quantity $\propto \Gamma_0 \cdot \frac{\Gamma_0}{\Gamma}$

    $\longrightarrow$ assumption in most analyses

    $$\frac{\Gamma_0}{\Gamma} = 1 \rightarrow \text{lower limit}$$

    $\longrightarrow$ alternatively correction with statistical model calculation $\rightarrow$ upper limit

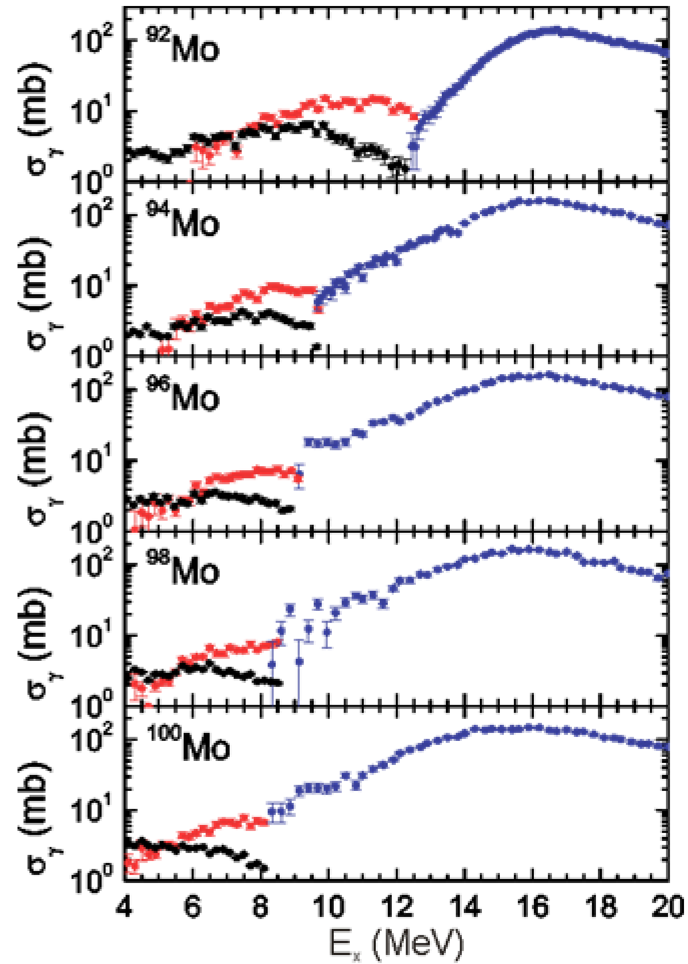

G. Rusev et al., PRC 79 (2009) 061302

Problems

- Experimental:
  - (γ,γ') reaction measures strength (roughly) up to threshold only
  - Experimental quantity $\propto \Gamma_0 \cdot \frac{\Gamma_0}{\Gamma}$

    $\longrightarrow$ assumption in most analyses

    $$\frac{\Gamma_0}{\Gamma} = 1 \rightarrow \text{lower limit}$$

    $\longrightarrow$ alternatively correction with statistical model calculation $\rightarrow$ upper limit

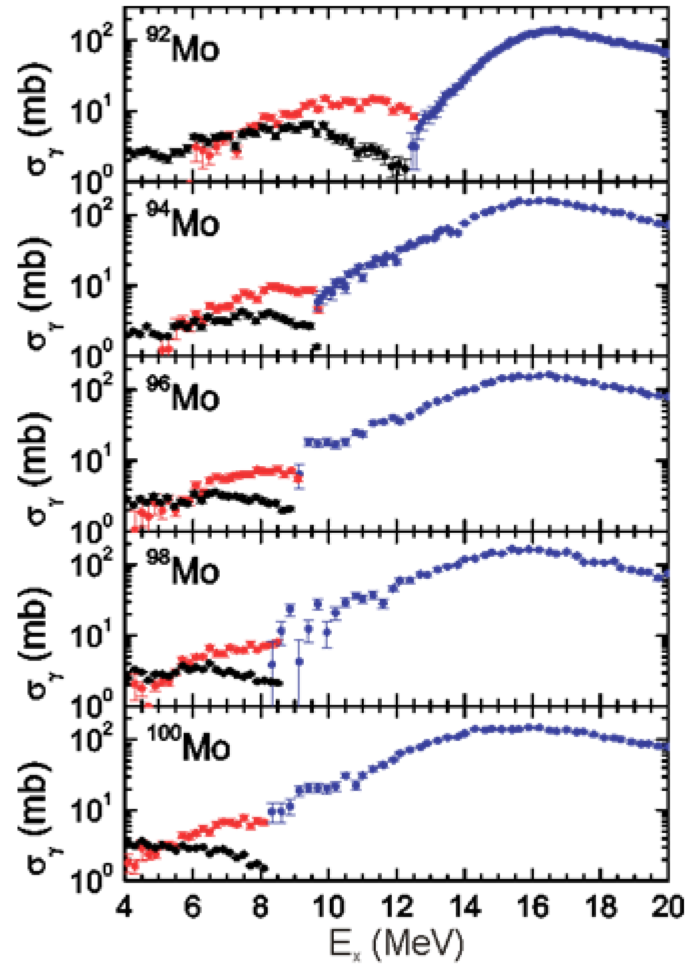

G. Rusev et al., PRC 79 (2009) 061302

Wavelets

- Wavelets: $d\int_{-\infty}^{\infty} \Psi^*(x)x = 0$

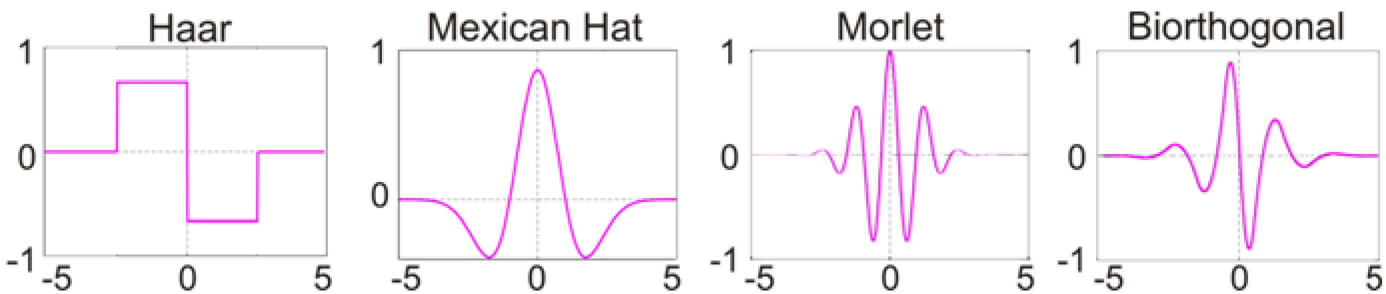

- Wavelet coefficients:

$$C(\delta E, E_x) = \frac{1}{\sqrt{\delta E}} \int \sigma(E)\, \Psi^*\left(\frac{E_x - E}{\delta E}\right) dE$$

scale position spectrum wavelet

- Discrete: $\delta E = 2^j$ and $E_x = k\delta E$
  with $k,j = 1, 2, 3, \ldots$

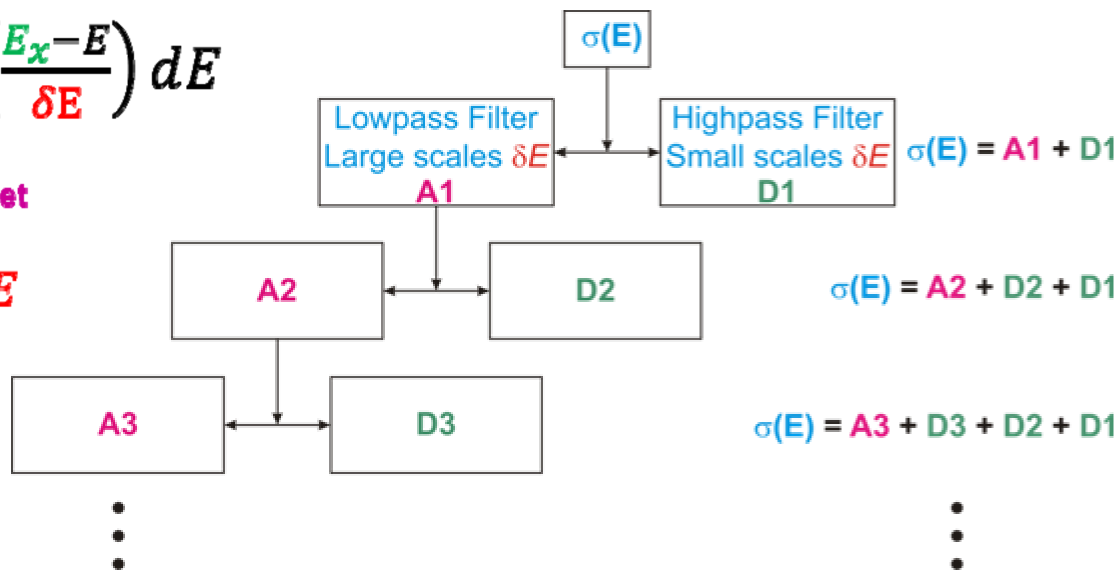

DWT of ^{208}Pb spectrum

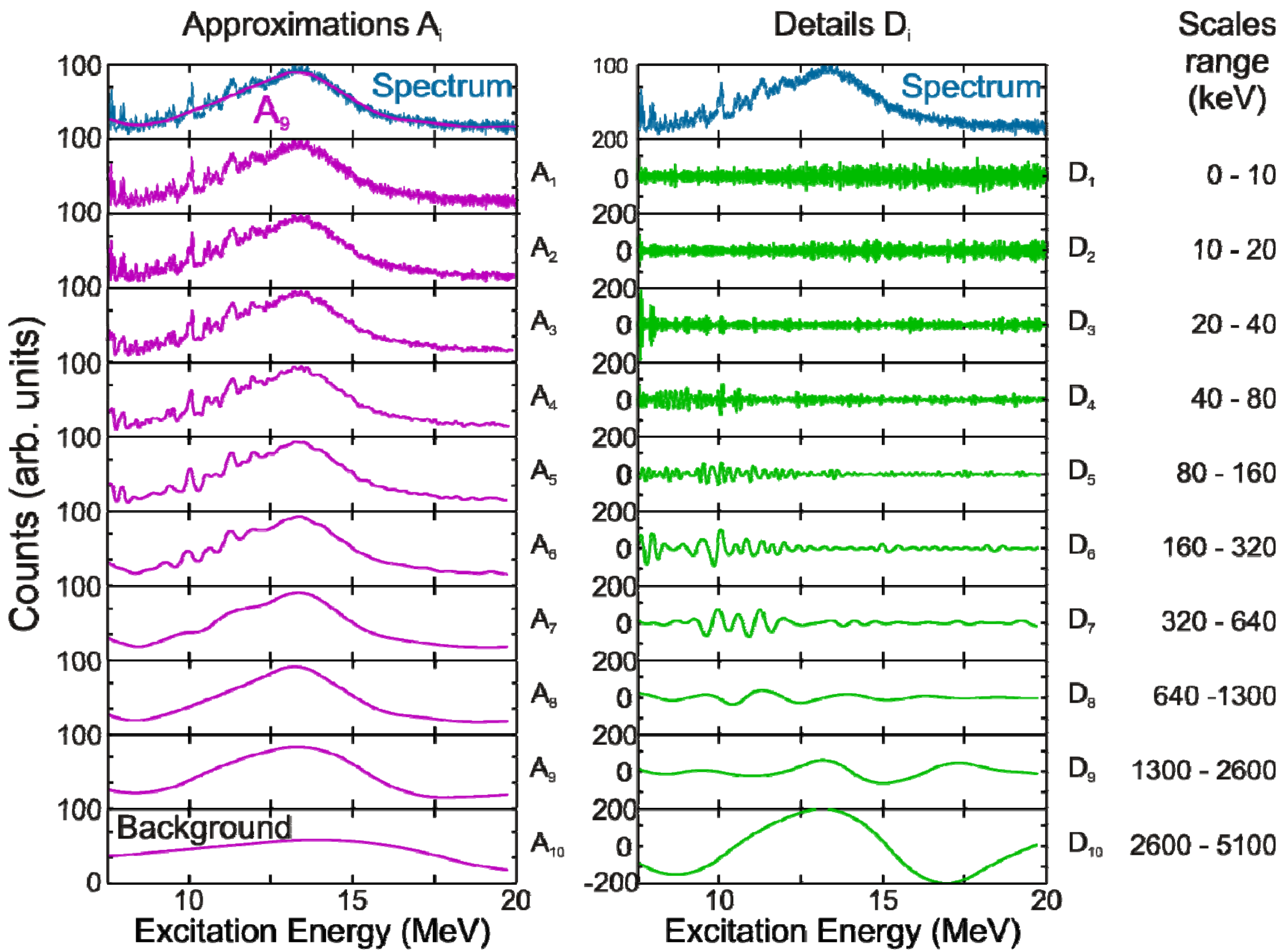

END